

**DEVELOPMENT AND CHARACTERIZATION OF BIOCOMPOSITES FROM
POLYLACTIC ACID AND GROUNDNUT SHELL ASH NANOPARTICLES**

BY

OLAYINKA SAMSON OLAJIDE

**DEPARTMENT OF METALLURGICAL AND MATERIALS ENGINEERING
FACULTY OF ENGINEERING
AHMADU BELLO UNIVERSITY,
ZARIA- NIGERIA**

MARCH, 2018

**DEVELOPMENT AND CHARACTERIZATION OF BIOCOMPOSITES FROM
POLYLACTIC ACID AND GROUNDNUT SHELL ASH NANOPARTICLES**

BY

**Olayinka Samson OLAJIDE B.ENG (A.B.U), M.Sc(UNILAG)
PHD/ENG/11957/2007-2008**

**A DISSERTATION SUBMITTED TO THE SCHOOL OF POSTGRADUATE
STUDIES,
AHMADU BELLO UNIVERSITY, ZARIA**

**IN PARTIAL FULFILLMENT OF THE REQUIREMENTS FOR THE AWARD
OF THE DOCTOR OF PHILOSOPHY DEGREE IN METALLURGICAL AND
MATERIALS ENGINEERING**

**DEPARTMENT OF METALLURGICAL AND MATERIALS ENGINEERING
FACULTY OF ENGINEERING
AHMADU BELLO UNIVERSITY,
ZARIA- NIGERIA**

MARCH, 2018

DECLARATION

I declare that the work in the Thesis entitled Development and Characterization of Biocomposites from Polylactic Acid and Groundnut Shell Ash Nanoparticles was performed by me in the Department of Metallurgical and Materials Engineering under the supervision of Prof. Shehu A.Yaro. The information derived from literature has been duly acknowledged in the text and list of references provided. No part of this Thesis has been used previously for another degree or diploma at any university.

OLAJIDE SAMSON OLAYINKA

Date

CERTIFICATION

This Thesis entitled “DEVELOPMENT AND CHARACTERIZATION OF BIOCOMPOSITES FROM POLYLACTIC ACID AND GROUNDNUT SHELL ASH NANOPARTICLES” by OLAJIDE Samson Olayinka meets the regulation governing the award of the degree of Doctor of Philosophy of Ahmadu Bello University, Zaria and approved for its contribution to knowledge and literary presentation.

Prof. ShehuAliyuYaro Chairman,
Supervisory committee

Date

DrFerdinardAsuke
Member Supervisory Committee

Date

Prof. Ola Aponbiede
Member Supervisory Committee

Date

DrAuwalKasim
Head of Department

Date

Prof. S. Z. Abubakar
Dean, school of postgraduate studies

Date

DEDICATION

This work is dedicated to Almighty God, the Apple of my eyes, OlajideOmoladeand our children – OlajideOreofeoluwa and OlajideImisioluwa. I love you all.

ACKNOWLEDGEMENT

I thank God Almighty, the Alpha and Omega, Jehovah El-Shaddai, who has brought peace and joy to my life and my family. Without Him, this work would not have been successful.

My sincere appreciation goes to my supervisor Prof. ShehuAliyuYaro for his positive criticism, suggestions, open-mindedness and tirelessness in going through my work. May God Almighty reward him for his hard work and dedication.

I wish to express gratitude to Dr Ferdinand Asuke who took pains to read this work and proffered insight in the course of the work. I am grateful to Prof. Ola Aponbede for his positive contribution to the work. I am also thankful to the Head of Department DrAuwalKasim, other academic staff like Prof. E.T. Dauda, Prof. T. Ause and entire member of the Department for contributing to my success.

My profound thanks go to Prof. Patricia Popoola, Department of Chemical, Metallurgical and Material Engineering, Tshwane University of Technology, Pretoria South Africa, and staff of National Centre for Nano-structured Materials at Center for Scientific and Industrial Research CSIR, Pretoria South Africa.

My love goes to my lovely Wife, the Apple of my eyes;OlajideOmolade and our lovely children OlajideOreofeoluwa and OlajideImisioluwa for their love and support. Special thanks to my brothers:DrSeyiOlajide, Arch. Paul Olajide, Arch. Emmanuel Olajide and my dear sister MrsFunkeFakeye. May God continue to bless you and your families. Without your moral, spiritual and financial supports from childhood, I would not have made it this far.

Abstract

Poly lactide (PLA) is an emerging material mainly because it can be synthesized from renewable resources and is thus environmentally and ecologically safe. It found application in packaging and biomedical. In terms of cost, however, PLA cannot rival the traditional packaging materials. Creative solutions are therefore needed to make PLA a more financially viable packaging alternative. This study was carried out in order to improve the properties and reduce the cost of PLA. Composites of Polylactic Acid (PLA) and Groundnut Shell Ash nanoparticles (GSAnp) were produced using injection moulding method. The GSAnp were produced by grinding groundnut shell ash in a ball mill and the optimal ball milling time of 10 hours with average nanoparticle size of 20nm was achieved. After the production, the GSAnp was characterized using Energy Dispersive Spectrum (EDS), X-ray Fluorescence (XRF), X-ray Diffractometer (XRD) and Brunauer-Emmett Teller (BET) analysis to determine the chemical composition, phase composition and specific surface area. Taguchi method was used to determine the combination of process parameters that gave the composite best combination of properties. Various process parameters varied were Wt% GSAnp, polyethylene glycol (PEG) %, annealing temperature ($^{\circ}\text{C}$) and time (hrs). The optimal combination of process parameters was obtained at 20wt% GSAnp, 4wt% PEG, annealing temperature of 100°C and time of 6 hours. This combination was found to produce a good interfacial bonding between the reinforcement and the matrix. The XRD spectrum of the PLA revealed two peaks located at $2\theta = 18.45^{\circ}$ and 45.6° while the composite exhibits major broad diffraction peak at $2\theta = 36, 45, 65$ and 78.5° with the presence of silica and alumina phases. Mechanical testing of the composite gave better tensile modulus, flexural strength and hardness values in comparison with the PLA used. After the mechanical test, SEM morphological study showed that the GSAnp at 20nm as a reinforcement has smooth spherical surface. The GSAnp was fairly dispersed in the polymer matrix. The maximum endothermic peaks shifted to higher temperature with GSAnp addition and improved the thermal stability of the produced composite. The storage modulus of the PLA decreases from 3100 to 500MPa, while that of the composite from 4250 to 700MPa at 30 and 90°C respectively, showing that the composite has better storage modulus. The weight loss as a result of biodegradation ranges from 2.5 to 20.5% after 20 days for PLA and 3.4 to 21.5% after 100 days for the composite. Hence, the mechanical, thermal and biodegradable properties of the developed nanocomposite material can be employed for use in food packaging and other disposable products as well as in fire-retardant materials.

TABLE OF CONTENT

TITLE PAGE	ii
DECLARATION	iii
CERTIFICATION	iv
DEDICATION	v
ACKNOWLEDGEMENT	vi
ABSTRACT	vii
TABLE OF CONTENT	viii
LIST OF TABLES	xiii
LIST OF FIGURES	xv
LIST OF PLATES	xvi
LIST OF APPENDICES	xvii
LIST OF ABBREVIATIONS	xviii
LIST OF SYMBOLS	xx
CHAPTER ONE	1
1.0 Introduction	1
1.1 Background	2
1.2 Statement of Problem	3
1.3 Aim and Objectives of the Research	5
1.4 Justification	5
1.5 Scope of the Work	6
CHAPTER TWO	7
2.0 Literature Survey	7
2.1 Composite Materials	7

2.2	Polymer Matrix Composites	9
2.2.1	Particulate Reinforced composites	11
2.2.2	Effect of filler particles on polymer matrix conformation	12
2.2.3	Polymer filler interface	13
2.3	Nanotechnology and Nanomaterials	15
2.3.1	Comparison of micron and nano-sized reinforcement	16
2.3.2	Polymer Matrix Nanocomposites	17
2.3.3	Mechanical Properties of Nanocomposites Coatings	18
2.3.4	Nanoparticles-polymer compatibility and their effect on the nanocomposite properties	20
2.4	Biodegradable polymers	22
2.4.1	Degradation of biopolymers by microorganisms	24
2.4.2	Factors affecting the biodegradability of biopolymers	27
2.4.3	Environmental Impacts of Biopolymers	27
2.5	Biocomposites from renewable resources	28
2.5.1	Applications of bio-based materials	30
2.6	Poly(Lactic Acid)	31
2.6.1	Modification of PLA	33
2.6.2	Poly(lactic Acid (PLA) nanocomposites	36
2.7	Hydrophilic Character of Natural Fibres/Particles	38
2.8	Solid Fillers	39
2.9	Groundnut Shell	42
2.10	Design of Experimental Technique	43
2.10.1	Taguchi Method and Research Model	45
2.11	Previous Works	46

CHAPTER THREE	53
3.0 Materials and Methods	53
3.1 Materials	53
3.2 Equipment	55
3.3 Methods	55
3.3.1 Production of Groundnut Shell Ash Nanoparticles (GSAnps)	55
3.3.2 Morphology and particles analysis of the produced Groundnut Shell Ash Nanoparticles (GSAnp).	57
3.3.2.1 Transmission Electron Microscopy (TEM)	57
3.3.2.2 Brunauer-Emmett-Teller (BET) Surface Area Analysis	57
3.3.2.3 X-ray diffractometer analysis(XRD)	58
3.3.2.4 Nanoparticle size analyzer	58
3.3.2.5 Fourier transform infrared spectrometry (FTIR) analysis	59
3.3.4 Experimental Design	59
3.3.4.1 Selection of Orthogonal Array (OA)	59
3.3.4.2 Analysis procedure of the selected orthogonal array	60
3.3.4.3 Development of PLA/GSAnp Composites	62
3.3.4.4 Determination of optimal production conditions for the composites	64
3.4 Morphological Analysis	65
3.4.1 Scanning Electron Microscopy (SEM) Analysis	65
3.5 Tensile Strength Test	65
3.5.1 Tensile Test Data Analysis	66
3.5.2 Signal to Noise (S/N) Data Analysis	66
3.6 Determination of the Mechanical Properties of the Composites	68
3.6.1. Tensile Strength Determination	68
3.6.2 Flexural Strength Determination	68

3.6.3	Impact Energy Determination	69
3.6.4	Hardness test	69
3.6.5	Dynamic Mechanical Analysis (DMA)	70
3.7.	Physical Test	70
3.7.1	Water Absorption	70
3.7.2	Determination of Density	71
3.7.3	Determination of Thermal Properties.	71
3.7.4	Cone Calorimetry	72
3.8	Biodegradability Test	73
3.9	Morphological and Phases Analysis	73
3.9.1	Scanning Electron Microscopy (SEM) Analysis	73
	CHAPTER FOUR	74
4.0	Results and Discussion	74
4.1	Results of Characterization of the Groundnut shell nanoparticles	74
4.1.1	Transmission electron microscope analysis(TEM)	74
4.1.2	X-ray fluorescence (XRF) analysis of the GSAnp	79
4.1.3	X-ray diffractometer (XRD) analysis of the GSAnp	80
4.1.4	Nano-Particle size analysis	82
4.1.5	Surface area (BET)	83
4.1.6	FTIR analysis of GSAnp	83
4.2	Visual Observation of the Composites	84
4.3	Tensile strength for optimal composite setting	84
4.3.1	Estimation of optimum performance characteristics	88
4.3.2	Confirmatory experiment at optimal conditions	89
4.3.3	Analysis of variance (ANOVA)	90
4.3.4	Regression model for optimum tensile strength	91

4.4	Properties of Composites at optimized condition	92
4.4.1	X-ray Diffraction	92
4.4.2	Morphology of the Composites	94
4.4.3	Tensile Modulus and Percentage of Elongation	96
4.4.4	Flexural Properties.	96
4.4.5	Hardness values	97
4.4.6	Impact Energy	97
4.4.7	Density	98
4.4.8	Water Absorption	98
4.4.9	Thermogravimetric Analysis (TGA)	99
4.4.10	DMA analysis	102
4.4.11	Cone Calorimeter Analysis	104
4.4.12	Biodegradability Analysis	108
	CHAPTER FIVE	109
5.0	Conclusions and Recommendation	109
5.1	Conclusions	109
5.2	Recommendation	110
5.3	Contribution to Knowledge	110
	References	112
	Appendices	121

LIST OF TABLES

Table 2.1: Types of application and examples of composite materials.	8
Table 2.2: Types of application and examples of composite materials	9
Table 2.3: Major areas of applications of Nanotechnology	16
Table 2.4: Physical properties of PLA(98%L-lactide) PLA(94%L-lactide), PS and PET	33
Table 2.5: Solid used as fillers or Reinforcement	41
Table 3.1 Properties of the Polylactic Acid (PLA) Resin Specification	53
Table 3.2: Process parameters and their values for different levels	59
Table 3.3: The L9 (3 ⁴) Orthogonal Array (OA) with parameters assigned and responses	61
Table 3.4: Various factor levels and manufacturing parameters for the formulations	62
Table 3.5: Extrusion parameter used	64
Table 4.1: EDS Quantitative Results of the GSAnp at 10hours ball milling	80
Table 4.2: Composition of the groundnut shell ash nanoparticles	80
Table 4.3: Peak List of the XRD pattern of GSAnp	82
Table 4.4: Identified Patterns List GSAnp	83
Table 4.5: Various Factor levels and manufacturing parameters for the formulations	86
Table 4.6: Response Table for Signal to Noise Ratios Larger is better (Larger is better)	89
Table 4.7: Response Table for Means (Larger is better)	90

Table 4.8: ANOVA for the Model	91
Table 4.9: Experimental values and Predicted values	92
Table 4.10: Optimum levels of process parameters (TENSILE strength after fracture)	93
Table 4.11: The results of physical and mechanical properties at optimized condition	98
Table 4.12: Summary of results of Cone Calorimeter	106

LIST OF FIGURES

Figure 2.1: Classification of biodegradable polymers.	25
Figure 2.2: Chemical structure of (a) L-lactic acid, D-lactic acid and (b) Polylactic acid	32
Figure 4.1: EDS analysis of the GSAnp at 10 hours ball milling	78
Figure 4.2: XRD pattern of the GSAnp	80
Figure 4.3: Particle size distribution by wt%	83
Figure 4.4: FTIR of the GSAnp	84
Figure 4.5: Main effects plot for the means.	86
Figure 4.6: Main effects plot for the S/N ratios.	86
Figure 4.7: XRD pattern of the PLA	93
Figure 4.8: XRD pattern of the composite at optimal condition	93
Figure 4.9: Variation of % Water absorption with Time of exposure	99
Figure 4.10: TGA curves of the GSAnp, PLA and Composite	101
Figure 4.11: Derivative weight curves of the GSAnp, PLA and Composite	101
Figure 4.12: Variation of Storage Modulus with Temperature	103
Figure 4.13: Variation of Damping factor with Temperature	103
Figure 4.14: Variation of heat release rate with time	106
Figure 4.15: Variation of Total heat release rate with time	106
Figure 4.16: Variation of mass loss with time	107
Figure 4.17: Variation of Biodegradation with incubation time	108

LIST OF PLATES

Plate 3.1: Photograph of Groundnut shell	54
Plate 3.2: Photograph of the Polylactic acid pellets	54
Plate 3.3: Photograph of the Ashed groundnut shell	56
Plate 4.1: TEM morphology of the GSAnp at 2 hours ball milling time x250,000	75
Plate 4.2: TEM morphology of the GSAnp at 4 hours ball milling time x250,000	75
Plate 4.3: TEM morphology of the GSAnp at 6 hours ball milling time x250,000	76
Plate 4.4: TEM morphology of the GSAnp at 8 hours ball milling time x250,000	76
Plate 4.5: TEM morphology of the GSAnp at 10 hours ball milling time x250,000	77
Plate 4.6: TEM morphology of the GSAnp at 12 hours ball milling time x250,000	77
Plate 4.8: SEM fracture morphology of the PLA	95
Plate 4.9: SEM morphology of the composite at optimum composition	95

LIST OF APPENDICES

APPENDIX A: Stress-Strain curves	127
APPENDIX B: Pictures of Equipment and facilities	132
APPENDIX C: Publication from this Research Work.	145

LIST OF ABBREVIATIONS

ABS	– Acrylonitrile-butadienesstyrene
ANOVA	– Analysis of Variance
ASTM	– American Society for Testing and Materials
ATR	– Attenuated Total Reflectance
AVR	– Average Response
BET	– Bruner-Emmet Teller
CNT	– Carbon Nanotube
CSIR	– Centre for Scientific and Industrial Research
DMA	– Dynamic Mechanical Analysis
DMAC	– Dimethylacetamide
DOE	– Design of Experiment
DOF	– Degree of Freedom
DTA	– Differential Thermal Analysis
EDS	– Energy Dispersive Spectroscopy
EV	– Expected Response
FTIR	– Fourier Transform Infrared Spectrometry
GSA _n P	– Groundnut Shell Ash Nanoparticles
HRR	– Heat Release Rate
IPP	– Isotactic Polypropylene
KGM	–konjacglucomannan
LDI	– Lysine-based Diisocyanate
LDPE	– Low-Density Polymer Polyethene
MCC	– Microcrystalline cellulose
MMT	– Montmorillonite

MWCNT	– Multi-walled Carbon Nanotube
OA	– orthogonall array
OMLS	– Organically Modified Clay Particles
PBAT	– Aromatic co-polymer
PBS	– Poly(butylenes succinate)
PCL	– Polycaprolactones
PEG	– Polythelene glycol
PEO	– Polyethene Oxide
PET	– Polyethene terephthalate
PHB	– Poly 3-hydroxybutyrate
PLA	– Polylactic Acid
PP	– Polypropylene
PS	– Polystyrene
PVA	– Poly (Vinyl) Acetate
RS	– Rice Starch
SEM	– Scanning Electron Microscopy
SSA	– Specific Surface Area
TEM	– Transmission Electron Microscope
TGA	– Thermogravimetric Analysis
THR	– Total Heat Release
XRD	– X-Ray Diffractometer
XRF	– X-Ray Fluorescence

LIST OF SYMBOLS

T_g	– Glass Transition Temperature
OH	– Hydroxyl
$^{\circ}\text{C}$	– Degree Celsius
wt	– Weight
h	– Height
\emptyset	– Titer
rpm	– Revolution per Minute

CHAPTER ONE

1.0 INTRODUCTION

The last decade brought a tremendous growth of interest in natural fibre/filler reinforced composites because of their good mechanical properties, significant processing advantages, chemical resistance, and the ratio of low cost to low density (Avella *et al.*, 2008). On the other hand, for environmental reasons, there is an increased interest in replacing reinforcement materials (inorganic fillers and fibres) with renewable organic materials. In this respect, natural fibre/particles reinforced composites (eco-composites) are subject of many scientific and research projects as well as many commercial interests (Fang and Hanna, 1999). The growing global environmental and social concern, high rate of depletion of petroleum resources, and the new environmental regulations have forced the search for new composites and green materials that are compatible with the environment. Also, the technology and machinery for blending, forming, and processing of these composites offers easy and cost-effective processes, apart from the fact that market for eco-composites seems to be promising and realizable for double-digit growth in the near future. Biodegradable thermoplastic polymers combined with renewable agricultural materials provides attractive, eco-friendly, qualitative and sustainable biocomposite.

Polylactic Acid (PLA) is a representative of semi-biosynthetic polymers, characterized by its transparency, humidity and oil resistance (Avella *et al.*, 2008). It is a biodegradable thermoplastic polymer with good mechanical properties, produced on a large scale from fermentation of renewable resources such as corn starch, cassava roots, sugar cane *e.t.c* to lactic acid and subsequent chemical polymerization. Pure PLA can

degrade in the environment to carbon dioxide, water and methane over a period of several months to two (2) years, while degradation of petroleum plastics takes much longer period (Nagata and Miyajima, 2008).

There are numerous results presented in scientific literature where groundnut shells were used to reinforce thermoplastic polymers such as polypropylene (PP) and polyethylene (PE) (Sobkowicz *et al.*, 2008), but apparently, no studies are reported on the use of groundnut shell particles as reinforcement in biodegradable polymers, especially PLA. The use of groundnut shell nanoparticles can be considered as an innovative alternative in reducing the cost of biodegradable composites while retaining some important properties such as rigidity, water resistance and biodegradability.

In the last decade biopolymers prepared from renewable resources have attracted great attention in both the academic and industrial worlds. In fact, renewable sources of polymeric materials reinforced with agricultural wastes derived from renewable resources, offer an answer to maintaining sustainable development of economically and ecologically attractive materials with respect to ultimate disposability and raw material use. In recent years, scientists and engineers have been working together to use the inherent strength and performance of the fibres and nanoparticles in combination with natural green polymer to produce a new class of bio-based composites. The special features of this type of bio-composites are their eco-attributes that make them environmentally friendly, completely degradable and sustainable.

1.1 BACKGROUND

Over the last decades, research has increasingly been conducted on renewable materials from sustainable resources for a variety of applications. This has been influenced by the ever-increasing demand for newer, stronger, stiffer, recyclable, fire repellent/retardant, less expensive and yet lighter-weight materials in fields such as aerospace, transportation, construction and packaging industries. Factors such as increased environmental and health concerns, the need for waste management solutions, the demand for more sustainable methods of manufacturing and reduced energy consumption, are reasons for the search for an alternative to conventional composites (glass, carbon and synthetic fibres). Therefore, material components such as natural fibres/particles and biodegradable polymers can be considered as alternatives for the development of new biodegradable composites or biocomposites (Mathew *et al.*, 2006).

At present, there is significant interest in the development of environmentally friendly polymers and polymer-based composites from renewable resources. Concerns about greenhouse gas emissions produced by using fossil fuel combined with low degradability of polymers derived from fossil fuel have led to an increase in research to develop degradable polymers and composites. Polylactic acid, (PLA) and cellulose are two such examples of degradable polymers that come from renewable resources.

1.2 STATEMENT OF PROBLEM

Nanocomposite is a class of composites in which the dimensions of the reinforcing particles are in the order of 1-100 nanometers. Because of this nanometer size characteristic, nanocomposites possess superior properties to the conventional composites due to larger interfacial adhesion. In the past, major interest has been in the use of synthetic materials such as aliphatic polyesters, aliphatic-aromatic polyesters, polyvinyl alcohols, polyesteramides, polystyrene, nanoclays, glass and carbon fibres and carbon nanotubes for the production of nanocomposite materials. The use of these materials, however, present great challenges (Nagata and Miyajima, 2008), which includes the shortage of the organic compounds due to declining oil and gas resources as well as fluctuation in oil and gas prices. Other disadvantages include environmental concerns for their degradation or incineration, global warming, uneconomical costs and cross contaminations during recycling and toxicity risks (Huda *et al.*, 2008). These concerns gave birth to the quest for materials that can withstand these challenges and also have the same properties (Huda *et al.*, 2008).

The use of polymer reinforced composites from renewable sources has advantages over synthetic sources, particularly as a solution to the environmental problems generated by plastic waste (Huda *et al.*, 2005). Green composite is today widely researched because of the need for innovations in the development of materials from biodegradable polymers, preservation of fossil-based raw materials, complete biological degradability and reduction in the volume of carbon dioxide released into the atmosphere. Applications of agricultural resources (wastes and products) for the production of green materials are some of the reasons why green composites have attracted tremendous research interests (Hu and Lim, 2007).

The use of these biocomposites is expected to improve manufacturing speed and recycling with enhanced environmental compatibility (Grozdanov *et al.*, 2006). Another problem is the low processing temperatures that must be used because of the possibility of thermal degradation of the fibres/particles, which might affect the biocomposite properties.

Therefore, studies aiming at the modification of polymer with groundnut shell ash nanoparticles to improve its thermal properties formed part of this research.

1.3 AIM AND OBJECTIVES OF THE RESEARCH

Aim

The aim of the project is to develop and characterize biocomposite from polylactic acid (PLA) and Groundnut Shell Ash nanoparticles (GSAnp).

Objectives

In order to achieve the aim of the project, the following objectives were pursued:

- i. Production and characterization of the groundnut shell ash nanoparticle.
- ii. Determination of the optimum production conditions that will give the highest tensile strength using Taguchi Method.
- iii. Development of the polylactic/groundnut shell ash nanoparticlebiocomposite.
- iv. Determination of the physical and mechanical properties of the composite produced at optimum conditions.
- v. Study of the morphological and thermal properties of the developed biocomposites using Scanning Electron Microscopy (SEM) with Energy Dispersive Spectroscopy (EDS), and Thermogravimetric analysis (DTA/TGA) respectively.
- vi. Determination of the biodegradability of the composites
- vii. Determination of the fire retardant characteristic of the developedbiocomposites using cone calorimeter.

1.4 JUSTIFICATION

Nanotechnology bridges the gap between molecules and particles and does not only opens new ways for the production and handling of particulate matter, but also for the design of advanced materials with special properties. In this context, organic/inorganic materials have received significant interest in the past few years. Improved material properties including scratch, abrasion, solvent and heat resistance, transparency, toughness and stiffness as well as gas barrier effects have been reported for

nanocomposites formed from inorganic nanoparticles accommodated in a polymeric matrix.

1.5 SCOPE OF THE WORK

The scope of the work covered in the research includes:

- i. Production and characterization of the groundnut shell ash nanoparticle using Transmission Electron Microscope (TEM), Brunauer-Emmett- Teller (BET) Surface Area Analysis and Nanoparticle size analyser.
- ii. Preparation of PLA/groundnut shell ash nanoparticles biocomposites.
- iii. Determination and evaluation of physical properties, water absorption, density and mechanical properties through tensile test, flexural test based on ASTM standards.
- iv. Study of surface morphology and thermal properties of the composites using Scanning Electron Microscopy (SEM) and Thermogravimetric analysis (DTA/TGA) respectively.
- v. Determination of the biodegradability of the composite using weight loss technique
- vi. Determination of the fire retardant characteristic of the composite using Stanton Redcroft Cone Calorimeter.

CHAPTER TWO

2.0 LITERATURE SURVEY

2.1 COMPOSITE MATERIALS

Composite materials can be defined as a material in which two or more distinct structurally complementary substances combined to produce structural or functional properties not present in either of the individual components. Composite can be produced either naturally (i.e. wood, teeth, etc) or synthetically (cement, aerospace materials, etc.) (Yang *et al.*, 2006). The most commonly used and studied composites are those used in structural applications, such as cement, fibre reinforced polymers, etc. however as technology develops and more materials with very specific properties are needed to meet the requirements, other functional applications have been studied and developed such as electronic, optical or biomedical.

An efficient way to categorize composite materials is by the application in which they are used (Osman *et al.*, 2010). Table 2.1 shows several types of composites for the most common types of applications and examples of those materials (Osman *et al.*, 2010).

Table 2.1: Types of application and examples of composite materials.

Application	Description	Examples
<i>Structural</i>	Composites that requires high mechanical performance. Often a low density is also required.	Steel-reinforced concrete race bicycles frames, tennis rackets, satellites, furniture, missiles.
<i>Thermal</i>	Applications that involve heat Transfer.	High thermal conductivity materials, thermal insulation materials.
<i>Electronic</i>	These materials include electrical, optical and magnetic applications.	Solar cells, heaters, light sources, optical lenses, magnetic field sensors, magnetic recording.
<i>Environment</i>	Relate to the protection of the environment from pollution by reduction of the amount of pollutant generated.	Biodegradable polymer composites, activated carbon fibre composites, macroporous filtering on absorption materials.
<i>Biomedical</i>	Related to the diagnosis and treatment of conditions, diseases and disabilities, as well as their prevention.	Implants (e.g. hips, teeth, heart, veins) surgical devices, pharmaceutical packaging.
<i>Prize reduction</i>	Related to composite materials with low coat inert filler	Materials like: chalk powder and CaCO_3 .

Source: Osman *et al.*, 2010.

Another method for classifying composite materials is by the type of matrix or majority phase it contains. Table 2.2 shows these different categories of composites and some examples and applications for each one (Osman *et al.*, 2010).

Table 2.2: Composites materials divided by the type of matrix or majority phase

Composite matrix	Examples	Applications
<i>Polymer</i>	Polymer-clay composites, polymer-carbon composites, polymer-metal composites, polymer-glass.	Structural, electronic, thermal, biomedical, environment.
<i>Metal</i>	Carbon fibre metal-matrix composites.	Structural, electronic, thermal.
<i>Ceramic</i>	Silicon carbide, silicon nitride, alumina composites.	Structural, thermal.
<i>Carbon</i>	Carbon fibre reinforced graphite (also called Carbon-carbon composites). Carbon-metal nanocomposites.	Structural, thermal, electronic, biomedical, environmental.
<i>Cement</i>	Concrete (cement, sand and gravel), carbon fibre reinforced concrete.	Structural, prize reduction.

Source: Osman *et al.*, 2010

2.2 POLYMER MATRIX COMPOSITES

Polymers have both advantages (flexible, low cost, low density, ease of process) and disadvantages (poor mechanical properties) as compared to other types of materials like metals and ceramics. One way to eliminate or mitigate these disadvantages is by producing polymer matrix composite materials. Polymer matrix composites are much easier to produce independently of the type of polymer (thermoplastic or thermoset) than other composites (metal-matrix, ceramic –matrix or carbon-matrix composite)(Osarenwinda and Nwachukwu, 2007). The reason is the relatively low temperatures needed to process the polymers. Normal processing temperature for epoxy resins range from room temperature to 200°C; for thermoplastics, such as

polyethersulfone (PES) and polyamide (PI) the respective temperatures range from 300°C to 400°C (Osarenmwinda and Nwachukwu, 2010). Thermoset composites have long been used and they remain most used polymer-matrix composites so far. A good example is the car tires where carbon black is added to natural rubber to give the structural properties needed to bear the load of the vehicle (Nourbakhsh and Ashori, 2009). The main use of thermoset composites is circuit boards and structural boards for ships. However, thermoplastic composites are growing in importance and production and they are under rapid development because they are inherently advantageous over thermoset polymers (Ichazo *et al.*, 2001). Some of the advantages are:

- a. No cure needed.
- b. Unlimited shelf life.
- c. Higher processing speed.
- d. Reprocessability (for recycling and repair).
- e. Reduced risks due to chemicals during processing.
- f. Thermal shaping possibilities
- g. Recently, also high-temperature thermoplastics.

Polymer composites can also be classified from the point of view of the dispersed phase they contain. By far, the most common types of polymer composites are the ones with added carbon. Whether in the form of fibres, laminates or particulates (Ichazo *et al.*, 2001). The use of ceramic and clay composites is growing rapidly because of properties achievable with the different types of additives available (Facca *et al.*, 2006).

2.2.1 Particulate Reinforced Polymer Composites

Factors that influence the properties of particulate filled composites are the properties of individual components, percentage composition and interaction of the components. Two kinds of interactions can occur in particulate filled composites (Facca *et al.*, 2006).

(i) Formation of an interphase—polymer adheres to the surface of particles forming an interphase. The interphase layer can have properties different from that of the polymer matrix

(ii) Aggregation— particles aggregate due to the interaction between particles

These two interactions are dependent on the forces of separation and adhesion between particles. Particle separation is influenced by the extent of shear forces exerted on the particles. Aggregation of the particles, on the other hand, is influenced by the particle size and surface tension of the particles (Facca *et al.*, 2006).

Pukanszky and Fekete (1999) gave factors that affect particle-particle interactions: particle size, specific surface area and surface energy. It has been shown for Polypropylene (PP) filled CaCO_3 composites that particle aggregation increases with decreasing particle size. However, increasing particle surface area by decreasing particle size, increases contact surface between filler and matrix and thus influences the filler matrix interactions.

Ess and Hornsby (1987) have identified the adhesive forces that cause particle agglomeration and have listed them in order of increasing adhesive strength as mechanical interlocking, electrostatic forces, van der Waals forces, liquid bridging and solid bridging.

Jancar (1989) has reported a much faster increase in composite

modulus with increasing filler volume fraction for untreated CaCO_3 compared to the surface treated CaCO_3 . He has attributed this difference to a higher thermodynamic energy of adhesion of the untreated filler. The higher thermodynamic energy of adhesion resulted in greater filler-matrix interactions. The rate of increase of modulus is thus seen to depend on interfacial interactions. However, reduction in filler energy achieved by surface treatment of CaCO_3 was observed to improve dispersion of the filler.

2.2.2 Effect of filler particles on matrix polymer conformation

The presence of filler particles can modify the conformation of the matrix polymer chains which in turn affects the properties of the polymer. Particles can restrict the conformation of polymer molecules in their vicinity which could expand the polymer chain.

Effect of crystallinity

It has been reported that particulate fillers can affect the crystallinity of some polymers and hence influence the mechanical properties of the polymer (Pozsgay *et al.*, 2002). Crystalline size and shape, orientation, percent crystallinity are some parameters that influence the properties. Since in thermoplastics the polymer chains have hindered motion, a high degree of supercooling may be required before crystallization (Rothon, 1995), this makes the thermoplastic polymers prone to nucleating effects with the addition of nucleating agents causing rapid nucleation. The nucleating agents, in general, affect the size and the number of crystallites formed.

Mitsuishi *et al.* (1991) have reported for samples of CaCO_3 filled PP change in crystallization rate of the matrix polymer due to the interactive motion of matrix chains at the particle surface. Decreasing particle size increases surface energy, which in turn increases the activity of the particle surface. This resulted in an increase in crystallization temperature

with increasing volume fraction of filler at all particle sizes. The authors have also reported a decrease in impact strength with increasing the nucleating effect of CaCO_3 .

Garlotta (2002) has shown that the mechanical properties of PLA depend on the degree of crystallinity which in turn can be influenced by annealing. Ray *et al.* (2003) have observed that dispersed organically modified clay particles, OMLS, act as nucleating agents in PLA and that the nature of OMLS influences the crystallization temperature.

Mathew *et al.* (2006) have studied the crystallization behaviour of PLA reinforced with microcrystalline cellulose, wood flour and cellulose fibres. They observed that the nucleating efficiency was more influenced by the surface topography than the chemical composition of the reinforcement.

2.2.3 Polymer filler interface

The interface in polymer composite systems is the surface between two mutually insoluble and chemically distinct phases which are at equilibrium with respect to each other. If there is no interaction between the phases, physical or chemical, then at larger strains the composite will respond as if the matrix contained holes of a shape identical to the shape of the filler. In the case when there is an interaction between the two phases, stress transfer can occur across the interface, resulting in filler carrying the load and thus reinforcing the matrix. However, if the interface is too strong then properties such as impact strength may be adversely affected as energy dissipation becomes difficult. In order to improve the interfacial strength, it is necessary that the polymer wet the fibre/particles (reinforcement) spontaneously during processing, wherein the adhesion energy between the polymer and fibre/particles can overcome the cohesive energy of polymer (Antonio *et al.*,

1997). Two methods are used for increasing the interfacial shear strength of the composite namely application of coupling/compatibilizing agent or chemical modification of the fibre/particle surface. Examples of coupling agents employed are those which are capable of condensing efficiently with surface hydroxyl groups present on the fibre/particle surfaces such as, carboxylic anhydrides, isocyanates, oxiranes and siloxanes. Improvement in mechanical properties, e.g., modulus and strength of thermoplastic composites reinforced with wood cellulose fibre have been reported after chemical modification of cellulose fibre surface (Bataille *et al.*, 1989). It is crucial, that modification takes place on the surface of the fibre but the cellulose backbone is not modified

Another important factor for achieving good interaction between matrix and fibre is the compatibility between their surface energies. Surface modification of cellulose fibres promotes adhesion by minimizing their interfacial energy with the non-polar polymer matrices. It is well established that the mechanical properties of the composite can be improved if chains (oligomer or polymer) grafted onto cellulose reinforce for surface modification can diffuse into and entangle with the matrix chains (Antonio *et al.*, 1997). Chemical or physical modification of polymer is another approach for modifying the properties of the polymer to meet some specific requirements/applications

Heux *et al.* (2000) have described a method for obtaining a stable dispersion of cellulose whiskers in non-polar solvents using surfactants. In general, a significant increase in the mechanical properties of the composite is observed with uniform dispersion of reinforcement.

Belgacem and Gandini (2005) have reviewed in detail the different procedures used for

surface modification of fibres/particles. Surface modification is necessary to increase the effect of cellulose as a reinforcing material to obtain new composites with desired properties. The surface of the cellulose whiskers can be chemically modified in order to improve dispersion in solvents such as water and organic solvents such as chloroform (Araki *et al.*, 2001).

2.3 NANOTECHNOLOGY AND NANOMATERIALS

In recent years, there has been a whole new area of research called nanotechnology. It includes nanocomposite materials involving polymer and nanoparticles. Nanomaterials are materials where the sizes of the individual building blocks are less than 100 nm, at least in one dimension (Fang and Hanna, 1999).

Depending on the above properties, nanomaterials find applications in many fields of engineering and it is expected to develop much more in the next decade. Table 2.3 shows several of the major fields where nanotechnology can be used (Fang and Hanna, 1999).

Table 2.3: Major areas of applications of Nanotechnology

Field	Application
Pharmacy	It can be possible to create nanoparticles that (because of the very small size) can be solubilized and carried in the blood. These particles can deliver the necessary drug for certain diseases.
Computer science	Nanoparticles are being used in video and audio discs that depend on the magnetic and optical properties of the ultrafine particles.
Ceramics and insulators	The compression efficiency of nanoscale ceramic particles allows creating more flexible solids due apparently to a large number of existing grains. Non-porous high-density materials can be also developed that can serve as metal replacements.
Metallurgy	When some nanoparticles are compressed into solid objects, they show a stronger surface, frequently five times more than the normal polycrystalline metals.
Environmental chemistry	Semiconducting nanoparticles can be used in a more efficient way to generate power via solar cells. Photoexcitation of nanoparticles produces oxidation and reduction of polluting agents, so that decontamination of water can be achieved.
Catalysis	Different nanoparticles have been tested for catalytic reactions. However, such reactions will depend on the type of materials used, its size and its shape, all these parameters change the net surface areas available for reaction.
Gas sensors	Materials with high superficial area whose electric conductivity changes when they absorb certain gases.
Electrodes	Magnetic metals such as iron can form dense magnetic materials with soft mechanical properties; thus, these materials can be used to create electric transformers.
Polymers	There are several effects produced when nanoparticles are added to polymers such as an increase in electric and thermal conductivity, mechanical reinforcement, fracture toughness, etc.
Paints	It has been demonstrated that when paintings are doped with nanoparticles such as TiO ₂ there is no need for cleaning the painting. This is related to the photo-oxidation of the contaminants by the TiO ₂ particles in water.

Source: Fang and Hanna, 1999

2.3.1 Comparison of micron and nano-sized reinforcement

Winey and Vaia (2007) compared microcomposites and nanocomposites of the same volume fraction of a spherical filler having volumes of $1 \mu\text{m}^3$ and 1nm^3 per

particle, respectively. In the nanocomposite, mean particle-particle separation was found to be smaller by three orders of magnitude, the total internal interfacial area increased by six orders of magnitude and the number density of constituents was found to increase by nine orders of magnitude. At extremely small particle size, the volume of the interface can be greater than the particle volume resulting in a majority of the volume fraction being occupied by the interfacial region. If this is the case, interface and particle-particle interaction dominate the macroscopic properties. Thus in an ideal polymer nanocomposite, the mean distance between the filler particles (nanoparticles), will be of the order of radius of gyration, R_g , of the matrix chains, which is the fundamental length scale characterizing the size of the matrix chains. The size of the filler is also of the order of R_g . The large aspect ratios observed with nanofillers can introduce orientationally correlations between particles giving rise to low percolation thresholds (Vaia and Wagner, 2004). Cypus *et al.* (2003) have observed the enhancements in mechanical and barrier properties of polymer nanocomposites to be a function of the aspect ratio of the nanofiller. In summary, the drastic improvements in material properties observed in nanocomposite systems at relatively low filler loadings can be related to short distances between particles, very high interfacial area per volume of particles, large number density of particles per particle volume and particle-particle interaction taking place at low volume fractions (Vaia and Wagner, 2004).

2.3.2. Polymer Matrix Nanocomposites

When additives are nano-scaled, there are of certain advantages to filled polymers and composites that lead to a better performance of the materials. This is a result of the filler size reduction and the consequent increase in surface area (Vaia and Wagner, 2004).

The concentration of the additive can be decreased by up to three orders of magnitude relative to the conventional fillers assuming an ideal mixture and dispersion. Moreover, many fields of engineering associated with electrical or optical properties benefit from quantum confinement effects induced by the nanoscale dimension of the materials (Vaia and Wagner, 2004). For instance, comparing a fraction of dispersed microcomposite and nanocomposite of the same volume. The main separation between particles is smaller by three orders of magnitude; the total internal interfacial area increased by six orders of magnitude; and the number density of particles increases in nine orders of magnitude (Bhatnagar and Sain, 2005). Although these numbers are impressive by themselves, the filler size must be observed relative to the size of the polymer chains –to capture the full potential impact of nanoscale fillers on composite materials properties.

A typical radius of gyration of a polymer chain is in the range of 3 to 30 nm. Depending on the strength of interaction between the filler surface and the matrix, the polymer chains in close proximity to the filler will be perturbed with respect to those in the bulk. As with traditionally filled plastics, enormous varieties of polymer plus nanoparticle combinations are possible. Thus, given the diversity of possible properties and tolerable costs, there is no "best universal" nanoparticle filler for polymer nanocomposites. The best nano-sized filler will be determined by meeting both a specific set of physical properties and a price associated with a particular product (Bhatnagar and Sain, 2005).

2.3.3. Mechanical Properties of Nanocomposites Coatings

The tailoring of properties is especially important for functional coatings. Therefore, composites are commonplace in the coatings field. The fillers may significantly improve properties like modulus, yield strength, impact resistance, and abrasion resistance (Rong *et al.*, 2001). For example, Qu *et al.* (1998) demonstrated that the addition of silica nanoparticles to nylon-6 resulted in increases in tensile strength, strain-to-failure, Young's modulus and impact strength.

Mammeri *et al.* (2003) filled PMMA coatings with silica nanoparticles, which resulted in an increase of the coating hardness. Vu *et al.* (2002) showed that incorporation of silica nanoparticles in UV- curable acrylate coatings can give a 2.5-fold increase of the E-modulus and higher abrasion resistance. Silica nanoparticles can be found in many performance materials like car tyres and scratch and abrasion resistant coatings (Rong *et al.*, 2001). The properties of a composite are not simply the sum of the properties of its components. The composite properties are also determined by the size, shape, and spatial distribution of the filler in the matrix and by the forces acting on the components (Rong *et al.*, 2001).

It has been found that decreasing the average size of the fillers from a few micrometers to a few nanometers can result in a higher gain in yield stress and modulus (Rong *et al.*, 2001). The larger effect of nanoparticles is attributed to their larger surface area. The surface area is an important parameter for interactions between the filler and the matrix which are very important for the composite properties. For a wide range of polymer matrices, it is observed that near the filler surface the glass transition temperature (T_g) is shifted by tens of degrees (Yang and Nelson, 2004). Moving away from the filler surface, the T_g returns to the bulk value of a gradient that stretches over tens of

nanometers (Yang and Nelson, 2004). The size and the direction of this T_g shift are determined by the interactions between the polymer and the filler. In the case of strong interactions, like strong physical or covalent bonding, a strong increase of the T_g will be found whereas very weak interactions may result in a decrease of the T_g (Yang and Nelson, 2004). Hence, modifications of the filler surface may affect the composite properties. For example, for silica-acrylate composites, it has been shown that the T_g increase when 3- methacryloxypropyltrimethoxysilane is grafted onto the silica surface, whereas with grafted acetoxo propyltrimethoxysilane the T_g decreases. Shifting of the T_g affects the mechanical properties, especially when a rubber polymer becomes glassy or vice versa(Bikiaris, 2006). If near the filler surface the T_g of a rubber polymer is raised above ambient temperature, a shell of glassy polymer around the filler is formed. This shell has a much higher E-modulus than the bulk rubber, consequently the modulus of the composite increases. The thickness of such a shell can be in the order of a few nanometers(Bikiaris, 2006); for nanocomposites, this shell may contain a major part of the matrix and large changes in the mechanical properties may be expected. For glassy polymer matrices, a similar increase of the T_g will have a smaller effect on the mechanical properties as no glass transition will take place.

2.3.4. Nanoparticles-polymer compatibility and their effect on the nanocomposite properties

Inorganic fillers are very hydrophilic and cannot be dispersed directly in low-polar resins. To improve the compatibility of the fillers with a polymer matrix, the surface of the fillers can be treated with an organic ligand. Surface modification of the inorganic nanoparticles can avoid homogeneity and compatibility problems between the two phases

and thus improve the mechanical properties of the composite (Bikiaris, 2006). Another interest in nanoparticles modification is to enable their self-organization.

Functionalization by using organic groups is still a relatively unexploited possibility; however, simple organic groups may be sufficient to protect nanoparticles against agglomeration. Unmodified silica nanoparticles were used to improve the mechanical properties of poly (ethylene 2, 6 – naphthalate) (PEN) (Bikiaris, 2006). However, the mechanical properties of the unmodified silica nanoparticle-reinforced composites tended to be worse than those of pristine (PEN). A major problem of such materials is the non-uniformity of the resulting properties attributed to the poor dispersion of the filler in the polymer matrix, and to adhesion occurring at the polymer-filler interface (Yang and Nelson, 2004). The mechanical properties were only improved after surface modification of the silica nanoparticles using stearic acid. Surface modification of the silica nanoparticles led to an increase in Young's modulus of the samples because of the improvement in adhesion between the silica nanoparticles and the PEN matrix.

Bikiaris (2006) prepared isotactic polypropylene (IPP)/silica nanocomposites by melt blending. The silica nanoparticles were first treated with dimethyldichlorosilane so that silica nanoparticles could be more compatible with IPP polymer matrix.

Rong *et al.* (2001) presented experimental results for epoxy/TiO₂ nanocomposites, indicating that the wear performance significantly depends on the dispersion state. The compatibility between nanoparticles and polymer matrix must be considered as a very important factor to obtain polymeric materials with the desirable properties.

Yang and Nelson (2004) successfully prepared PMMA/silica nanocomposites by solution polymerization and found that the nanoparticle-doped materials exhibited better mechanical properties when the nanoparticles size decreased or the nanoparticles surface was modified. Calcium carbonate (CaCO₃) nanoparticles were surface modified using stearic acid and an anionic surfactant in order to improve their dispersion in a polymeric matrix, thus the mechanical properties of the corresponding nanocomposite coating.

2.4 BIODEGRADABLE POLYMERS

In recent years, there has been a marked increase in interest in biodegradable materials for use in agricultural, medicine, packaging, and other areas. In particular, biodegradable polymer materials (known as biopolymers) are of interest to many researchers. Since polymers form the backbone of plastic materials, they are continually being employed in an expanding range of areas. As a result, many researchers are investing time into modifying traditional materials, to make them user-friendly and to design novel polymer composites out of naturally occurring materials (Kolybaba *et al.*, 2003). Biodegradable polymers are plastics obtained from renewable resources synthesized from petroleum-

based chemicals, and which can be degraded by microorganisms. They are capable of undergoing decomposition when exposed to environmental conditions (Mohanty *et al.*, 2002). Polymer materials are classified into three primary classes, which define their degradation behaviour. The first class is the conventional plastics, that are resistant to degradation when disposed into the natural environment. The resistance to degradation is due to their impenetrable petroleum based matrix, which is reinforced with carbon or glass fibres and it is unable to be consumed by microorganisms. The second class of polymer materials are partially degradable. The production of these materials typically includes naturally produced fibres with a traditional matrix. When exposed to environmental conditions, microorganisms are able to consume the natural macromolecules within the plastic matrix, leaving the matrix weakened with rough and open edges, resulting in further degradation. The final class of polymer materials is completely biodegradable; the polymer matrix is derived from natural resources such as starch or microbial grown polymers, and their reinforcement is produced from common crops such as flax, kenaf or hemp. According to the American Society for Testing of Materials (ASTM), biodegradable polymers are defined as those that undergo a significant change in chemical structure under specific environmental conditions (Kolybaba *et al.*, 2003), such as photodegradation, hydrolysis, oxidation and microbial-induced chain scission, leading to mineralization which alters the polymer during the degradation process. They are capable of undergoing decomposition primarily through the enzymatic action of microorganisms (fungi,

algae, bacteria, etc.) into CO₂, methane, biomass or inorganic compounds in a specified period of time (Mohanty *et al.*, 2000).

Avérous and Boquillon (2004) presented the classification of biodegradable polymers in different families (Figure 2.1). Except for the fourth family, which is of fossil origin, most biodegradable polymers are obtained from renewable resources (biomass). The first family are the agro-polymers (polysaccharides), obtained from biomass by fractionation. The second and third families are polyesters obtained by fermentation from biomass or from genetically modified plants or synthesized from monomers obtained from biomass. The fourth families are polyesters that are totally synthesized through petrochemical processes from fossil resources.

Figure 2.1: Classification of biodegradable polymers. (Avérous, and Boquillon, 2004)

2.4.1 Degradation of biopolymers by microorganisms

Biodiversity and occurrence of polymer-degrading microorganisms vary depending on the environment, such as soil, sea, compost, and activated sludge (Avérous and Le Digabel, 2006). It is necessary to investigate the distribution and population of polymer-degrading microorganisms in various ecosystems.

Generally, the adherence of microorganisms on the surface of plastics, followed by the colonization of the exposed surface, is the major mechanism involved in the microbial degradation of plastics (Kozłowski and Władyska-Przybylak, 2008). The enzymatic degradation of plastics by hydrolysis is a two-step process (Kozłowski and Władyska-Przybylak, 2008): (i) the enzyme binds to the polymer substrate then subsequently catalyzes a hydrolytic cleavage. Polymers are degraded into low molecular weight oligomers, dimers, monomers and finally mineralized to CO_2 and H_2O ; (ii) the clear zone method with agar plates is a widely-used technique for screening polymer degraders and for assessment of the degradation potential of different microorganisms on a polymer. Agar plates containing emulsified polymers are inoculated with microorganisms and the presence of polymer-degrading microorganisms can be confirmed by the formation of clear halos around the colonies. This happens when the polymer-degrading microorganisms secrete extracellular enzymes which diffuse through the agar and degrade the polymer into water-soluble materials. Through several studies, researchers investigated the population of aliphatic polymer-degrading microorganisms in different ecosystems, and the degradation order was found to be as follows: PHB > PCL > PBS > PLA where, poly(3-hydroxybutyrate) = (PHB), poly(ϵ -

caprolactone) = (PCL), poly (butylenesuccinate) = (PBS) and poly(lactic acid) = (PLA) (Tokiwa *et al.*, 2009, Cheung *et al.*, 2008).

2.4.2 Factors affecting the biodegradability of biopolymers

Biopolymers were originally designed for the packaging and farming sector, because they were not suitable to be used as matrices in biocomposites. In particular, they show either too high values of elongation at failure, or their rheological behaviour is a strong restriction for application in biocomposites (Tokiwa *et al.*, 2009). The performance limitation and high cost of biopolymers are major barriers for their widespread acceptance as substitutes for traditional non-biodegradable polymers. The high cost of biopolymers compared to traditional plastics is mainly attributed to the low volume of production rather than the raw material costs for biopolymers synthesis. However, biopolymers are now of interest due to the current environmental threat and social concerns. New applications for these bio-based materials will result in increased production of biocomposites (Tokiwa *et al.*, 2009). The development of biodegradable polymers is challenging in view of the fact that such materials should be stable during storage and usage, and should degrade once disposed of after their intended lifetime. Bioplastic modifications are applied to make the polymer a suitable matrix for composite applications.

2.4.3 Environmental Impacts of Biopolymers

Engineers are attempting to integrate environmental considerations directly into material selection processes, in order to respond to an increased awareness of the need to protect the environment. The use of renewable resources in the production of polymer

materials achieves this in two ways (Tokiwa *et al.*, 2009). First of all, the feedstocks being employed can be replaced, either through natural cycles or through intentional intervention by humans. The second environmental advantage of using renewable feedstocks for biopolymer development is the biodegradable nature of the end products, thereby preventing potential pollution from the disposal of the equivalent volume of conventional plastics. At the end of their useful period, biopolymer materials are generally sent to landfills or composted. Recycling of plastic materials is encouraged and well-advertised, but attempts at expanding this effort have been less than effective. In the United States, currently less than 10% of plastic products are recycled at the end of their useful life (Fowler *et al.*, 2006). Recycling must be recognized as a disposal technique, not a final goal for material development. A complacent attitude regarding recycling processes ignores the fact that advanced infrastructure is needed to properly house recycling. As discovered, in underdeveloped countries plastics are almost completely recycled, as the return on investment is positive in their economic situation. This appears to be positive at the onset, but the open systems by which the plastics are recycled allow the emission of toxic gases at crucial levels.

2.5 BIOCOMPOSITES FROM RENEWABLE RESOURCES

Biocomposites are composite materials comprising of biodegradable polymers as the matrix material and biodegradable fillers, usually bio fibres/particles (Fowler *et al.*, 2006). Natural fibres/particles, such as cotton, flax, hemp, kenaf etc. or fibres from recycled wood or waste paper, or even by-products from food crops are examples used for the production of biocomposite materials (Fowler *et al.*,

2006). Hence composites made with natural fibres/particles are known as “green composites”. In contrast to synthetic polymer composites, biocomposites have polymer matrices ideally derived from renewable resources such as vegetable oils or starches. Polymer matrices from renewable resources are becoming attractive alternatives, due to their abundance, availability, renewability and relatively low cost (Guduri *et al.*, 2006). Various biodegradable polymers have been used for the matrix such as polyesters (polyhydroxybutyrate (PHB)) or starch (polysaccharides). Incorporating biopolymers with natural fibres/particles is a promising solution to replace conventional composites because they are environmentally friendly (Guduri *et al.*, 2006).

Biodegradable matrices are available commercially in large numbers and exhibit a wider range of properties. At present, they can compete with non-biodegradable matrices in different industrial fields (packaging, agricultural products and cutlery) (Guduri *et al.*, 2006). In this wider range, there also are the lignocellulose-based fibres/particles used as biodegradable fillers. These fibres/particles have a number of significant mechanical and physical properties. These attractive properties also motivate more and more industrial sectors (e.g. structural and automotive parts, building materials) to replace commonly used glass fibre with natural fibres, because they are of low cost and composites made from them are expected to be lightweight (Le Duigou *et al.*, 2008). With their environmentally friendly character and some economic advantages, investigations of biocomposite materials have not only been a challenge to materials scientists, but their use has

also been an important provider of opportunities to improve the standard of living of people around the world (Mehta *et al.*, 2004).

Biocomposites materials provide a competitive advantage over glass-reinforcement composites in many applications. They can contribute to economic improvements, such as new agricultural activities and environmental issues. Several critical issues related to biofibres/particles are (i) surface treatment to make it a suitable reinforcing filler for composite application, (ii) their hydrophilic properties, which may affect the properties of the biocomposite material, and (iii) the development of appropriate processing techniques, depending on the type of fibre form (chopped, non-woven/woven fabric, yarn) (Biagiotti *et al.*, 2004).

2.5.1 Applications of bio-based materials

Recent work on biocomposites reveals that in most cases the specific mechanical properties of biocomposites are comparable to widely used glass fibre reinforced plastics. Various complex structures, i.e., tubes, sandwich plates and car door interior panelling have been made from biocomposites (Biagiotti *et al.*, 2004). Starch-based materials based on recycled fibres are currently used in the packaging industry for boxes and other rigid packing media (Mohanty *et al.*, 2002). The use of natural fibres as reinforcement has grown significantly in the automotive and aerospace industries. This is due

to the hollow structure of natural fibres that provides a better insulating property against noise and heat (Mohanty *et al.*, 2002). Mostly these fibre/particle reinforced biocomposites are used for the door or ceiling panels, and panels separating the engine and the passenger compartment. They are usually applied in formed interior parts because these components do not need load bearing capacity, but dimensional stability is important. Biobased vehicles are lighter, making them a more economical choice for consumers. They reduce fuel cost (Mohanty *et al.*, 2002). They exhibit a favourable non-brittle fracture on impact, which is an important requirement in the passenger compartment. In addition to the components for the interior design of motor vehicles, they find use in panelling railway, cars and aircraft. It is also important for these composites to be flame resistant (Herrmann *et al.*, 1998).

2.6 POLY (LACTIC ACID)

Poly(lactic acid) (PLA) is a class of crystalline biodegradable thermoplastic polymer with relatively high melting point and excellent mechanical properties. PLA has been highlighted because of its availability from renewable resources such as corn and sugar beets (Garlotta, 2002). PLA is synthesized by the condensation polymerization of D- or L-lactic acid or ring-opening polymerization of the corresponding lactide (Zhao *et al.*, 2008). Under specific environmental conditions, pure

PLA can degrade to carbon dioxide, water and methane over a period of several months to two years, a distinct advantage compared to other petroleum plastics that need much longer periods. Advanced industrial polymerization technologies have been developed to obtain high molecular weight pure PLA, which leads to a potential for structural materials with enough lifetime to maintain mechanical properties without rapid hydrolysis (Fang and Hanna, 1999).

The final properties of PLA strictly depend on its molecular weight and crystallinity. PLA has been extensively studied as a biomaterial in medicine, but only recently it has been used as a polymer matrix in composites. In fact, PLA resins are nowadays marketed for different applications. In 2002, Cargill-Dow LLC started up a commercial PLA plant, with the aim of producing PLA fibres for textiles and nonwovens, as well as PLA films for packaging applications and rigid containers (Huda *et al.*, 2005).

PLA consists of lactic acid as the basic constitutional unit. It is manufactured by carbohydrate fermentation or chemical synthesis (Huda *et al.*, 2005). Lactic acid (2-hydroxy propionic acid) is a hydroxy acid with an asymmetric carbon atom and exists in two optically active configurations, the L (+) and D (-) isomers. In general, lactic acid can be manufactured from petroleum-based sources or from a renewable source such as glucose and maltose from corn or potato, sucrose from cane or beet sugar etc. Chemical structure of PLA is shown in Figure 2.2.

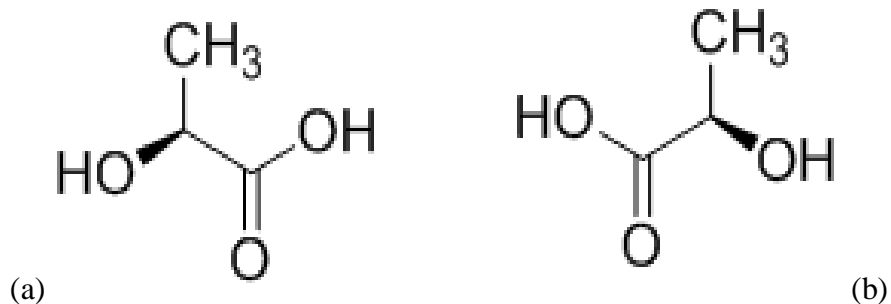


Figure 2.2: Chemical structure of (a) L-lactic acid, D-lactic acid and (b) polylactic acid (PLA) (Bax and Mussig, 2008).

In addition to its biodegradable character, other advantages of PLA polymer are biocompatibility, availability from renewable resources, non-toxic byproducts, metabolization or mineralization of biodegradable byproducts and chance to cover a large range of properties through copolymerization or blending (Bax and Mussig, 2008).

Depending on the synthesis route and the chiral monomer(s) used, the resulting distribution of chiral repeating units can be very different. The use of cyclic dimer (lactide) together with controlled residence time, temperature and catalyst type used, makes it possible to control the ratio and sequencing of D- and L-lactic acid units in the final polymer (Huda *et al.*, 2008). The optical components of the polymers significantly affect crystallization kinetics and the ultimate extent of crystallinity. PLA derived from greater than 93% L- or D-lactic acid can be semi-crystalline whereas PLA containing greater than 7% of the second isomer is found to be amorphous (Huda *et al.*, 2005). This second isomer acts as an impurity leading to the introduction of twists in the otherwise regular polymer molecular architecture. The molecular imperfections result in a decrease in both the rate and extent of PLA crystallization. Garlotta (2002) have reported that the glass transition temperature, T_g , is determined by the proportion of different lactides present, which results in PLA polymers with a wide range of stiffness and hardness values. Table 2.4 gives the physical

properties of PLA (98%L-lactide), PLA (94%L-lactide), polystyrene (PS) and polyethyleneterephthalate (PET).

Table 2.4: Physical properties of PLA (98% L-lactide), PLA (94% L-lactide), PS and PET.

Sample	PLA (98% L-lactide)	PLA (94% L-lactide)	PS (atactic)	PET
T _g (°C)	71	66	100	80
T _m (°C)	160-170	140-150	-	240-245
Enthalpy of fusion (J. g ⁻¹)	37.5	21.9	-	47.7
% Crystallinity	40	25	-	38

Source: Garlotta (2002)

2.6.1 Modification of PLA

The major drawbacks of PLA limiting its applications are its poor chemical modifiability and mechanical ductility, slow degradation profile, and poor hydrophilicity. In order to be suitable for specific biomedical applications, the PLA has been modified mainly concerning two aspects: Bulk properties and surface chemistry. To achieve this, both chemical modification and physical modification have been tried, involving the incorporation of functional monomers with different molecular architectures and compositions, the tuning of crystallinity and processibility via blending and plasticization, etc., Polymer blending is an effective, simple, and versatile method to develop new materials with tailored properties without synthesizing new polymers (Peesan *et al.*, 2005). The properties of different polymers (biodegradable and non-biodegradable) can be combined by blending with PLA, or even new properties can arise in the products due to interactions between the components. Biodegradable components blended with PLA include polyethylene glycol (PEG), poly-

hydroxybutyrate)(PHB), polycaprolactone(PCL), polybutylene adipate-co-terephthalate(PBAT), chitosan, and starch (Sheth *et al.*, 1997). While blends of PLA and non-biodegradable polymers have not been as extensively studied low-density polyethylene(LDPE), poly(vinyl acetate)(PVA), and polypropylene(PP) have been examined. Reddy *et al.*, 2008 found that PLA in blends obtained from five ratios of PLA/PP had substantially better resistance to biodegradation and hydrolysis, and improved dyeability with dispersed dyes. However, most of these blends are immiscible (phase-separated) and display poor mechanical properties due to low interfacial adhesion between the polymer phases.

To improve the processing and mechanical properties of PLA without sacrificing its degradability and biocompatibility, Xu *et al.*, 2009 blended PLA with a new degradable thermoplastic derived from konjac glucomannan (TKGM), synthesized by graft copolymerization of vinyl acetate and methyl acrylate onto konjac glucomannan (KGM).

The carboxyl and hydroxyl groups of PLA make it possible to copolymerize it with other monomers through polycondensation with lactone-type monomers such as caprolactone, which generally lead to low molecular weight copolymers, or alternately through ring-opening copolymerization of lactide with other cyclic monomers including glycolide, valerolactone, and trimethylene carbonate, as well as with monomers like ethylene oxide (EO) to produce high molecular weight copolymers.

The hydrophobicity and crystallinity of the copolymers can be increased for low to moderate comonomer contents. Besides, poly(ethylene oxide)(PEO) and PEG have been most commonly copolymerized with PLA to

prepare copolymers on account that it is highly biocompatible, hydrophilic and non-toxic, non-immunogenic and non-antigenic (Metters *et al.*, 2000). Such properties reduce protein adsorption and enhance resistance to bacterial and animal cell adhesion.

Di-block PLA-PEG copolymers and Tri-block PLA-PEG-PLA copolymers allow modulation of the biodegradation rate, the hydrophilicity, and the mechanical properties of the copolymers, while phase separation can be tailored with PLA-PEG multi-block copolymers of predetermined block lengths (Wang *et al.*, 2005).

Among numerous modifiers that have been researched, the excellent biocompatibility, biodegradability, non-toxicity and chain flexibility make the Polyethylene Glycol (PEG) a good choice for the modification for PLA, in either chemical way (e.g. the PLA-PEG block polymer) or physical way (the blend mixture). Usually, the PEG is used as the plasticizer to improve the mechanical properties of PLA. The phase miscibility, stability, and thermal properties of PEG-PLA materials have also been intensively investigated. On the other hand, as one of the most important properties of PLA, the degradability is an addressed concern in its modifications. Particular biological applications require either slow or fast degradation, especially in the biomedical field. For the PEG modification on PLA, the degradation property was also investigated, and a general conclusion is that PEG content will increase the degradation rate of PLA due to its flexibility, hydrophilicity and wettability to degrade in aqueous environment.

2.6.2 Poly(lactic Acid (PLA) nanocomposites

The incorporation of nanoparticles in certain biodegradable matrices could significantly affect the crystallization behaviour, morphology, mechanical properties as well as biodegradation (Rhimet *et al.*, 2009). Also, water barrier and antimicrobial properties are very important characteristics when using biodegradable polymers for special purposes like packaging. For example, PLA nanocomposites based on different types of nanoclays such as Cloisite Na⁺, Cloisite 30B and Cloisite 20A are effective in improving the water vapour barrier properties and bacteriostatic function against certain microbes (Rhimet *et al.*, 2009).

Thenanocomposites based on PLA are of special interest for medical purposes. Special attention has been paid to novel nanomaterials capable of facilitating the biorecognition of anticancer drugs. For example, blending of titanium dioxide (TiO₂) nanoparticles and polylactide (PLA) nanofibres has been adopted as a new nanomaterial that lets drug molecules readily self-assemble on the surface of the nanocomposite (Rhimet *et al.*, 2009). These novel nanocomposites imply some potential valuable application as a kind of drug carriers in view of the respective good biocompatibility of PLA and large surface area of the nanoparticles (Song *et al.*, 2008).

Tissue engineering has become an alternative method to traditional surgical treatments for the repair of bone defects, and an appropriate scaffold supporting bone formation. For these purposes, special nano-sized demineralized bone powders with PLA were electrospun for engineering bone (Ko *et al.*, 2008). Electrospinning is known as a novel fabrication method to form nanofibrous scaffolds for tissue engineering application. Previously, many

natural biopolymers of protein have been electrospun. In some cases, the introduction of special components, like keratin or gelatin electrospun with PLA result in nanofibres that better adhere to the cells (Yuan *et al.*, 2008).

In some cases, the properties of nanocomposites depend on the intercalated or exfoliated structures. In order to improve the intercalated or exfoliated structures of the nanocomposites, twin-screw extrusion is usually employed. The effective increase of the binding force between the phases could be improved by the addition of compatibilizer. For example, in poly (lactic acid)/montmorillonite (PLA/MMT) nanocomposites prepared by twin-screw extrusion, the addition of polycaprolactone (PCL), as a compatibilizer, can improve the thermal properties (Yu *et al.*, 2008).

In order to improve the thermal and mechanical properties of the biodegradable matrix sometimes it is necessary to modify nanosized particles. In PLA/nanosized calcium carbonate (CaCO_3) composites, calcium stearate was used as a modifier to improve the adhesion between the CaCO_3 particles and the PLA matrix. The tensile strength and modulus values of the composite could be improved greatly without a significant loss in the elongation at break when the nanosized CaCO_3 was incorporated up to 30% wt (Kim *et al.*, 2008).

Nanotubes are nowadays commonly used in nanocomposites. In some cases, these nanofillers could form a conductive network structure in an appropriate polymer matrix, which is the key for liquid sensing. Liquid sensing properties have been identified in PLA/multi-walled carbon nanotube

(MWCNT) composites. Very interesting properties, like changing the electrical properties upon solvent contact have been observed (Kobashi *et al.*, 2008).

Multi-walled carbon nanotubes (MWCNTs) are usually functionalized to achieve their better dispersion within the polymer matrix. Both the dispersion state and the surface functionalization of MWCNTs are very important for the thermal stability of the biopolymer. Different functionalities of the MWCNTs could have a different effect on the dispersion and therefore on the thermal stability of the nanocomposites (Wu *et al.*, 2008). MWCNTs are used in many cases to achieve high electrical conductivity at low carbon nanotube loadings. When only 0.5 parts per hundred part of resin (phr) modified multi-walled carbon nanotubes are added to low-crystalline PLA, the surface resistance of the composite could fall by 10-13 order. The effect is usually realized due to the enhanced MWCNT dispersion by covalent or hydrogen bonding between the modified multi-walled carbon nanotube and PLA. The degree of crystallinity of PLA can influence the electrical property of MWCNT/PLA composites apparently as well (Kuan *et al.*, 2008).

2.7 Hydrophilic Character of Natural Fibres/Particles

Shortcomings associated with natural fibres/particles have to be overcome before using them in composites reinforcement. The most serious concerned problem with natural fibres is its hydrophilic nature, which causes the fibre/particles to swell and ultimately rotting takes place through an attack by fungi. Natural fibres are hydrophilic, is that they are derived from lignocellulose, which contains strongly polarized hydroxyl

groups. The major limitations of using these fibres as reinforcement in matrices include poor interfacial adhesion between polar-hydrophilic fibre and non-polar-hydrophilic matrix; difficulty in mixing because of poor wetting of the fibre with the mixture; and the high moisture absorbance of the fibres. To reduce the moisture absorption, the fibre has to be changed chemically and physically through fibres pretreatments.

Mercerization leads to fibrillation which causes the breaking down of the composite fibre bundle into smaller fibres. Mercerization reduces fibre diameter, thereby increases the aspect ratio which leads to the development of rough surface topography that results in better fibre-matrix interface connection and an increase in mechanical properties (Joseph *et al.*,2000). Moreover, mercerization increases the number of possible reactive sites and allows better fibre/particles wetting. Mercerization has an effect on the chemical composition of fibres/particles, degree of polymerization and molecular orientation of the cellulose crystallites due to cementing substances like lignin and hemicellulose which were removed during the mercerization process. Several workers have performed work on alkali treatment (Joseph *et al.*, 2000 and Mishra *et al.*, 2003) and reported that mercerization leads to an increase in the amount of amorphous cellulose at the cost of crystalline cellulose and the removal of hydrogen bonding in the network structure.



2.8 SOLID FILLERS

Almost any solid can be used in a polymer as filler given that the particle size and adhesion of the matrix are suitable and there is an opportunity to improve the sustainability of the composite. The original purpose of filling polymers was to lower the

cost of moulded compounds, but of increasing importance is a selective modification of properties or the formation of completely new materials using traditional fillers and reinforcements (De Silva *et al.*, 2002).

The different particulate and fibrous materials that have been tested for their suitability in sustainable materials are listed in Table 2.5. This table highlights the extensive range of materials used to manufacture composites that are sustainable, biodegradable or composite that simply utilizes waste materials. It also shows that almost any material has the potential to be used in these composites, given that it is a sustainable source and imparts desirable properties on the final product. Fillers not covered in Table 2.5 include traditional particulate and fibrous materials, such as calcium carbonate, talc, glass fibres and other synthetic polymer fibres. They are not considered novel approaches to achieve sustainability or as a pathway to re-use other materials. These materials may, however, be included in some applications in addition to materials listed in Table 2.5.

Table 2.5: Solid used as fillers or reinforcement

Particle	Fibres
Cork (Hernandez <i>et al.</i> 1999)	Weeds (Kalita <i>et al.</i> 1999)
Blast furnace slag (Savastano <i>et al.</i> 1999)	Old newsprint (Nada <i>et al.</i> 1999)
Sand (Zahran 1998)	Wheat straw (Mo,2003, Han1998, Patil, 2000, Nemil,2003 and Parker, 1997)
Waste rubber powder (Kim <i>et al.</i> 2000)	Read straw (Han <i>et al.</i> 1998)
Microcrystalline starch (Dufresne <i>et al.</i> 1998)	Banana, hemp and sisal fibres (Mishra, 2000 and Siriardena, 2001)
Mineral fillers (Haworth <i>et al.</i> 2001)	Rice husk ash (Siriardena <i>et al.</i> , 2001)
Minerals waste (D'Almied <i>et al.</i> 2002)	Rice husk (Mishra, 2000 and Nemil, 2003)
Recycled urea-formaldehyde resin (Bliznakov <i>et al.</i> 2000)	Jute fibre felt and fabric (Deng, 2002 and Nemil, 2003)
Lignin (Casenave <i>et al.</i> 1996)	Coffee husk (Bisanda <i>et al.</i> 2003)
Polymer waste, powder rubber, Tire rubber, tire fibres,	Coconut fibre (Mishra <i>et al.</i> 2000)
Milled electrical wire (Bignozzi <i>et al.</i> 1999)	Bamboo strips and mats (Nemil <i>et al.</i> 2003)
Fly ash (Guhanathan <i>et al.</i> 2001)	Vegetable fibres
Mixed waste plastic (Xanthos <i>et al.</i> 2002)	Wood flour (Wu <i>et al.</i> 1999)
Waste leather particles (Andreopoulos <i>et al.</i> 2000)	Leaf fibre residue of sugar beet (Das 2000)
Industrial waste from zinc plant (Rodelheimer <i>et al.</i> 2001)	Cane bagasse pith (Mishra <i>et al.</i> 2003)
Coir pith (Viswanathan <i>et al.</i> 1999, Viswanathan <i>et al.</i> 2000)	Sawdust
Oil palm wood flour (Ismail <i>et al.</i> 1999)	Cane bagasse (Patil, 2000 and Nemil, 2003)
Waste of tea leaves (Yalinkilic <i>et al.</i> 1998)	Agave bagasse (Iniguez-Covarrubias <i>et al.</i> 2001)
	Kiwi prunings (Nemil <i>et al.</i> 2003)
	Groundnut shells (Nemil <i>et al.</i> 2003)
	Cotton (Nemil <i>et al.</i> 2003)
	Maize husk and cob (Nemil <i>et al.</i> 2003)

Source: Verbeek and Pickering (2007).

2.9 GROUNDNUT SHELL

Groundnut (*Arachis hypogaea L*) also known as peanut, is one of the world's principal oil seed crops. Groundnut originated from South America but is now widely cultivated throughout the tropical, sub-tropical and the warm temperate areas. Groundnut is put to many uses. It is an economic crop. The haulms are an important fodder for livestock, especially, sheep and goat and in particular ram. The plant, through its biological activities nitrogen fixation, is an important soil fertility conserver. The nuts are consumed roasted, boiled or as confectionary, snack nuts, peanut butter or in cookies. The nut is crushed to produce oil which is principally used for cooking (Onuegbu *et al.*, 2013). But is also used for other industrial purposes such as; pharmaceuticals as carrier, cosmetics. It is also used for the production of margarine. The by-product, meal (cake) is used for both human and livestock consumption.

Groundnut in Nigeria, as in other major producing areas, is largely a smallholder crop, grown under rainfall conditions in semi-arid areas. Although it is grown in commercial farms in America and Europe, the developing countries, with their small-scale production, account for over 95 and 94 percent of world groundnut area and production respectively (Onuegbu *et al.*, 2013). Production is concentrated in Asia and Africa. Asia accounts for 60 and 70 percent of world area and product respectively. India (35% area 28% production) and China (17% area, 34% production) are the major producers in Asia. Africa accounts for 35 percent of the global area but only 21 percent of the production. The major producers in Africa are Senegal, Nigeria and Sudan. The other major world producers are USA and Argentina.

Nigeria is one of the foremost producers of groundnut in the world, producing up to about 2.699 million metric tonnes in 2002 and 1.55 million metric tonnes in 2008. Groundnut shell is found in large quantities as agricultural farm wastes in Northern parts of Nigeria such as Sokoto, Kebbi, Zaria, Borno and Yobe States (Onuegbu *et al.*, 2013).

Groundnut shell is a byproduct of groundnut processing industry. In Nigeria and many other neighbouring countries, in addition to industrial extraction of oil, groundnut is consumed directly as nut fresh, dry or cooked. It is also grown as a cash crop for export. Groundnut shell is a waste produced when the nut is being processed for consumption by breaking the shell open manually or mechanically. In Nigeria, the shell is abundantly available from May to October(Rajuet *al.*, 2012). The shell, though sometimes heaped and burnt, are usually just left lying around in unsightly, rotting, smelly heaps, thus constitute an environmental pollution problem. For now, groundnut shell could be very cheap because, being a waste, the only costs would be those of gathering, processing and transporting to points of use.

Over the years, groundnut shell constitutes common solid waste especially in the developing part of this world. It's potential as a useful engineering material has not been investigated. The utilization of Groundnut shell will promote waste management at little cost, reduce pollution by these wastes and increase the economic base of the farmer when such waste is sold thereby encouraging more production(Raju *et al.*, 2012).

2.10 DESIGN OF EXPERIMENTAL TECHNIQUE

In an experiment, we deliberately change one or more process variables (or factors) in order to observe the effect which the changes have on one or more response variables. The (statistical) Design of Experiments (DoE) is an efficient procedure for

planning experiments so that the data obtained can be analysed to yield valid and objective conclusions. In other words, an experimental design is the laying out of a detailed experimental plan. A well-chosen experimental design maximizes the amount of information that can be obtained for a given amount of experimental effect. There are several designs that are in use in the design of experiments such as incomplete block designs, Youden square designs, lattice square designs, Taguchi designs, fractional factorial designs, Graeco-latin square designs, split-plot designs, covariance design or time-series, factorial designs, Plackett-Burman design, etc. According to Ben-Gal *et al.* (2008), among the several experimental design methods, Taguchi method has made valuable contributions to statistics and engineering.

Genichi Taguchi emphasis on loss to society techniques for investigating variation in experiments, and his overall strategy of the system, parameter and tolerance design have been influential in improving manufactured quality products worldwide. It reduces testing cycle time and analysis is simple. Although some of the statistical aspects of the Taguchi methods are disputable, there is no dispute that they are widely applied to various processes. A quick search at World Wide Web reveals that the method is being successfully implemented in diverse areas, such as optimization of communication and information network, development of electronic circuits, laser engineering of photomasks, cash-flow optimization in banking, policy making, runway utilization improvement in airports and even robust eco-design. The approach provides complete interaction information than typical fractional factorial design (Ben Gal *et al.* 2008).

2.10.1 Taguchi Design Method

Taguchi approach to parameter design provides the design engineer with a systematic and efficient method for determining near optimum design parameter for performance and cost. The first concept of Taguchi is what he refers to as “noise factor”. Noise factors are viewed as the cause of variability in anything that causes a measurable product or process characteristics to deviate from its target value (Ben Gal *et al.* 2008).

Target values may be (Ben Gal *et al.* 2008):

Smaller is better: Chosen when the goal is to minimize the response.

The S/N ratio can be calculated as given in equation (2.1) for smaller the better:

$$S/N = -10 \log_{10} \left(\frac{1}{n} \sum_{i=1}^n y^2 \right) \quad (2.1)$$

The larger the better: Chosen when the goal is to maximize the response.

The S/N ratio is calculated as given in equation (2.2) for large the better

$$S/N = -10 \log_{10} \left(\frac{1}{n} \sum_{i=1}^n \frac{1}{y^2} \right) \quad (2.2)$$

Nominal is better: Chosen when the goal is to target the response and it is required to base the S/N ratio on standard deviation only. The S/N ratio is calculated as given in equation (3.4) for normal the better.

$$S/N = -10 \log_{10} \left(\frac{1}{n} \sum_{i=1}^n (y_1 - y_0)^2 \right) \quad (2.3)$$

Equations (2.1) to (2.3), y shows the measured value of each response and n is the number of runs. When variability occurs, Taguchi (1987) says this is because the physics active in the design and environment promote change. Noise factor can be classified into three groups: External noise factor, sources of variability that occurs from outside the product.

Unit -to- unit noise due to the fact that no two manufactured components or products are ever exactly alike and internal noise due to deterioration, ageing and wear incurred in storage and use.

The objective is to select the best combination of control parameters so that the product or process is noise robust with respect to the noise factor. Taguchi method utilizes orthogonal arrays from the design of experiments theory to study a large number of variables with a small number of experiments. Using orthogonal arrays significantly reduces the number of experimental configurations to be studied.

Before selecting a particular orthogonal array (OA) to be used for conducting the experiments, these points must be considered (Roy, 1990).

- i) The number of parameters and interaction of interest.
- ii) The number of levels for the parameters of interest

The non-linear behaviour, if exist, among the process parameters can only be studied if more than two levels of the parameters are used (Roy, 1990).

Furthermore, the conclusion drawn from small-scale experiments are valid over the entire experimental region spanned by the control factor and their settings (Taguchi, 1987).

2.11 PREVIOUS WORKS

Yew *et al.* (2005) prepared and examined composites consisting of PLA, rice starch (RS) (0-50 wt.%) and epoxidized natural rubber. They concluded that incorporation of 20wt.% rice starch achieves a good balance of strength and stiffness. Incorporation of epoxidized natural rubber remarkably increase the tensile strength and elongation at break of the PLA/RS composites, owing to the

rubber elastomeric behaviour and its compatibilization effect, and enhanced composites biodegradability when exposed to water and α -amylase enzymatic treatment.

Oksman *et al.* (2003) studied the processing and material properties of PLA/flax fibre composites having flax fibre content of 30 and 40 wt.% and compared them to the more commonly used PP/flax fibre composites. Preliminary results showed that the composite strength is about 50% better when compared to similar PP/flax fibre composites.

Lee *et al.* (2006) investigated the effect of lysine-based diisocyanate (LDI) as a coupling agent, on the properties of bio-composites from poly(lactic acid) and bamboo fibre (BF). Tensile properties, water resistance, and interfacial properties were enhanced.

Serizawa *et al.* (2006) developed high-performance composites (PLA/kenaf fibre and PLA/kenaf fibre/flexibilizer) with good practical characteristics for housing material of electronic products, in comparison with petroleum-based plastics used in housing, such as glass fibre reinforced acrylonitrile-butadiene-styrene (ABS) resin. Adding kenaf fibre to PLA greatly increased its heat resistance (distortion temperature under load) and modulus and also enhanced its crystallization, so the ease of moulding of this material was improved. They concluded that elimination of short particles from kenaf fibres improves its effect on the impact strength, comparable to the effect of glass fibre. Furthermore, by adding a flexibilizer (a copolymer of lactic acid and aliphatic polyester) composite strength was improved.

Huand Lim (2007) fabricated hemp fibre reinforced PLA biodegradable composites and concluded that the composite with 40 vol.% of alkali treated fibre possesses the uppermost mechanical properties.

Ogata *et al.* (2006) in their study prepared nanocomposites using polylactic acid (PLA). PLA/ organically modified clay (OMLS) blends were made by dissolving the polymer in hot chloroform in the presence of dimethyl distearyl ammonium modified MMT (2C18MMT). X-ray diffraction results of PLA/MMT showed that the silicate layers forming the clay could not be intercalated in the PLA/MMT blends when prepared by the solvent-cast method. The clay existed in the form of tactoids with several stacked silicate monolayers. The formation of geometrical structures in the blends was attributed to the tactoids, which led to the formation of superstructures in the thickness of the blended film. This could lead to a structural feature that promotes an increase in Young's modulus of the hybrid.

Oksman *et al.* (2003) incorporated cellulose fibres as reinforcement in PLA. Due to the brittle nature of PLA, triacetin was used as a plasticizer for the matrix as well as PLA/flax composites in order to improve the impact properties. Plasticizers can be used during processing in order to lower the viscosity of the matrix polymer, which can then facilitate better fibre dispersion within the matrix polymer. Fibre dispersion is a critical factor to be considered during the development of biodegradable natural fibre composites.

Shibata *et al.* (2003) evaluated the use of short abaca fibres in the development of biocomposites using biodegradable polyesters. It was shown that strength and modulus increase with decreasing fibre diameter for both untreated and treated abaca fibre.

Mathew *et al.* (2005) conducted a study towards developing PLA based high-performance nanocomposites using microcrystalline cellulose as reinforcement. The study was concerned with achieving the best possible outcome for dispersion of the MCC

within PLA during processing. Comparisons were also made using wood flour and wood pulp as an alternative reinforcement for PLA.

Tzerki *et al.*(2006) investigated the usefulness of lignocellulosic waste flours derived from spruce, olive husks and paper flours as potential reinforcements for the preparation of cost-effective bio-composites using PLA as the matrix.

Petinakis *et al.*(2009) studied the effect of wood-flour content on the mechanical properties and fracture behaviour of PLA/wood-flour composites. The results indicated that enhancements in tensile modulus could be achieved, but the interfacial adhesion was poor. Therefore, it can be seen that incorporation of lignocellulosic materials into biodegradable polymer matrices, such as PLA, has the effect of improving mechanical properties, such as tensile modulus. But the strength and toughness of these bio-composites are not necessarily improved. This can be attributed to several reasons, such as the hydrophilic nature of natural fillers, compatibility with the hydrophobic polymer matrix can be problematic. In addition to the poor interaction between the phases, the hydrophilic nature of natural fibres leads to a tendency for fibres to mingle or form agglomerations, which can generally result in low impact properties, especially at high fibre loadings

Onuegbu *et al.*(2013) reported on Polypropylene composites of groundnut husk powder were prepared with filler contents of 0 to 40 wt. %. The particle sizes of the groundnut husk powder investigated were 0.2, 0.4, 0.6, 0.8, and 1.0 μm . The polypropylene composites were prepared in an extrusion moulding machine and the resulting composites were extruded as sheets. Some mechanical properties of the prepared composites determined using Instron testing machine and Izod impact tester respectively.

Presence of pulverized groundnut husk improved the tensile strength, modulus, flexural strength and impact strength of the composites and these properties increased with increase in filler contents and decrease in the filler particle size. The strain-at-break of the composites was however observed to decrease with increase in the filler contents, and particle sizes.

Nanocomposites of PLA with a compatibilizer and cellulose fibrils have been developed by Qu, *et al.*(1998). Bleached wood pulp was used as the fibre and commercial grade PLA as the matrix. A chemo-mechanical method was used to prepare cellulose nanofibrils dispersed uniformly in an organic solvent. Polyethylene glycol (PEG) was added to the matrix as a compatibilizer to improve the interfacial bonding/adhesion between the matrix and the fibre. The composites were obtained by solvent casting methods using N, N-Dimethylacetamide (DMAC) and characterized PLA reinforced with cellulose nanofibrils resulted in no improvement in tensile strength (30 MPa compared with pure PLA) and percent elongation (2.5% compared with pure PLA) of the composites. The authors attributed this to the poor interfacial bonding between cellulose nanofibrils and the PLA matrix. Addition of PEG to the blend of PLA resulted in significant improvement in tensile strength (28.2%) and percentage elongation (25%) compared to pure PLA. The authors posited that PEG covers the surface of the cellulose nanofibrils and act not only as a plasticizer for PLA to improve its elongation but also as a compatibilizer between the hydrophobic PLA and the hydrophilic cellulose nanofibrils. It was also evident that PEG also prevents the aggregation of the nanofibrils so that the cellulose nanofibrils disperse in the PLA matrix homogeneously to form a network structure. It was also noted by the authors that the optimum composition of cellulose

nanofibrils to obtain the best properties was 3% and above which tensile strength and percentage elongation decreased. The FT-IR analysis shows that PEG improved the intermolecular interaction, which is based on the existence of intermolecular hydrogen bonding among PLA, PEG, and cellulose nanofibrils.

Abdalla *et al.*(2013) design poly(lactic acid) multiwalled carbon nanotube nanocomposites (PLA/MWCNTs) using a simple fabrication technique. the PLA sheet was first dissolved in dichloromethane, and MWCNTs were subsequently added at various concentrations (0.5, 1.5 and 5%) while applying shear strain stirring to achieve dispersion of carbon nanotubes (CNTs). These solutions were then moulded and a hot press was used to generate sheets free of voids with free entrapped solvent. The results showed that a very good dispersion of MWCNTs in a PLA matrix could be observed. Further, the composite samples illustrated free of defects and voids, indicating that the hot press is capable of generating sufficiently compact polymer matrices. The investigation of the (fracture-) mechanical properties resulted in an increase of strength and Young's modulus at a nanotube content of both 0.5 and 1.5 wt%. Collectively, our results suggest that incorporation of CNTs as nano-fillers into biodegradable polymers may have multiple applications in many different sectors.

Goswami et al. (2013) studied three-components material systems (poly(lactic acid) (PLA), poly(ϵ -caprolactone) (PCL) and wollastonite (W)) in view of the possible application as a biomedical scaffold construct. Melt extruded PLA/PCL/W composites (PLCL15, PLCLW1, PLCLW4, PLCLW8 containing 0, 1, 4, 8 per hour filler respectively) are batch foamed using compressed CO₂ and the porous foams are studied for *in vitro* biocompatibility by seeding osteoblast cells. SEM images of the unfoamed

polymers show immiscibility in all compositions. Materials have been tested under compressive load using dry and wet conditions (using phosphate buffered saline at pH 7.4) for *in vitro* study. Contact angle measurement shows enhanced hydrophilicity in the composites changing from 80° in PLCL15 to 72° in PLCLW8. The foams are found to be microcellular (5–8 µm) in morphology showing quite a uniform pore distribution in the composites. The prepared foams, when studied as scaffold constructs, show osteoblast cell attachment and proliferation over the incubation period of 7 days. As expected, PLCLW8 containing the highest amount of CaSiO₃ supported maximum cell growth on its surface as visible from MTT assay data and SEM scans.

Fukushima *et al.* (2009) studied the PLA and PLA nanocomposites. Their study found that the degradation rates of PLA increased by adding nanoclays. The study also found that the clays can influence the polymer bacterial degradation depending on their chemical structure and affinity of the bacterium towards the clay.

Despite the availability of these studies, no investigation has been conducted on the application of the groundnut shell ash nanoparticles in polylactic acid composite materials. This work, therefore, reports for the first time the potential use of groundnut nanoparticles in reinforcing polylactic acid composites to the best of my knowledge. A relationship between the mechanical properties of the polymer composites and the process parameters was desirable to obtain the better understanding of the mechanical properties.

Finally, information based on utilization of PLA and waste groundnut shell generated in Nigeria for thermoplastic composite manufacturing is not available hence the need for this research work. Readily available information on the use of waste materials in

composites manufacturing will help industrialists in establishing industries that will provide employment.

CHAPTER THREE

3.0 MATERIALS AND METHODS

In this chapter, the detailed procedures and descriptions were given for the materials used, processing techniques employed and instruments used for preparation and characterization of samples. All the various experimental methods required to achieve the objectives of this research work were considered in detail. The Taguchi design method was also articulated.

3.1 MATERIALS

The Groundnut-shell was obtained from Oil Mill in Zaria city, Kaduna State, Nigeria (Plate 3.1). Polylactic acid biopolymer pellets were obtained from Dalian Zhonggang Chemical Products Co.Ltd, China. (Plate 3.2), The properties of the pure polylactic acid are shown in Table 3.1. Polyethylene glycol (PEG) of 100,000Mw was added to the matrix as a compatibilizer and was purchased from Sigma-Aldrich, South-Africa

Table 3.1 Properties of the Polylactic Acid (PLA) Resin Specification

Item	Standard	Unit	Values
Density	ISO1183	g/cm ³	1.18-1.2
Melting Point	DSC, 10°C/min	°C	110-120
Melt Flow Index	ISO1133	g/10min (190 °C,2.16kg)	≤10
Tensile Strength	ISO527	MPa	≥12
Elongation at Break	ISO527	%	≥180
Bending Strength	ISO178	MPa	≥4
Flexural Modulus	ISO178	MPa	≥100

Source: Dalian Zhonggang Chemical Products Co.,Ltd, China.



Plate 3.1: Typical Photograph of Groundnut shell



Plate 3.2: Photograph of the Polylactic acid pellets

3.2 EQUIPMENT

Equipment used in this research were: Digital Weighing Machine, Drying Oven, Vernier Caliper, Rockwell Hardness Testing Machine (Model 5023-A), Impact Testing Machine, Transmission Electron Microscope (TEM, Jeol, JSM2010), Micromeritics Surface Area Analyzer (ASAP 2020), X^oPertProPANalytical, LR 39487C X-Ray Diffractometer, Nanoparticle Size Analyzer (HORIBA LB 550), Perkin Elmer Spectrum 100 FT – IR Spectrometer, Planetary Ball Mill (Retsch, PM 400), Scanning Electron Microscope (JEOL 6480 LV), Fourier Transform Infrared Spectrometry (Perkin Elmer spectrum 100), Differential thermal Analysis (DTA) Machine. and Cone Calorimeter (Stanton Redcroft cone calorimeter).

3.3 METHODS

The methodology employed in this project work from the preparation of test samples to the final testing of mechanical properties are given in chronological order as follows:

3.3.1 Production of Groundnut Shell Ash Nanoparticles (GSAnps)

The groundnut shell was packed in a graphite crucible and heated in a controlled atmosphere muffle electric furnace at a temperature of 1200°C for 5hours to form groundnut shell ash particles (Plate 3.3). The groundnut shell ash was then fed into the high energy planetary ball mill (Appendix B, Plate B1). The objective of this milling was to reduce the groundnut shell ash particle size. The grinding jars of the planetary ball mill are arranged eccentrically on the sun wheel of the planetary ball mill. The direction of movement of the sun wheel was opposite to that of the grinding jars with speed in the ratio 1: -2. The grinding balls in the grinding jars were subjected to superimposed rotational movements, the so-called Coriolis forces. The difference in speeds between the balls and grinding jars produces an interaction between frictional and impact forces, that released high dynamic energies. The interplay between these forces produces the high and very effective degree of size reduction of the powder. The balls fell freely and impact the groundnut shell ash and balls beneath them. The kinetics of the process depends on the energy transferred to the powder from the balls during milling. In order to obtain the optimal milling time to produce the optimal particles size, the mechanical milling was done at a time of 2, 4, 6, 8 10 and 12hours. This milling time was chosen in accordance with the previous work by Fukushima *et al.*(2009).The milling was carried out at the speed of 300 rpm, with a ball to powder ratio of 10:1.

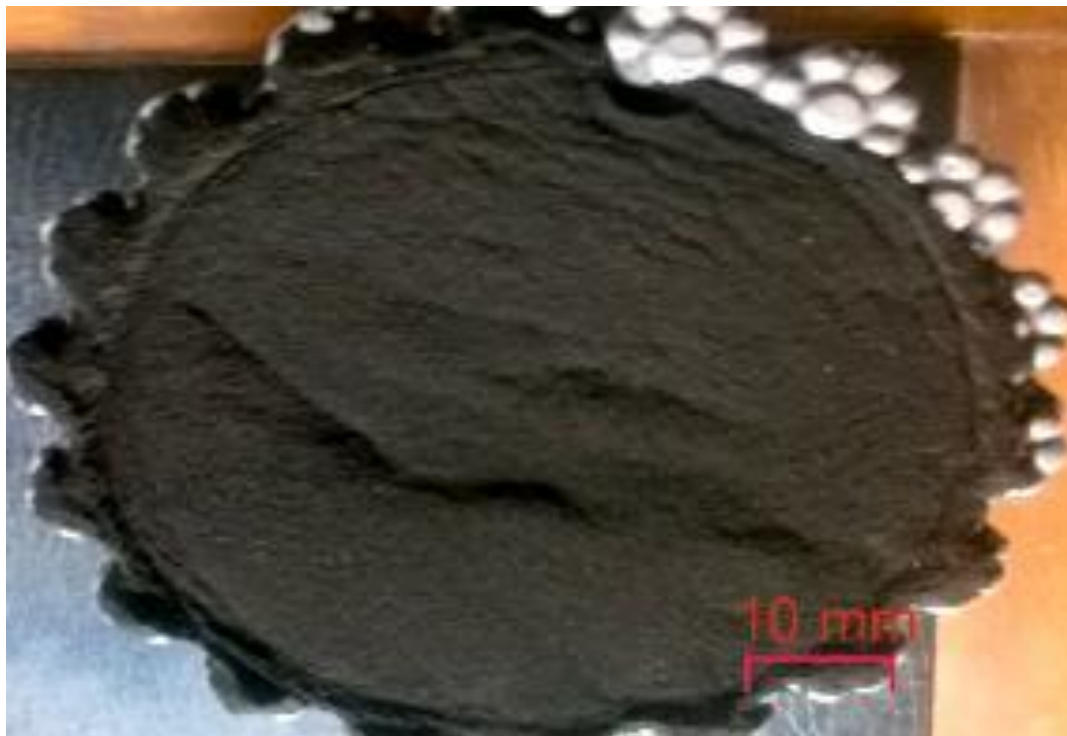


Plate 3.3: Photograph of the groundnut shell ash particles

3.3.2 Morphology and particles analysis of the Groundnut Shell Ash Nanoparticles (GSAnp).

The morphology and particle size determination of the GSAnp was carried out using Transmission Electron Microscopy (TEM), Brunauer-Emmett-Teller (BET) Surface Area Analysis, X-ray Diffractometer (XRD) analysis, Nanoparticle size analyzer and Fourier Transform infrared spectrometry (FTIR) analysis.

3.3.2.1 Transmission electron microscopy (TEM)

Particle size and morphology of GSAnp were examined by TEM (Jeol, JSM2010) at the Council for Scientific and Industrial Research (CSIR) Pretoria, South Africa using a 200 keV electron beam on the sample mounted on a carbon coated copper grid. With the assumption of spherical shape, the size of the particle was determined from the number

averaged particle radius. Ball milled nanoparticles sample (10mg) was sonicated for 3hours in isopropyl alcohol (5ml). The GSAnp suspension was taken using a dropper and spread on the carbon-coated copper grid and allowed to dry at room temperature. The copper grid was introduced into the instrument and the sample chamber was evacuated. The sample was scanned along the path of the electron beam and photograph of the sample was taken. The various sample produced using varied milling time were analyzed and the milling time that produced the smallest particles size was used in this research. The micrograph of the TEM is attached in Appendix B (Plate B.2).

3.3.2.2 Brunauer-Emmett-Teller (BET) Surface Area Analysis

Specific surface area of synthesized nanoparticles was measured by Nitrogen adsorption/desorption isotherms using ASAP 2020 Micromeritics Surface Area Analyzer at 196°C (Appendix B,Plate B.3). The specific surface areas were assessed according to the standard Brunauer- Emmett-Teller (BET) method. Samples were degassed in an oven at 110°C for 6 h and a five points BET analysis was conducted by using Quantachrome Autosorb-1 to obtain the specific area of the synthesized nanoparticles powder.

3.3.2.3 X-ray Diffractometer Analysis (XRD)

The X-ray diffraction (XRD) patterns of GSAnp samples were obtained by X-ray diffractometer using Cu K α radiation (40 kV, 40 mA)at Council for Scientific and Industrial Research (CSIR)Pretoria, South Africa. Stepwise increase for small angle was 0.01° over the range of 1 to 8° and wide angle rate of 1° 2 θ min⁻¹ over the range of 8 to 90° 2 θ respectively. Samples were prepared as thin layers on glass slides. The particle sizes of the samples were calculated employing the Scherrer equation (Mammeri *et al.*, 2003):

$$D = \frac{K\lambda}{\beta \cos \theta} \quad (3.1)$$

Where θ is the angle between the incident and diffracted beams, β the full width half maximum (rad.), D the particle size of the sample (nm) and λ is the wavelength of the X-ray. A photograph of the machine is shown in Appendix B (plate B.4)

3.3.2.4 Nanoparticle Size Analyzer

The nanoparticle analyzer as shown in (Appendix B, Plate B.5) was used to determine the nanoparticles size. The dynamic light scattering theory method and a measurement range of 1nm to 600nm were used. The dispersion of GSAnp in water was done before the analysis. Light source of a 650nm Laser diode, 5mW (Class 1) was used for the analysis.

3.3.2.5 Fourier Transform Infrared Spectrometry (FTIR) Analysis

Fourier transform infrared spectrometry (FTIR) was carried out on synthesized groundnut shell ash nanoparticles. IR spectra of the groundnut shellash nanoparticles were recorded using Perkin Elmer spectrum 100 FT – IR spectrometer (Appendix B, Plate B.6) in the frequency range $4000 - 400\text{cm}^{-1}$, operating in ATR (attenuated total reflectance) mode.

3.3.3 Experimental Design

In this study, Taguchi's parameter design approach was adopted to investigate the effect of manufacturing process parameters on the tensile properties of developed biocomposites.

3.3.3.1 Selection of Orthogonal Array (OA)

In this study, four parameters operated at three levels were analyzed. The process parameters and their level values are given in Table 3.3.

Table 3.2: Process parameters and their values for different levels

Process Designation	Parameter	Process Parameters	Level 1	Level 2	Level 3
A		Wt% GSA np	10	20	30
B		PEG(%)	4	8	12
C		Annealing Temperatures($^{\circ}$ C)	60	80	100
D		Annealing Time(hrs)	2	4	6

The choice of values for the parameters and their levels (minimum, intermediate, and maximum) for wt% groundnut shell nanoparticles, PEG, Annealing temperature and Time are in line with production parameters of conventional biocomposites (Youngquist, 1999, Abdalla *et al.*, 2013, Fukushima *et al.*, 2009) and represent a wide enough range for evaluating the effect of the variables on the composites properties.

To limit the study, it was decided not to study the second order interaction among the parameters, each three-level parameter has 2 degree of freedom (DOF) that is, number of levels minus one. The total degree of freedom for four parameters each at three levels is eight [$4 \times (3 - 1) = 8$]. By Taguchi's, the total degree of freedom of selected orthogonal array (OA) must be greater than or equal to the total degree of freedom required for the experiment. So, an L_9 OA (a standard three-level OA) having eight(9 – 1) degree of freedom was selected for the present analysis. This OA has four columns and nine experimental runs. The four parameters at three levels were assigned to these four columns as presented in Table 3.3 and 3.4.

3.3.3.2 Analysis procedure of the selected orthogonal array

In the analysis, parameter A assigned to column 1 of the L₉ OA. The same step by step is applicable to all the parameter and their respective levels assigned to the various columns and rows of the OA in coded form (Table 3.3). Experiments for each trial condition of the selected OA's have been repeated three times and recorded accordingly as shown in Table 3.4. Three responses (X_{ij}) are shown under R₁, R₂ and R₃ of the response column. R stands for repetition. In Table 3.4, the levels designated as 1, 2, 3, and the parameters A, B, C, D we replaced with the actual values to yield Table 3.5 showing the different formulations/parameters and their levels.

Table 3.3: The L9 (3⁴) Orthogonal Array (OA) With Parameters Assigned and Responses

S/N	RUN ORDER	PARAMETERS TRAIL CONDITIONS				TENSILE STRENGTH		
		A	B	C	D	R ₁	R ₂	R ₃
1	3	1	1	1	1	X ₁₁	X ₁₂	X ₁₃
2	7	1	2	2	2	X ₂₁	X ₂₂	X ₂₃
3	5	1	3	3	3	X ₃₁	X ₃₂	X ₃₃
4	1	2	1	2	3	X ₄₁	X ₄₂	X ₄₃
5	4	2	2	3	1	X ₅₁	X ₅₂	X ₅₃
6	6	2	3	1	2	X ₆₁	X ₆₂	X ₆₃
7	9	3	1	3	2	X ₇₁	X ₇₂	X ₇₃
8	2	3	2	1	3	X ₈₁	X ₈₂	X ₈₃
9	8	3	3	2	1	X ₉₁	X ₉₂	X ₉₃
Total						Σ	Σ	Σ
<p>R₁, R₂, R₃ represent responses values for three repetitions of each trial. The 1's, 2's and 3's represent levels 1, 2, and 3 of the parameters, which appear at the top of the column. (-) represents no assignment in the column. X_{ij} are the measured values of the quality characteristic (response).</p>								

Table 3.4: Various Factor Levels and Manufacturing Parameters for The Formulations

Exp. No.	Randomized Run order	A(wt%)	B(%)	C(°C)	D(hrs)	Tensile strength MPa T ₁	Tensile strength MPa T ₂	Tensile strength MPa T ₃	Average TS	S/N ratio
1	3	10	4	60	2					
2	7	10	8	80	4					
3	5	10	12	100	6					
4	1	20	4	80	6					
5	4	20	8	100	2					
6	6	20	12	60	4					
7	9	30	4	100	4					
8	2	30	8	60	6					
9	8	30	12	80	2					

3.3.3.3 Development of PLA/GSAnp Biocomposites

The composites were produced using the parameters in Tables 3.3 and 3.4 by the addition of the groundnut shell ash nanoparticles to the polylactic acid matrix and PEG, properly mixed and fed into extruder line with twin screw, temperature profile of 114 °C up to 185 °C and cold granulation on the end of the line (Appendix B, Plate B.7). The extrusion process was done with TE-30 Co-rotating screw extruder with extrusion length(L) of 1200mm and diameter(D) of 30mm with L/D = 40. Table 3.6 showed the extruder parameter used during the operation. The production was done in accordance with L₉ (3⁴) Taguchi experimental design method as presented, Tables 3.3 and 3.4.

The PLA was dried at 80±°C for 12 hours to remove water before processing through the extruder. A high drying temperature was chosen because by using adequate drying, significantly

higher adhesion could be developed between the phases. The residual moisture could induce degradation and it could also weaken the adhesion between the GSAnp and the PLA material. The extrudates were pelletized Appendix B (Plate B. 8) and oven dried prior to injection moulding to avoid cold crystallization of pellet.

After the extrusion and pelletization of the extrudates, the pellets were injection moulded with an ENGEL e-mac 50, injection moulding machine (Germany) equipped with a 30mm diameter, $L/D = 25$ screw (Appendix B, Plate B.9). The injection moulding machine was used to produced ISO standard dumbbell, tensile, three-point bending and Charpy specimens with a cross-section of 4x10 mm, and 100x 100mm cone calorimeter and dynamic mechanical analysis samples.

In Injection moulding, the beginning of mould close is usually taken as the start of an injection moulding cycle. Immediately after the moulds clamp up, the nozzle opens and the screw moves forward, injecting the polymer melt into the mould cavity. To compensate for the material shrinkage during cooling in the mould, the screw was maintained in the forward position by a holding pressure. At the end of the holding phase, the nozzle is shut off and the screw began to recover, while the part continues to be cooled in the mould. During the recovery phase, the screw rotated and conveyed the polymer forward along the screw. At the same time, the screw was allowed to slide backward within the barrel. In the moulding cycle, heat removal took place predominantly in the fill, hold and cool phases, although mould opening phase also contributes to partial cooling. Prior to the test, the samples were annealed, Tables 3.3 and 3.4. Annealing of PLA is reported to be an efficient treatment to increase modulus, tensile strength and reduce gas permeability, as a consequence of the reduced free volume of the polymer and increased crystallinity.

Table 3.5: Extrusion parameter used

Heating zone	Temperatures(°C)
Zone 1	114
Zone 2	158
Zone 3	183
Zone 4	173
Zone 5	178
Zone 6	178
Melt heat zone	185
Zone 7	185
Zone 8	178
Zone 9	175
Zone 10	182
Extrusion speed	209rpm

3.3.3.4 Determination of optimal production conditions for the composites

In this study, the L_9 (3^4) orthogonal array of Taguchi design method was adopted to determine the optimal manufacturing conditions of the composites. The performance characteristics for the “larger the better” situations were evaluated for maximization properties of tensile strength. Tensile strength was used as performance characteristics to deduce the optimal manufacturing parameters by using the analysis of variance (ANOVA) and signal-to-noise ratio on the test results. Noise matrix involving the use of the outer orthogonal arrays were not

considered since it was assumed that the noise effect was negligible and that by randomization of the inner array during the experimentation the noise effect was minimized.

The response data was analyzed using analysis of variance (ANOVA) technique at 0.05 levels of significance. Finally, the degree of contribution of each significant factor was obtained so as to determine the level of its statistical importance in the model. The percentage (%) contribution gives an idea about the degree of contribution of the factors to the measured response. If the contribution percent is high, the significance of the factors to that particular response is more. Likewise, if the contribution percent is low, the effect of the factors on that particular response is also low.

3.4 MORPHOLOGICAL ANALYSIS

3.4.1 Scanning Electron Microscopy (SEM) Analysis

Scanning Electron Microscopy (SEM) observations of developed composites were carried out with a JEOL 6480 LV electron microscope. A field emission gun and an accelerating voltage of 5kV were used. The surfaces of the samples were coated with gold before analysis.

3.5 TENSILE STRENGTH TEST

The performance characteristic measured in this work was the tensile strength after fracture for each trial conditions and replication was recorded. Tensile strength measurement of samples was determined using universal testing machine W3179 Appendix B (Plate B.10). The cross-head speed during the test was 3mm/min. Three (3) specimens from each sample were tested. The specimen was loaded using self-aligning, self-tightening grip that distributes the force evenly

over the grip surface and did not allow slipping. The load was applied continuously throughout the test at a uniform rate of motion of the moveable crosshead of the testing machine.

3.5.1 Tensile Test Data Analysis

The experiments were conducted under the specified conditions and the data obtained were analysed using the method(s) by Kumar *et al.* (2008) described in this section: The average values of the response at each parameter level was obtained by adding the result of all trial conditions at the level considered, and then divided by the number of data points added. The average values for parameter A, which are the levels' total of the responses at A₁, A₂, and A₃ was calculated using the method developed by Roy (1990).

$$A_1 = (x_{11} + x_{12} + x_{13}) + (x_{21} + x_{22} + x_{23}) + (x_{31} + x_{32} + x_{33}) \quad (3.2)$$

$$A_1 = (x_{41} + x_{42} + x_{43}) + (x_{51} + x_{52} + x_{53}) + (x_{61} + x_{62} + x_{63}) \quad (3.3)$$

$$A_1 = (x_{71} + x_{72} + x_{73}) + (x_{81} + x_{82} + x_{83}) + (x_{91} + x_{92} + x_{93}) \quad (3.4)$$

The average values of the responses at A₁, A₂ and A₃ are

$$\bar{A}_1 = \frac{A_1}{9}, \quad \bar{A}_2 = \frac{A_2}{9}, \quad \bar{A}_3 = \frac{A_3}{9} \quad (3.5)$$

3.5.2 Signal to Noise (S/N) Data Analysis

The raw data were converted to S/N ratio (dB). This transformation consolidates the repeated responses (raw data) in each trial condition into a single number. The S/N ratios were calculated which in turn reduced the total DoF of the experiments (Roy, 1990). The quality

characteristics for tensile strength after fracture is higher the better type so the signal-to-noise ratio (S/N ration) for the larger the better type was used and is given below:

$$\left(\frac{S}{N}\right)_{HB} = -10 \log \left[\frac{1}{n} \sum_{j=1}^R \left(\frac{1}{x_j^2} \right) \right] \quad (3.6)$$

Where x_j , $j = 1, 2, \dots, n$ the response values for the trial conditions repeated "n" times.

In this study, Design Expert 6.0 was utilized for the data analysis. The analysis provided the optimal values for the parameters that were used for the production of the composites.

3.6. DETERMINATION OF THE MECHANICAL PROPERTIES OF THE COMPOSITES

The following mechanical properties of the composites were determined:

3.6.1. Tensile Strength

The tensile strength of the samples was measured using universal notion W3179. The cross-head speed during the test was 3mm/min. Three (3) specimens from each sample were tested. The specimen was loaded using self-aligning, self-tightening grip that distributes the force evenly over the grip surface and did not allow slipping. The load was applied continuously throughout the test at a uniform rate of motion of the moveable crosshead of the testing machine.

The experiments were conducted under the specified conditions and the data obtained were analyzed using the method(s) by Kumar *et al.* (2008) described in this section: The average values of the response at each parameter level was obtained by adding the result of all trial conditions at the level considered, and then divided by the number of data points added. Those for parameter A, which are the levels' total of the responses at A₁, A₂, and A₃ was calculated using the method developed by Roy (1990) as shown earlier in equation 3.2 – 3.5.

3.6.2 Flexural Strength

The Flexural Strength of the composite was determined using universal testing machine model: W3179 equipped with a 500kg load cell, after conditioning at 25°C, in accordance with ASTM D790 standard. The load was applied continuously throughout the test at a uniform rate 3mm/min. Three-point bending method was used. Samples of dimension 150×50×4mm³ and a

span of 96mm were loaded from the top while resting on the two supports. The modulus of rupture was calculated in accordance with the equation 3.7 (ASTM D790)

$$R_b = \frac{3P_{max}L}{2bd^2} \quad (3.7)$$

Where b = width of specimen measured in dry condition (mm), d= thick of specimen (mm), L = length of span in mm, P_{max} = maximum load (N)

3.6.3 Impact Energy Determination

The Charpy impact test was used to determine the impact energy of the composite materials. The sample was supported and loaded in flexure by the pendulum striker. The striker was fixed at the end of the pendulum. The test specimen was clamped vertically in Charpy support anvils, fitted on the base of the machine and placed with the notch facing the striker. The striker swings downward, hitting the test specimen above the notch at the bottom of its swing. The test was carried out according to ASTM D256 standard using Advanced Pendulum Impact Tester Instron- IT 9050- type testing machine. Three specimens were tested from each sample and the average results recorded. All the specimens were conditioned at 23°C for 24 hours before testing.

3.6.4 Hardness test

Hardness test was performed using Rockwell hardness testing machine (Model 5023-A). The method is based on the rate of penetration of a specified indenter force into the material, under specified conditions. The samples were placed on a flat surface and pressure impacted on the specimens. The samples were subjected to three indentation hardness and readings taken.

3.6.5 Dynamic Mechanical Analysis (DMA)

Dynamic mechanical analysis (DMA) test was determined for the developed biocomposites. It is a thermal analysis technique that measures the properties of materials as they are deformed under periodic stress. Specifically, in DMA a variable sinusoidal stress is applied, and the resultant sinusoidal strain is measured. Dynamic Mechanical Analysis (DMA) was performed on a TA Q800 tester by using the injection moulded three-point bending specimens and dual cantilever. The dual cantilever was used in order to obtain storage modulus information above glass transition temperature (T_g). Amplitude of 20 μm with a span length of 35 mm and a frequency of 1 Hz was used from 0 to 160°C at a heating rate of 2°C/min.

3.7 PHYSICAL TEST

3.7.1 Water Absorption

The samples with dimension 50×50×4mm were used to examine water absorption behaviour (ASTM 570-98). Before the measurement, the samples were dried in an oven at 50 ± 2 °C temperature for 24 hours, cooled to room temperature in a desiccator, and then immediately weighed to the nearest 0.1 mg which was then taken as the dry initial weight of the sample designated m_1 . Then the samples were immersed in a container of distilled water and maintained at a temperature of 23 ± 2 °C. Three samples of the same composition were placed together in the same container with the required amount of water. In this process, care was taken to avoid the significant surface contact between test specimens or with the walls of the container. During 45

days – soaking time, the specimens were removed from the water at 5-day intervals, gently blotted with tissue paper to remove excess water from their surfaces, immediately weighed to the nearest 0.1 mg designated m_2 , and returned to the water. Each m_2 value was an average value obtained from three measurements. The percentage of weight increase due to water absorption (C) was calculated to the nearest 0.01% according to the Equation 3.8.

$$W_c(\%) = \frac{w_1 - w_0}{w_0} \times 100\% \quad (3.8)$$

Where w_0 and w_1 are weights of the specimen before and after immersion in water respectively.

3.7.2 Determination of Density

One of the major physical properties of a composite is its density and it is dependent on the amount of reinforcement present in the structure. The basic method for the determination of the density of composite samples is by measuring the mass and volume of the sample used. A clean sample is weighed accurately in air using a laboratory balance and then suspended in water. The weight of the sample when suspended in water was determined, and the volume of the sample was determined by the effect of displacement by water (Archimedean principle). The density of the sample was estimated from the equation below:

$$Density = \frac{mass}{volume} (g/m^3) \quad (3.9)$$

3.7.3 Determination of Thermal Properties.

Thermal decomposition of the samples was observed in terms of global mass loss by using a TA instrument TGA Q50 thermogravimetric analyzer (Appendix B, Plate B.13). This apparatus detects the mass loss with a resolution of 0.1 as a function of temperature. The samples were evenly and loosely distributed in an open sample pan of 6.4mm diameter and 3.2 mm deep

with an initial sample amount of 8-10mg. The temperature change was controlled from room temperature ($25\pm 3^{\circ}\text{C}$) to 700°C at a heating rate $10^{\circ}\text{C}/\text{min}$. The sampling segment was set to 0.5 seconds per point.

A high purity Argon was continuously passed into the furnace at a flow rate of 60 ml/min at room temperature and atmospheric pressure to maintain the inert environment. Before starting each run, the Argon was used to purge the furnace for 30 min to establish an inert environment in order to prevent any unwanted oxidative decomposition. The TG and DTA curves that were obtained from TGA runs were carefully smoothed at a smoothing region width of 0.2°C least squares smoothing method, and analyzed by using universal analysis 2000 software from TA Instruments.

3.7.4Cone Calorimetry Test

Artificial fire tests were performed on the small composite panels using a Stanton Redcroft cone calorimeter. Appendix B, Plate B.14 revealed a general view of the cone calorimeter and a close-up view of a burning panel. The artificial fire tests were performed by the rapid heating to one surface of the panels using a high-energy heating coil. For this study, the heat flux of $50 \text{ kW}/\text{m}^2$ was adopted because it caused the GRP panel to ignite after heating for 30 seconds. Greene suggests that the heat flux of $50 \text{ kW}/\text{m}^2$ is about the heat energy radiated by a medium intensity room fire. The panels were exposed to the heat flux at different times up to 10 minutes. A thermocouple was placed at the heat-exposed surface of the panel to measure the temperature reached by the composite inside the cone calorimeter. A second thermocouple was used to measure the air temperature close to the heating coil. At the end of the fire tests, the

burning composite panels were removed from the cone calorimeter, extinguished and then cooled to room temperature. The following quantities were measured using the cone calorimeter:

Peak heat release rate: This was the maximum heat release rate measured at any point over the test period.

Average heat release rate: This was calculated from the integral of the heat release rate over the entire period that heat was released by the specimen.

Time-to-ignition: This was defined as the minimum exposure time required for the specimen to ignite and sustain flaming combustion. The spark igniter to the cone calorimeter was used to induce ignition.

Average smoke density: This was measured by the decrease in transmitted light intensity of a helium-neon laser beam located within the fume extraction duct. The smoke density is expressed in terms of average specific extinction area (SEA) with units of m^2/kgK , which is a measure of the instantaneous amount of smoke being produced per unit mass of specimen burnt

Yields of carbon monoxide and carbon dioxide: These were measured using a CO/CO₂ gas analyzer located in the exhaust duct. Both the peak and average yields of these gases were determined.

Mass loss: The peak and average mass loss rates together with the total mass loss were measured using the load cell located beneath the specimen holder.

3.8 BIODEGRADABILITY TEST

The biodegradation of the materials was evaluated by means of weight loss measurements. The surface area and initial weight (W_0) of three specimens were measured before being immersed in polystyrene containers with Simulated Body Fluid (SBF). A surface/volume ratio of 1 g/10 ml was kept constant during the test. At the end of Each week, the specimens were recovered from

the fluid and dried at 37°C until the weight stabilized. After that, the weight was recorded (W_t) and the fluid was changed. The percentage of weight loss was determined using the following equation:

$$\%W = \frac{W_0 - W_t}{W_0} \times 100\% \quad (3.10)$$

Where W_0 is the initial weight of the specimen and W_t is the weight of the dried specimen at time t

CHAPTER FOUR

4.0 RESULTS AND DISCUSSION

This chapter presents and discusses all the results generated in the course of carrying out this research work.

4.1 CHARACTERIZATION OF THE GROUNDNUT SHELL ASH NANOPARTICLES

4.1.1 Transmission electron microscope analysis (TEM)

The TEM morphology of the GSAnp after various milling times are shown in Plates 4.1 to 4.6. As can be seen from the plates, the GSAnp were observed to be irregular in shape. Some spherical shape particles could also be seen. The average particles size obtained are 500nm, 500nm, 200nm, 100nm, 20nm and 2 μ m at 2, 4, 6, 8, 10 and 12 hours ball milling time respectively. It can be seen that ball milling time of two (2) and four (4) hours have the particles of size average of 500nm, but there were more distribution of the particles at 4 hours' ball milling than 2 hours (Plates 4.1 and 4.2).

There was a decrease in particles size with increase in surface area as the ball milling time was increased from four (4) hours to ten (10) hours. It was clearly observed that the

particles size of GSA ball milled at ten (10) hours were spherical in shape and had a larger surface area than sample ball milled at 12 hours Plate 4.5 and Plate 4.6. GSAnp at higher ball milling time of 12 hours tended to agglomerate and clusters of the fine particles are formed. Agglomeration of the fine powder particles occurred due to mechanical interlocking caused by atomic bonding. According to Hiremath(2012), particles in the nanometer size range possess a strong tendency to agglomerate owing to their relatively large surface area and other properties, which in turn accentuates their van der Waals interactions. Hence, the optimal ball milling time for the groundnut shell ash was found to be 10 hours with the particle size of 20 nm. This average particle size was used in this research.

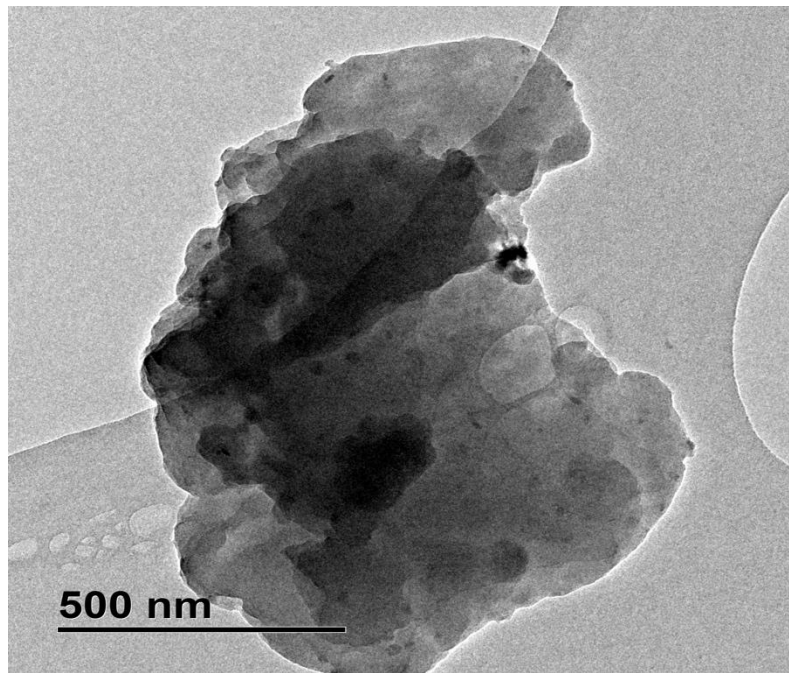


Plate 4.1: TEM morphology of the GSAnp at 2 hours balling time (x 250,000)

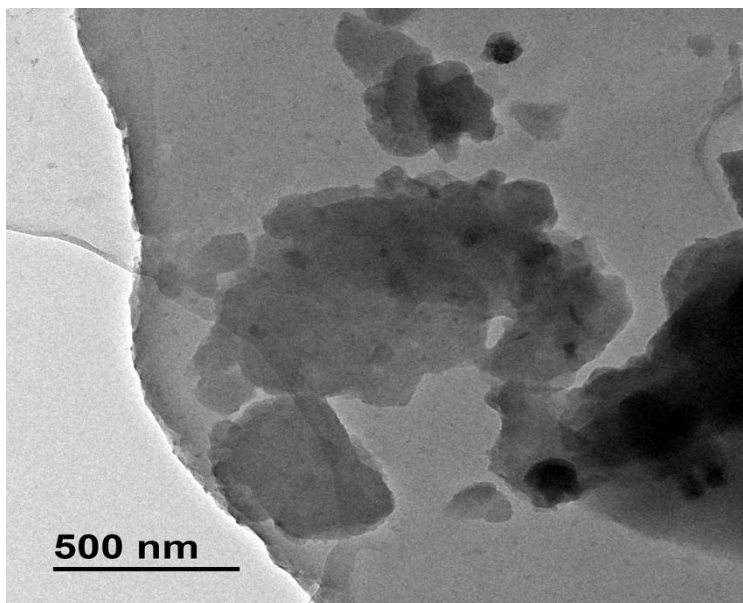


Plate 4.2: TEM morphology of the GSAnp at 4hours balling time (x 250,000)

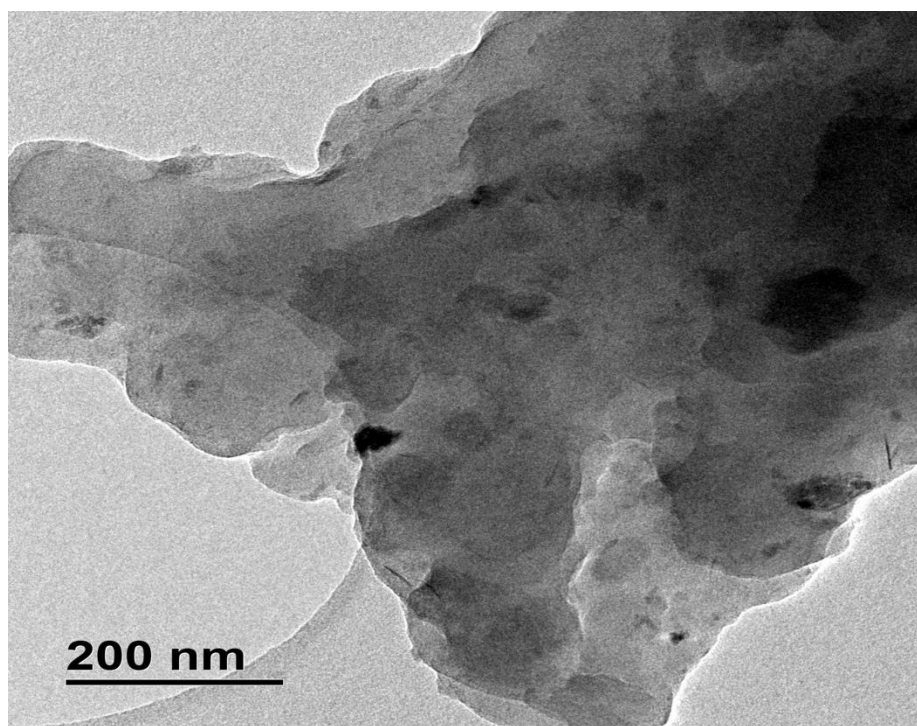


Plate 4.3: TEM morphology of the GSAnp at 6 hours balling time (x 250,000)

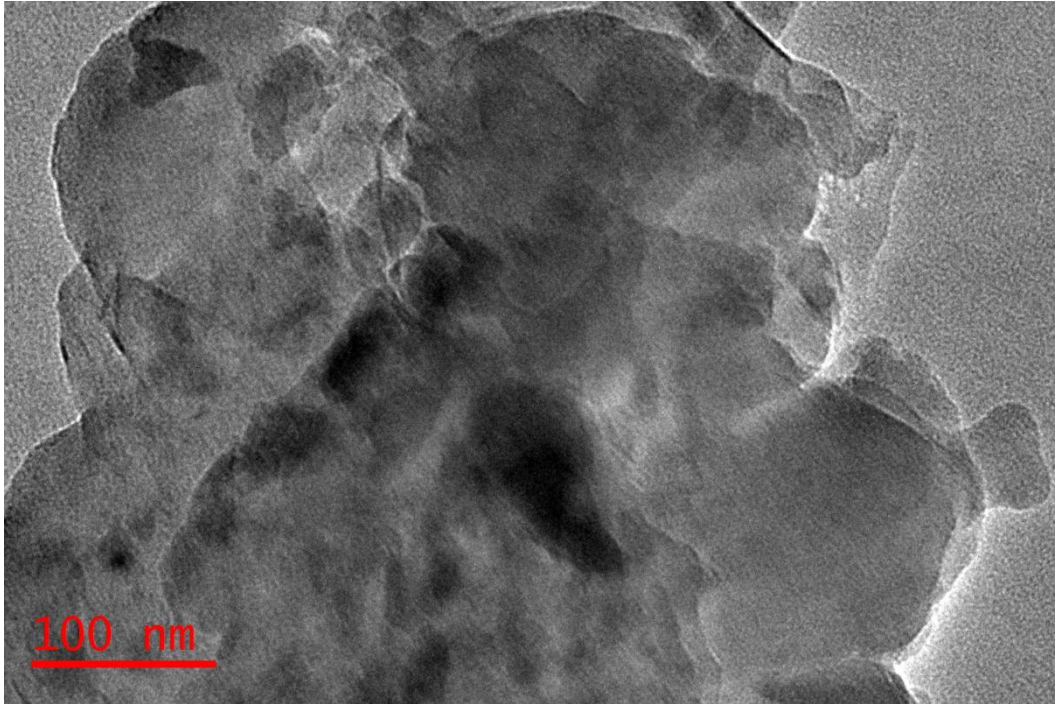


Plate 4.4: TEM morphology of the GSAnp at 8 hours balling time (x 250,000)

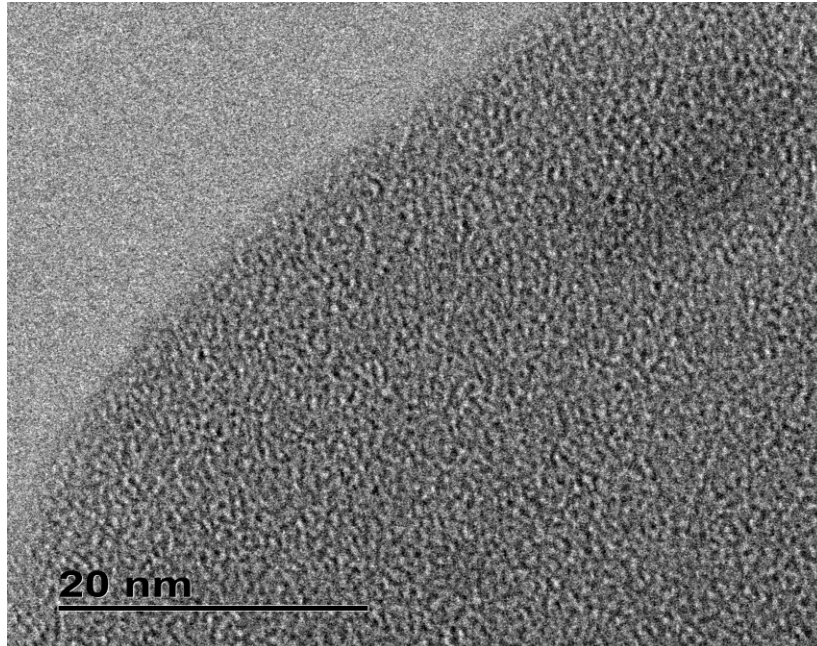


Plate 4.5: TEM morphology of the GSAnp at 10 hours balling time (x 250,000)

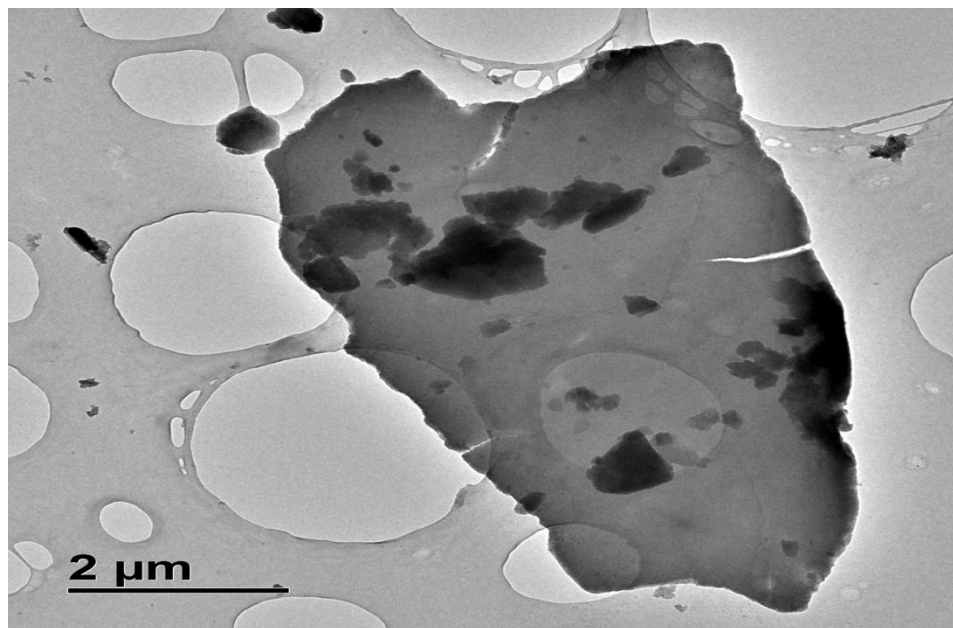


Plate 4.6: TEM morphology of the GSAnp at 12 hours balling time x (250,000)

The EDS analysis of the GSAnp at 10hours of balling milling is shown in Figure 4.1 and Table 4.1. It was observed that the micro-analysis of the EDS revealed the presence of carbon, oxygen, silicon, aluminium, and potassium. The higher peak of carbon (C) in Figure 4.1 was due to the effect of ashing of the groundnut shell at high temperature. Also, the presence of the high peak of oxygen (O) confirmed that the various elements in the groundnut shell ash were not pure.

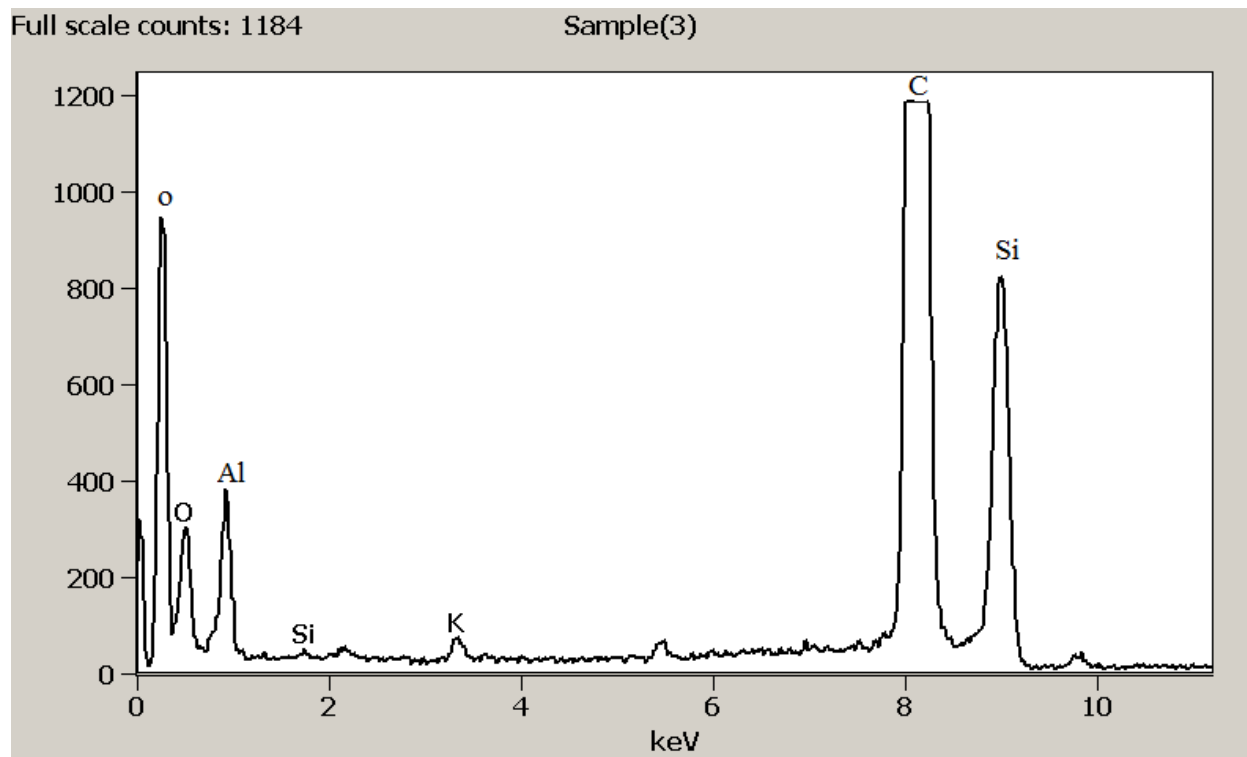


Figure 4.1: EDS analysis of the GSAnp at 10hours ball milling

Table 4.1: EDS Quantitative Results of the GSAnp at 10hours ball milling

<i>Element</i>	<i>Weight %</i>	<i>Weight %</i>	<i>Atom %</i>	<i>Atom %</i>	<i>Formula</i>
<i>Line</i>		<i>Error</i>		<i>Error</i>	
<i>C K</i>	76.95	± 1.09	82.38	± 1.16	C
<i>O K</i>	21.52	± 0.94	17.30	± 0.75	O
<i>Al K</i>	0.04	± 0.01	0.02	± 0.00	Al
<i>Si L</i>	---	---	---	---	(null)
<i>K K</i>	0.02	± 0.00	0.01	± 0.00	K
<i>K L</i>	---	---	---	---	(null)
<i>Si K</i>	1.47	± 0.01	0.30	± 0.00	Si
<i>Cu L</i>	---	---	---	---	(null)
<i>Total</i>	100.00		100.00		

4.1.2 X-ray fluorescence (XRF) analysis of the GSAnp

The chemical composition of the GSAnp determined by XRF analyzer is given in Table 4.2. The XRF analysis confirmed SiO₂, Al₂O₃ to be the major constituents of the ash. Silica and alumina are known to be among the hard substances (Laine *et al.*, 1989). Some other oxides viz: CaO, K₂O, Na₂O were also found to be present in traces. However, the presence of carbon was not detected by XRF. The carbon is the incombustible carbon in the ash

Table 4.2: Composition of the groundnut shell ash nanoparticles

Compounds	SiO ₂	Al ₂ O ₃	Fe ₂ O ₃	CaO	MgO	Na ₂ O	K ₂ O	L OI
Wt%	80.24	15.67	0.5	0.32	0.6	0.24	3.2	9.5

4.1.3 X-ray diffractometer (XRD) analysis of the GSA np

The XRD pattern of the GSA np revealed that the main diffraction major peaks are 24.27° , 31.06° , 49.69° , 64.74° and 42.74° and their inter-planar distances are 3.68\AA , 2.87\AA , 1.83\AA , 1.32\AA and 2.17\AA . Phases at these peaks as fullerite (carbon) C_6O , Quartz $\text{syn}(\text{SiO}_2)$ Moissanite (SiC), Potassium Oxide (K_2O), Potassium Aluminum Oxide K_3AlO_3 . Crystal structure of Monoclinic Tetragonal, Cubic, Monoclinic and crystallographic plane of: (313), (110), (220) and (131) respectively (Figure 4.2 and Tables 4.3 - 4.4). The result showed that silicon carbide has the highest percentage of all the compound present. The broad X-ray diffraction pattern which is typical of amorphous solids was also observed. This is similar to results obtained in another biomass ash (Janewit *et al.*, 2008).

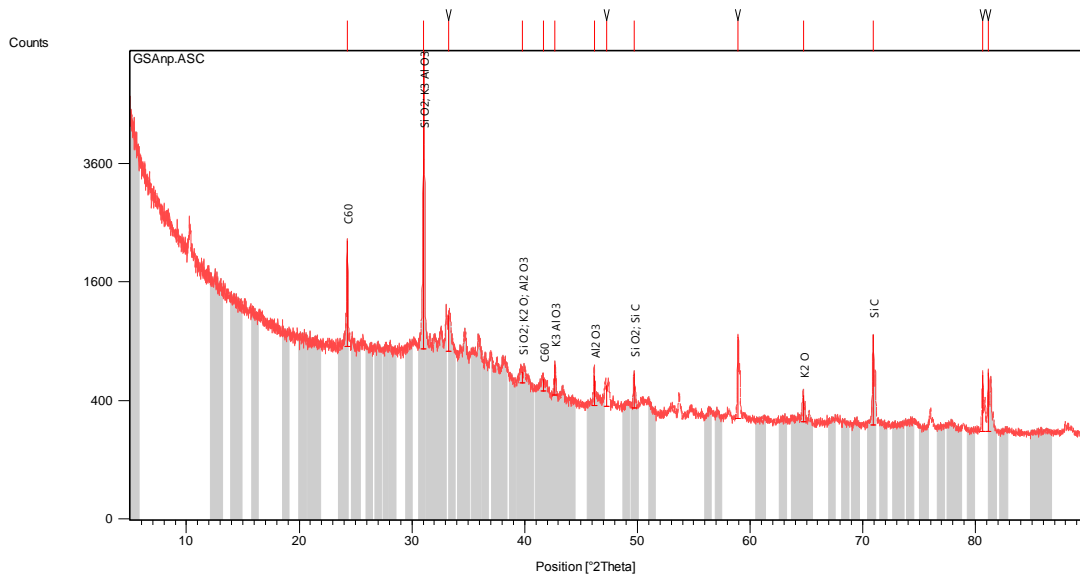


Figure 4.2: XRD pattern of the GSA np

Table 4.3: Peak List of the XRD pattern of GSAnp

Pos. [°2Th.]	Height [cts]	FWHM [°2Th.]	d-spacing [Å]	Rel. Int. [%]	Tip width [°2Th.]	Matched by
24.2737	1364.53	0.0945	3.66681	25.05	0.0960	49-1719
31.0645	5446.25	0.0708	2.87898	100.00	0.0720	82-0513; 27-1336
33.2471	388.36	0.5038	2.69481	7.13	0.5120	
39.8012	94.40	0.5038	2.26487	1.73	0.5120	82-0513; 77-2151; 49-0134
41.6630	96.72	0.6298	2.16786	1.78	0.6400	49-1719
42.6915	244.00	0.1260	2.11799	4.48	0.1280	27-1336
46.1890	220.13	0.1889	1.96543	4.04	0.1920	49-0134
47.2924	149.27	0.3779	1.92211	2.74	0.3840	
49.6990	255.29	0.1260	1.83453	4.69	0.1280	82-0513; 19-1138
58.9564	653.15	0.1152	1.56535	11.99	0.0960	
64.7387	166.10	0.2519	1.44000	3.05	0.2560	77-2151
70.9306	719.06	0.0960	1.32762	13.20	0.0800	19-1138
80.6324	375.45	0.1152	1.19056	6.89	0.0960	
81.1460	392.96	0.1152	1.18432	7.22	0.0960	

Table 4.4: Identified Patterns List GSAnp

Visible	Ref. Code	Score	Compound Name	Displacement [°2Th.]	Scale Factor	Chemical Formula
*	49-1719	33	Fullerite	0.000	0.015	C60
*	82-0513	23	Stishovite	0.000	0.055	Si O2
*	19-1138	17	Moissanite-2\ITH\RG, syn	0.000	0.013	Si C
*	77-2151	26	Potassium Oxide	0.000	0.020	K2 O
*	27-1336	17	Potassium Aluminum Oxide	0.000	0.033	K3 Al O3
*	49-0134	15	Aluminum Oxide	0.000	0.039	Al2 O3
*	75-1544	9	Silicon Oxide	0.000	0.003	Si O2
*	49-1717	14	Fullerite	0.000	0.012	C60
*	50-0511	14	Silicon Oxide	0.000	0.461	Si O2

4.1.4 Nano-Particle size analysis

Figure 4.9 represents the size distribution curve of GSAnp produced after milling and it could be observed that the GSAnp has a bimodal particle distribution curve with a particle size distribution range of 0–200 nm and peak maxima around 22.5 nm. This is in agreement with the particle size analysis carried out using TEM.

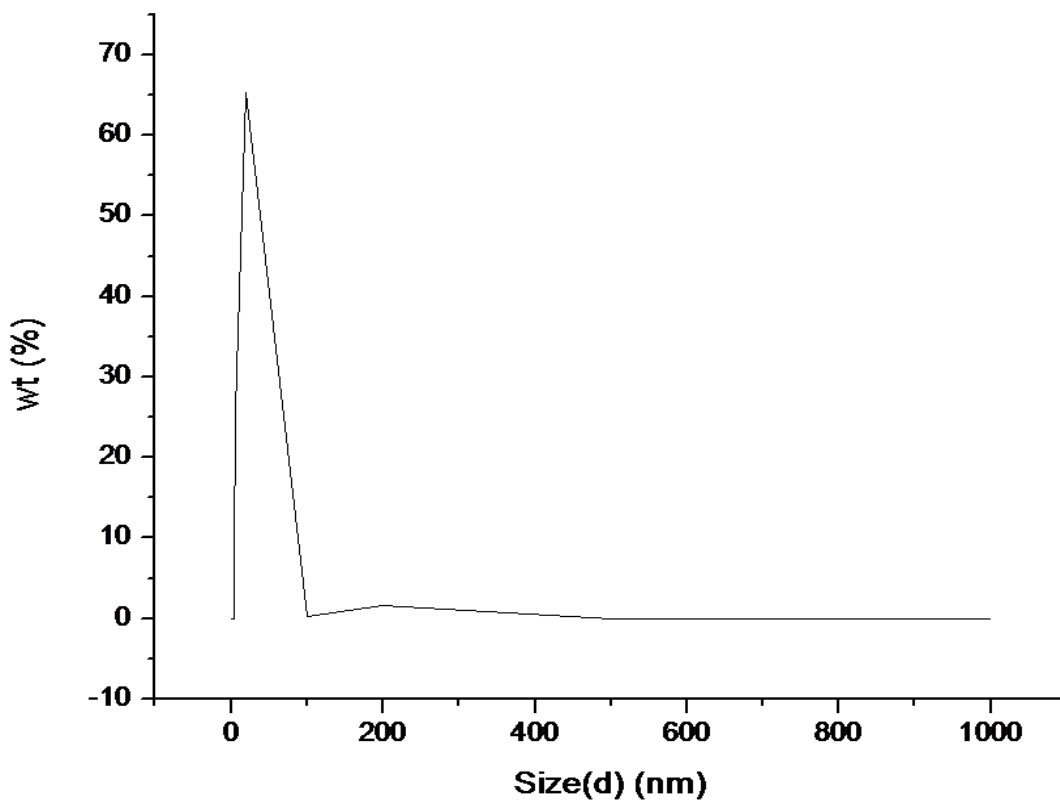


Figure 4.3: Particle size distribution by wt%

4.1.5 Surface area (BET)

The specific surface area (SSA) of the 20nm GSAnp nanoparticles was measured on a Brunauer-Emmett-Teller (BET). The GSAnp powders consist of nanoparticles with a specific surface area (SSA) of 56.7 m²/g which is also in agreement with the result of the TEM analysis which revealed nanoparticles of a high surface area.

4.1.6 FTIR analysis of GSAnp

The major chemical groups present in the GSAnp were identified by FTIR spectra as shown in Figure 4.4. The bands were scanned from 400 to 4000 cm⁻¹. The broadband at 3015.24cm⁻¹to

3972.36 cm^{-1} is due to the stretching vibration of the O-H bond from the (Si- OH) group. The band at 1013.64 cm^{-1} to 1624.2 cm^{-1} is attributed to the Si-O-Si asymmetric stretching vibration, while the band at 826.44 cm^{-1} to 885 cm^{-1} is assigned to the network Si-O-Si symmetric bond stretching vibration. The band at 425.16 cm^{-1} to 550.92 cm^{-1} is assigned to network O-Si-O bending vibration modes.

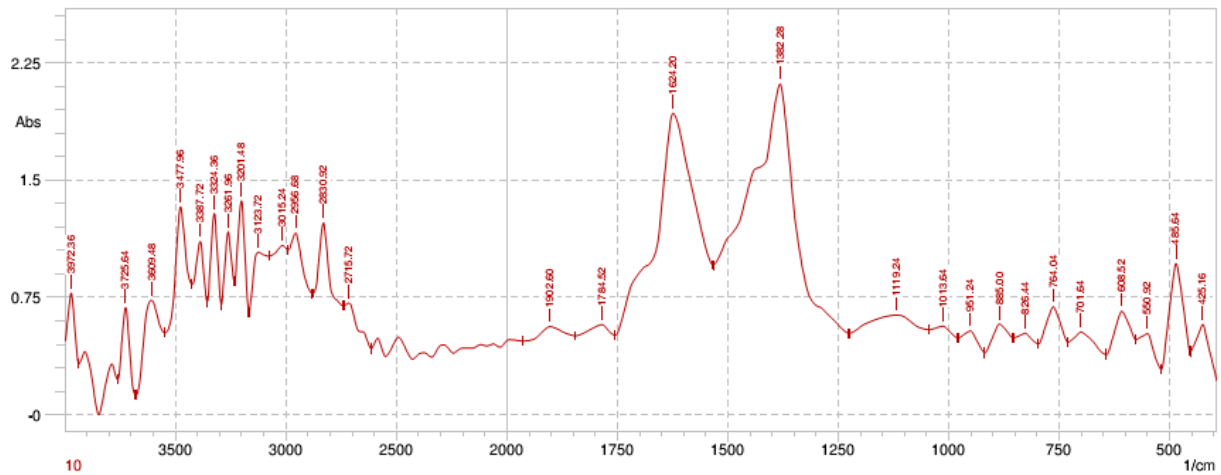


Figure 4.4: FTIR of the GSAnp

4.2 VISUAL OBSERVATION OF THE COMPOSITES

The physical appearance of the composites after production revealed that there was a change in colour from white to black for the composites reinforced. The composites revealed a fair distribution of GSAnp within the PLA matrix. The distribution of particles is influenced by the compounding of the GSAnp with the PLA matrix, which resulted in fair bonding.

4.3 TENSILE STRENGTH FOR OPTIMAL COMPOSITE SETTING

The results for tensile strength were presented Table 4.4 and Figures 4.5 – 4.6. Taguchi S/N ratio was employed to analyze the experimental data. Since larger values of tensile strength

were required, the larger the better (LB) criterion was selected for the analysis. S/N ratio for each combination of parameters was calculated and presented Table 4.5.

Analyses of the influence of each control factors: Wt% GSA_np (A), wt% PEG (B), Annealing Temperatures (°C) (C), Annealing Time (hrs)(D) on the responses were obtained from the response tables of mean S/N ratio Table 4.5. The main effects plots for mean and S/N ratios are presented in Figures 4.5 - 4.6.

Table 4.5: Various factor levels and manufacturing parameters for the formulations

Exp. No.	Randomized Run order	A(wt%)	B(%)	C(°C)	D(hrs)	Tensile strength MPa T ₁	Tensile strength MPa T ₂	Tensile strength MPa T ₃	Average (Mpa)	S/N ratio
S1	3	10	4	60	2	46.27	60.5	72.93	59.9	35.10
S2	7	10	8	80	4	60.5	56.33	80.27	65.70	36.06
S3	5	10	12	100	6	92.3	120.2	110.3	107.6	40.48
S4	1	20	4	80	6	104.67	121.90	118.04	114.87	41.15
S5	4	20	8	100	2	73.17	80.71	79.52	77.8	37.79
S6	6	20	12	60	4	80.85	98.27	80.2	86.44	38.62
S7	9	30	4	100	4	62.8	69.31	60.73	64.28	36.12
S8	2	30	8	60	6	66.01	48.33	60.5	58.28	35.09
S9	8	30	12	80	2	40.69	40.5	40.31	40.50	32.15
Control						42.27	46.19	46.54	45.01	33.04

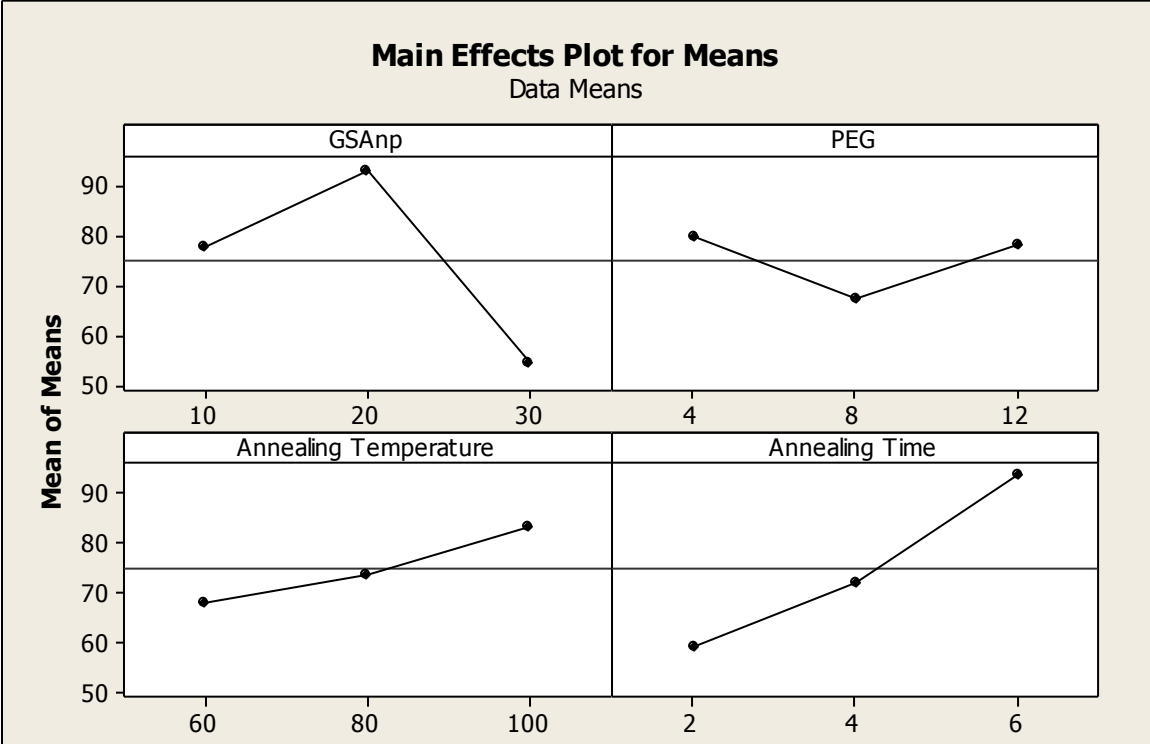


Figure 4.5: Main effects plot for the means.

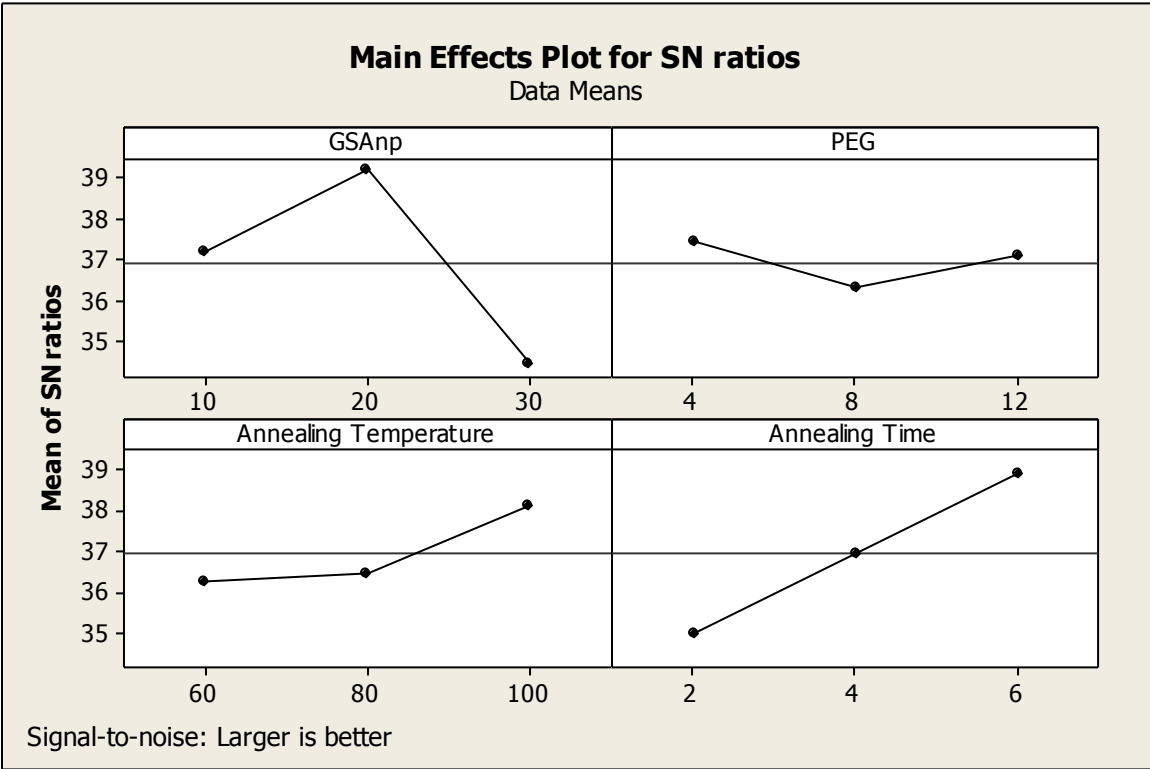


Figure 4.6: Main effects plot for the S/N ratios.

It was observed in Figures 4.5 and 4.6 that the increase in the weight % of GSAnp (A) to 20wt% consequently led to increase of the tensile strength of the composite. Increase in the weight% of GSAnp beyond 20wt% led to decrease in the tensile strength. Therefore, at 20wt% GSAnp, the optimized composite was obtained. The decrease in tensile strength at 30wt% GSAnp might also be attributed to weak interfacial bonding between the PLA and GSAnp. This is in agreement with an earlier observation by Vignesh *et al.* (2016).

The addition of PEG did not have a specific pattern in the tensile strength of the developed composites. It was observed that from 4 to 8wt% the tensile strength decreased, but 8 to 12wt%, the tensile strength of the composites increased. This only confirms that PEG served as a compatibilizer that created the environment to increase the interfacial bonding between the PLA and GSAnp. This phenomenon was observed in the work of Vignesh *et al.* (2016). Annealing of the composites after the injection moulding increases its thermal stability. It is quite clear from the Figures 4.5 and 4.6 that there was wide variation in the tensile strength when annealing was done at the temperature of 60°C and 80°C. The highest tensile strength was obtained when the annealing temperature was increased to 100°C. Also, a corresponding increase in the annealing time from 2 to 6 hours was found to raise the tensile strength. It can be concluded that higher annealing temperature of 100°C and time of 6 hours gives the composites good thermal stability and reduces the probability of production of brittle composites. Therefore, the S/N analysis revealed that the optimal process parameters are the wt% GSAnp at level 2 (20wt%), %PEG at level 1(4%), annealing temperature at level 3 (100°C) and annealing time at level 3(6 hours)

4.3.1 Estimation of Optimum Performance Characteristics

The optimum values of tensile strength are predicted at each level of significant parameters using the S/N ratio and the means effects. The estimated response characteristic of S/N ratio and mean for means were computed using equation 4.1:

$$\text{Factor} = \frac{L_1 + L_2 + L_3}{3} \quad (4.1)$$

The response tables for the average tensile strength values Tables 4.5 and 4.6. It indicates the S/N ratio and means at each level of control factor and how it changed when settings of each factor were changed from level one to three. The ranking of the process parameters using the signal to noise and means are stated in Tables 4.6 and 4.7. From the two tables, it could be seen that percentage weight of GSAnp in the composite (rank=1) has the dominant effect on the tensile strength characteristic, followed by annealing time (rank=2), annealing temperature (rank =3) and percentage weight of PEG (rank=4). The optimal condition for the tensile strength was achieved at GSAnp L₂ PEG L₁ Annealing temperature L₃ Annealing time L₃.

Table 4.6: Response Table for Signal to Noise Ratios Larger is better(Larger is better)

Level	GSAnp	PEG	Annealing Temperature	Annealing Time
1	37.21	37.45	36.27	35.01
2	39.19	36.31	36.45	36.93
3	34.45	37.08	38.13	38.90
Delta	4.74	1.14	1.86	3.89
Rank	1	4	3	2

Table 4.7: Response Table for Means (Larger is better)

Level	GSAmp	PEG	Annealing Temperature	Annealing Time
1	77.73	79.68	68.21	59.40
2	93.04	67.26	73.69	72.58
3	54.35	78.18	83.23	93.58
Delta	38.68	12.42	15.02	34.18
Rank	1	4	3	2

The estimated optimal tensile strength was calculated using equation 4.2:

$$EV = AVR + (A_{opt} - AVR) + (B_{opt} - AVR) + (C_{opt} - AVR) + (D_{opt} - AVR) \quad (4.2)$$

Where, EV= expected response, AVR = average response, A_{opt} = mean value of response at optimum setting of factor A, B_{opt} = mean value of response at optimum setting of factor B, C_{opt} = mean value of response at optimum setting of factor C, D_{opt} = mean value of response at optimum setting of factor D

$$EV = 75.04 + (93.04 - 75.04) + (79.68 - 75.04) + (83.23 - 75.04) + (93.58 - 75.04)$$

$$EV = 75.04 + 18.0 + 4.64 + 8.19 + 18.54$$

$$EV = 124.41\text{Mpa}$$

4.3.2 Confirmatory Experiment and validation (error(s)) at optimal Conditions

A confirmatory experiment was conducted at the optimum setting of the process parameters. The percentage weight of GSAmp was set at the second level L_2 , wt% PEG was set at the first level L_1 , the annealing temperature was set at the third level L_3 , and annealing time was also set at third level L_3 . The average tensile strength after fracture of the composites was found

to be 118.9MPa. The values are within the confidence interval of predicted optimal of tensile strength after fracture.

$$Error = \frac{124.4 - 118.9}{118.9} \times 100\% = 4.625\% \approx 4.6\%$$

$$\% \text{ improvement} = \frac{118.9 - 114.87}{118.9} \times 100\% = 3.57\% \approx 3.6\%$$

4.3.3 Analysis of variance (ANOVA)

The experimental results were also analyzed with ANOVA to find the percentage contribution of each independent control variable. The analysis was evaluated at a confidence level of 95%, that is for a significance level of $\alpha=0.05$ using design expert software 6.0. The result of the ANOVA is presented in Table 4.8. From Table 4.8 it was observed that GSAnp has the highest influence (48.55%) on the tensile strength, followed by annealing time (38.18%), annealing temperature (7.39%) and the least PEG (5.88%). The Model F-value of 6.54 implies the model is significant. There is only a 4.82% chance that a "Model F-Value" this large could occur due to noise. Values of "Prob > F" less than 0.0500 indicate model terms are significant. In this case, A(GSAnp) is significant model terms. Values greater than 0.1000 indicate the model terms are not significant. The "Pred R-Squared" of 0.9575 is in reasonable agreement with the "Adj R-Squared" of 0.9768 with a standard deviation of 12.47 and mean of 75.04.

Table 4.8: ANOVA for the Model

Source	Sum of Squares	DF	Mean square	F _{value}	P _{value}	% Contribution	Remarks
Model	4067.84	4	1016.96	6.54	0.0482		Significant
A	2277.22	2	1138.61	7.32	0.0461	48.55	
B	275.85	2	137.92	0.886	0.1678	5.88	
C	346.62	2	173.31	1.11	0.1545	7.39	

D	1790.62	2	895.31	5.75	0.0665	38.18	
Residual	622.46 4	2	155.62				
CorTotal	4690.30	8				100	

4.3.4 Regression model for optimum tensile strength

The model equation for the tensile strength of composites was expressed as:

$$\begin{aligned} \text{Tensile Strength} = & 75.0411 + 2.6922 A[1] + 17.9956A[2] + 4.6422 B[1] - 7.7811 B[2] \\ & - 6.8344 C[1] - 1.3511 C[2] - 15.6411 D[1] - 2.9011D[2] \quad (4.3) \end{aligned}$$

By substituting the coded values of the variables for any experimental condition in Equation 4.3, the tensile strength of the composites can be calculated and shown in Table 4.9. Also, from Table 4.9, it was clear that the actual experimental values are also very close proximity to the predicted values.

Table 4.9: Experimental values and Predicted values

Experimental order	Actual value	Predicted value	Residual
S1	59.90	62.09	-2.19
S2	65.70	74.83	-9.13
S3	107.60	96.28	11.32

S4	114.87	111.58	3.29
S5	77.80	77.40	0.40
S6	86.44	90.14	-3.70
S7	64.28	51.45	12.83
S8	58.28	72.90	-14.62
S9	40.50	38.71	1.79

Table 4.10: Optimum levels of process parameters (TENSILE strength after fracture)

Process parameter	Parameter designation	Optimal levelCBPp	Optimal tensile strength(Mpa)	Validation	
				% error	% improvement
GSAnp	A	L2(20wt%)	124.41	4.6	3.6
PEG	B	L1 (4wt%)			
Annealing Temperature	C	L3(100°C)			
Annealing Time	D	L3(6hours)			

4.4 PROPERTIES OF COMPOSITES AT OPTIMIZED CONDITION

4.4.1 X-ray Diffraction

Figures 4.7 and 4.8 are the XRD patterns of the PLA and composites produced at optimal conditions. From Figures 4.7 - 4.8, one can observe that there are clear differences between the spectrums. The X-ray diffraction spectrum of the PLA shows two peaks located at $2\theta = 18.45^\circ$ and 45.6° . The sharp peak at 18.45° indicates high crystalline structure which strongly agrees with work reported by Giita Silverajah *et al.* (2012). The composite XRD spectrum exhibits major broad diffraction peak at $2\theta = 36, 45, 65$ and 78.5° with the presence of silica and alumina phases. This behaviour could be attributed to the addition of GSAnp to the PLA. The XRD pattern of the composite show that they are semi-crystalline. These facts confirmed that the presence of the GSAnp in the PLA structure altered the regularity of the polymer.

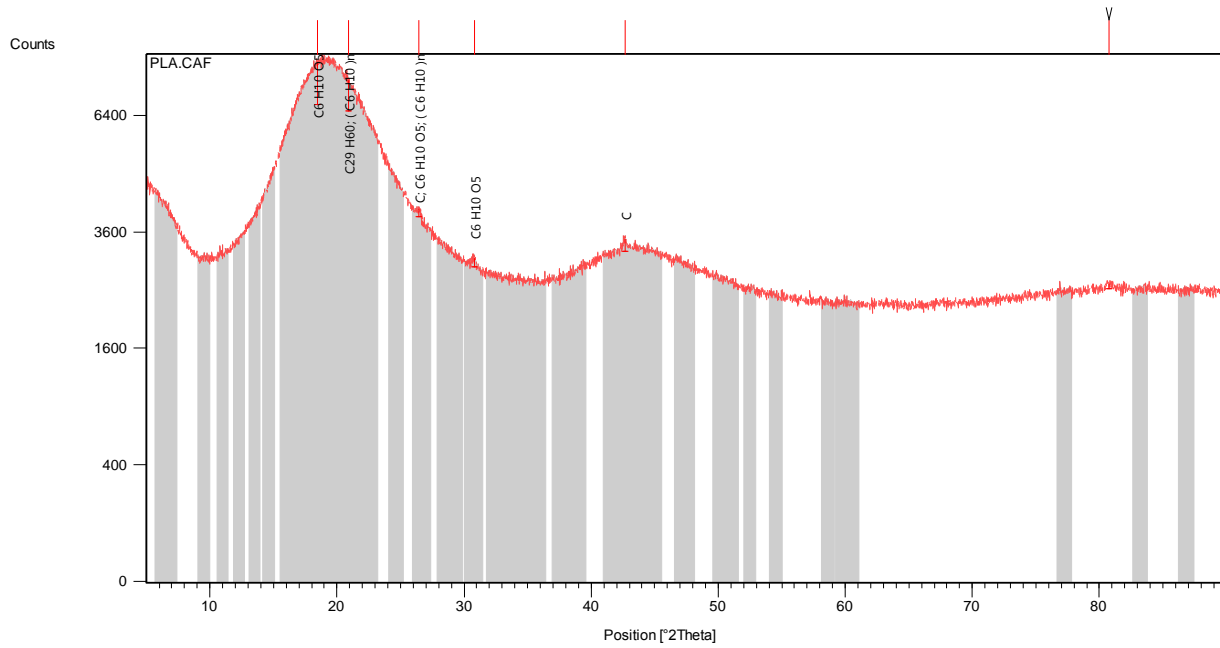


Figure 4.7: XRD pattern of the PLA

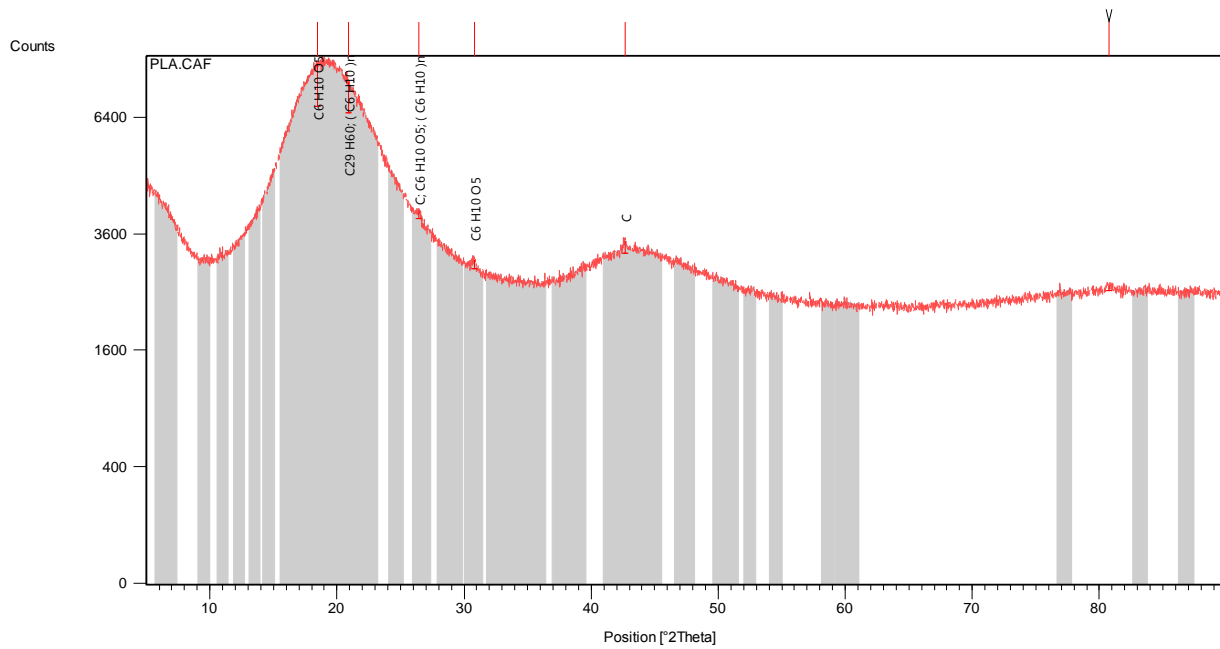


Figure 4.8: XRD pattern of the composite at optimal condition

4.4.2 Morphology of the Composites

SEM was used to study the morphology of the tensile fractured PLA/GSAnp composites surfaces. Plate 4.8 shows the SEM micrograph of the PLA surfaces, while Plate 4.9 shows the SEM micrographs of the composites surfaces. The morphological study showed that the GSAnp as a reinforcement has smooth spherical surface and higher surface area for interaction. There is a fair dispersion of GSAnp in the polymer matrix. Morphology of the composite in Figure 4.9 clearly shows that there is proper mixing of GSAnp with the PLA in the composites. Particles - matrix interface plays an important role in composite properties. A strong particle-matrix interface bond is critical for high mechanical properties of composites. It was observed that PLA surrounds the GSAnp in the form of an isotropic homogeneous material. GSAnp is found to be evenly distributed over the entire PLA. There are no noticeable gaps or pores in either PLA or PLA/GSAnp composites.

Pulling out of the GSAnp from the PLA, delamination between the particles and the polymer matrix was not observed in the study. All the composites contain polymer fibres attached to the GSAnp an indication of improved adhesion between the phases. The PLA- GSAnp based composite particles pull-out as well as holes resulting from particles delamination was not observed. The good interfacial bonding achieved in this research work was attributed to the use of PEG, oven drying of the compound blends before injection moulding and thermal treatment. These actions expelled trapped moisture, ensured interfacial bonding and reduced residual stress after injection moulding.

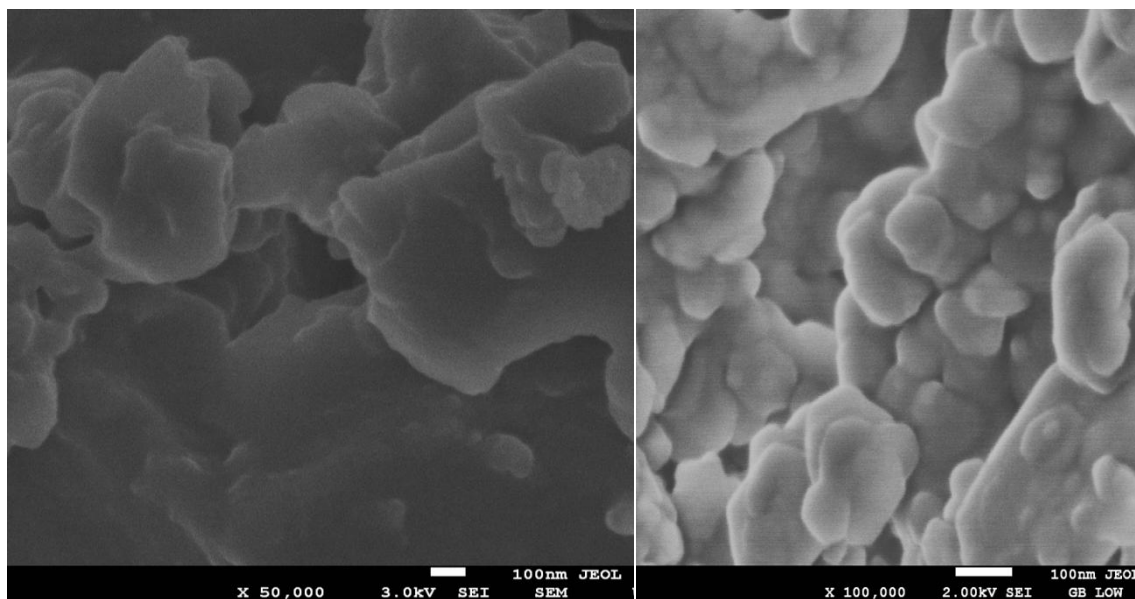


Plate 4.8: SEM fracture morphology of the PLA

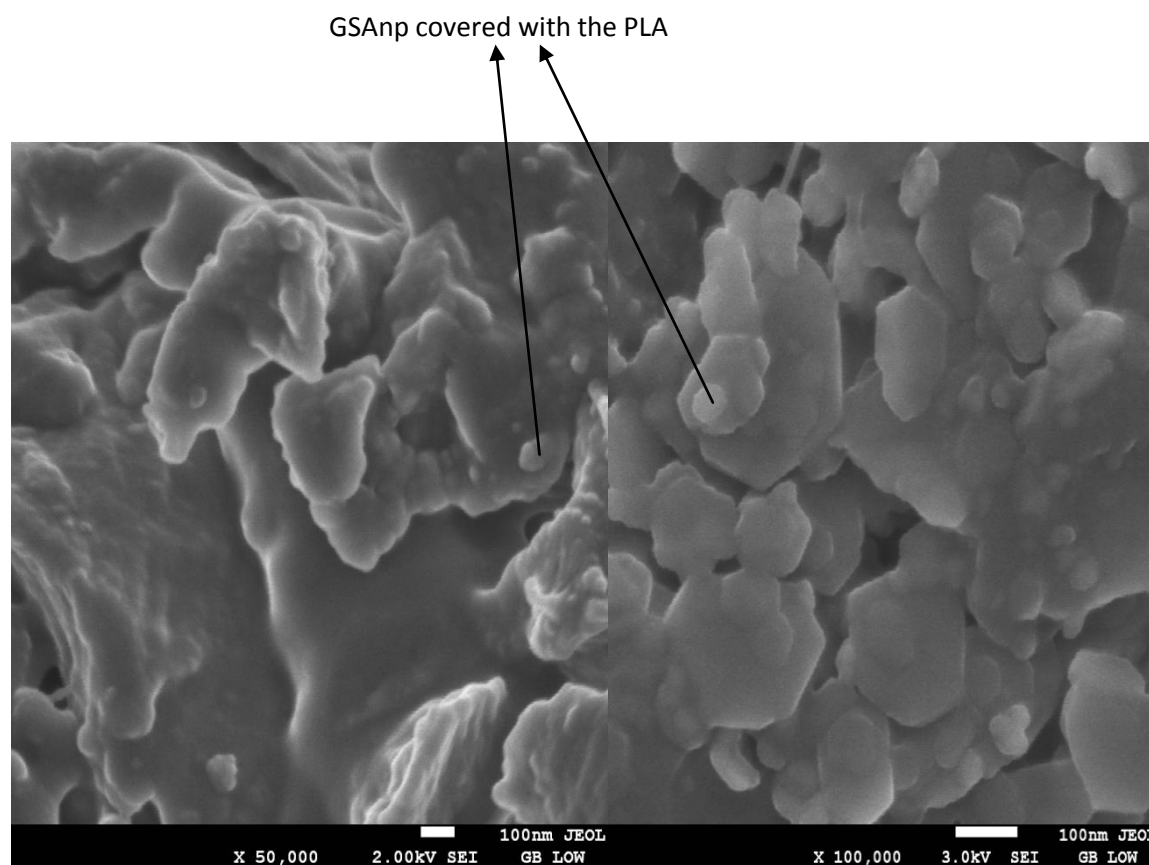


Plate 4.9: SEM morphology of the composites at the optimal composition

4.4.3 Tensile Modulus and Percentage of Elongation

The Young's modulus of PLA and composites were 2226.39 and 2305.361MPa, as shown in table 4.11 whilst the corresponding elongation at break was 7.81 and 8.61%, respectively. The results show that the composites have a relatively higher Young's modulus and %elongation than the PLA, as shown in Table 4.11. The Young's modulus of the composites with GSA_{np} increment was attributed to the inherent high stiffness strength of the reinforcement.

PEG plasticized the PLA and increased the chain mobility of the PLA which obviously lowered the stress required for craze initiation and growth, resulting in higher Young's modulus, tensile strength and higher elongation-at-break. Nevertheless, the tensile strength obtained in this study remained within the acceptable levels for outdoor and indoor structural applications (polymer ceiling board, food packaging) (ASTM, 2002). The tensile strength obtained at the optimum point was due to the stability of the filler to support stresses transferred from the polymer matrix (Chapple *et al.*, 2013).

4.4.4 Flexural Properties.

The composites produced better flexural strength 189.7MPa compared to pure PLA which was 135.8MPa. Also, there was an increment in flexural modulus to 2345.78MPa as shown in Table 4.11 against that of PLA of 2012.65MPa. The increase in flexural modulus and flexural strength of the composite with increase in GSA_{np} could be attributed to the higher stiffness of the GSA_{np} in the matrix. A similar observation was reported by Chapple *et al.* (2013). It follows that the addition of GSA_{np} has a positive effect on flexural modulus and strength of the composites due to better interfacial adhesion between matrix and GSA_{np} which aids stress transfer from matrix to reinforcement resulting in higher values of flexural strength. Weak particle/matrix interfacial bonding may result in poor flexural properties.

Table 4.11: The results of physical and mechanical properties of the PLA and Composite produced at optimum condition.

Conditions	PLA	Composite at the Optimal condition
Tensile modulus (N/mm ²)	2226.39	2305.36
%Elongation	7.81	8.61
Flexural modulus(N/mm ²)	2012.65	2345.78
Flexural strength(N/mm ²)	135.8	187.7
Impact Energy(J)	5.4	5.9
Hardness values HV	27.5	29.8
Density(g/cm ³)	1.198	1.145
% of water absorption	0	0

4.4.5 Hardness values

Hardness values of PLA matrix and composites at optimum are 27.5 and 29.8HRB respectively (see Table 4.11). There was 8.36% increase in hardness values of the composite over the PLA. It was assumed that the hardness values of the composites increased due to the addition of GSA_np in the polymer matrix. This may be due to the hardening of the matrix by GSA_np (Zhuang *et al.*, 2008).

4.4.6 Impact Energy

High strain rates or impact loads may be expected in many engineering applications of composite materials. The suitability of a composite for such applications should, therefore, be determined not only by usual design parameters but also by its impact energy absorption. The results of the

impact energy of the composites and PLA are close. It was observed that there was not much change in the impact energy when GSAnp was added at the optimal condition. Impact energy values of 5.4 and 5.9J were obtained for the PLA and composite respectively Table 4.11. The GSAnp addition at the optimal condition enhanced the ability of the matrix to absorb energy and thereby led to increase in toughness. The impact energy of 5.9Joules was in agreement with the work of other researchers (Yew *et al.*, 2005) and within the standard level for biocomposites (Raju *et al.*, 2012).

4.4.7 Density

The density of the GSAnp is 0.85g/cm^3 , which means that GSAnp is a light material. The value obtained fall within the range of density of others biomass materials which are between 0.65 and 2.2 g/cm^3 respectively (Onuegbu *et al.*, 2013). The density of the composites is shown in the Table 4.11; from the results, it would be observed that the density of the composite (1.145g/cm^3) is lower density than the PLA (1.198g/cm^3). This is because the density of the GSAnp is lower than that of the PLA matrix. Nevertheless, the density obtained in this study remained within acceptable levels for biocomposites (ASTM, 2002).

4.4.8 Water Absorption

The water absorption of the composites is shown in Figure 4.9, from the results obtained it revealed that the water absorption characteristics of the PLA and composite are similar. The results showed straight line pattern. It can be observed that the water intake of the composite is almost 0%. These results were expected since PEG and injection moulding was used in the production. However, the water absorption obtained in this study remained within acceptable levels for the production of biocomposites for food packaging (ASTM, 1998).

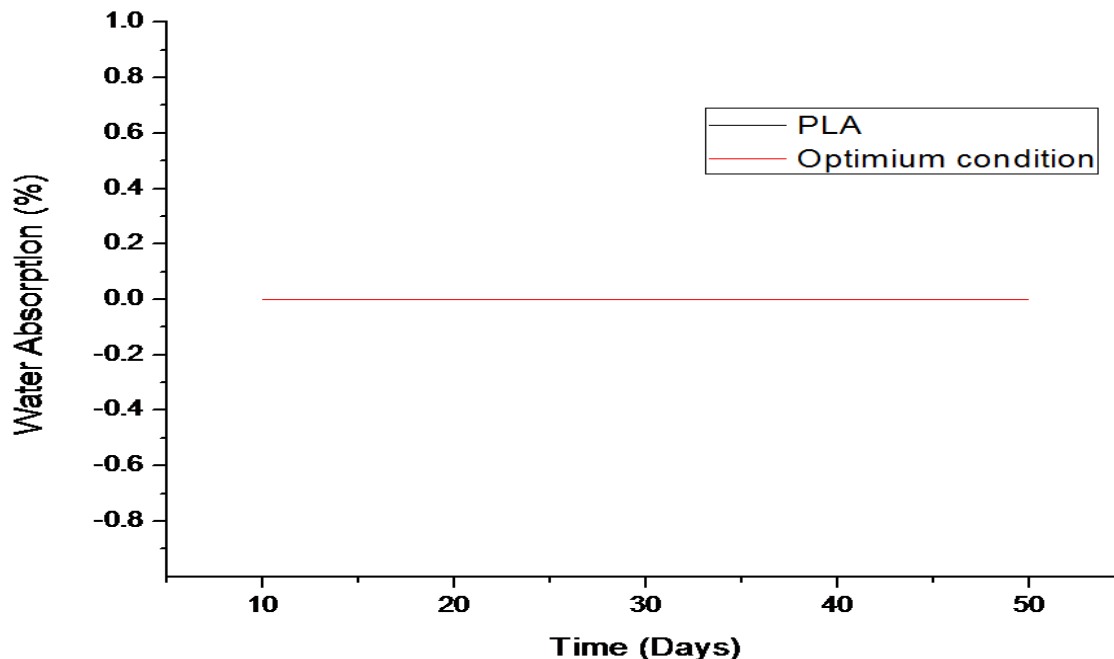


Figure 4.9: Variation of % Water absorption with Time of exposure

4.4.9 Thermogravimetric Analysis (TGA)

The results of the TGA scan of the GSAnp, PLA matrix and that of the composites at optimized condition are shown in Figures 4.10 and 4.11. The pronounced endothermic effects of the composite were observed in the Derivative Weight curves, which is due to the oxidative degradation process and to the release of volatile matters Figure 4.11. TGA curve of the GSAnp indicates that the GSAnp show less percentage of decomposition. At a temperature above 700°C, the residual weight stabilized due to the presence of silica and carbon in the GSAnp which is in line with earlier reports by (Avérous and Boquillon, 2004). As the samples were heated close to 700°C, the sample started to decompose and the decomposed byproducts including silica and carbon were formed. The silica delays the degradation process and makes the GSAnp more thermally stable. From the thermal analysis, it was clear that the GSAnp still retained above 80% of its weight at temperature around 1000°C (see Figure 4.10).

From Figure 4.10, the PLA shows the onset decomposition temperature ($T=5\%$) at 220 °C, and the thermal decomposition process only has one stage with a T_{max} at 352 °C. Pure PLA leaves almost no char residue at 500 °C. The result indicates that addition of GSAnp to PLA shift the decomposition temperature to higher temperature. The composite shows less percentage of decomposition with T_{max} of 395 °C. At a temperature above 500 °C, the residual weight stabilized which is as a result of the silica and carbon contained in GSAnp. This is also in line with the earlier reports by Huda *et al.*, 2005. From figure 4.10, the composite started to decompose at about 300 °C and the decomposed byproducts include silica and carbon. The silica ash gradually accumulated on the polymer matrix which delays the degradation process and makes the polymer more thermally stable.

The endothermic effects observed in the temperature range indicated above are probably as a result of the double bonds formed in the polymer backbone, cross-linkage of the dehydrogenated PLA macromolecules and continuous oxidation of the composite during thermal degradation Figure 4.11. The maximums of the endothermic peaks shift to higher temperature with GSAnp which reflects the improved thermal stability of polymer matrix due to the incorporation of GSAnp particles. It is established that the GSAnp reinforced PLA became more stable and the temperature of the maximal decomposition/ destruction rate was increased.

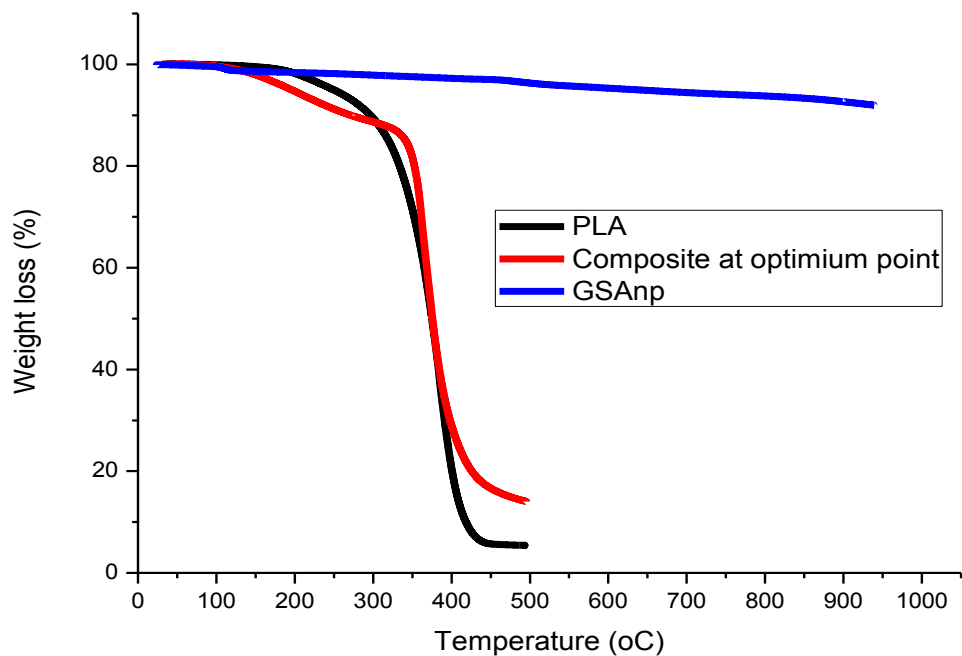


Figure 4.10: TGA curves of the GSAnp, PLA and Composite

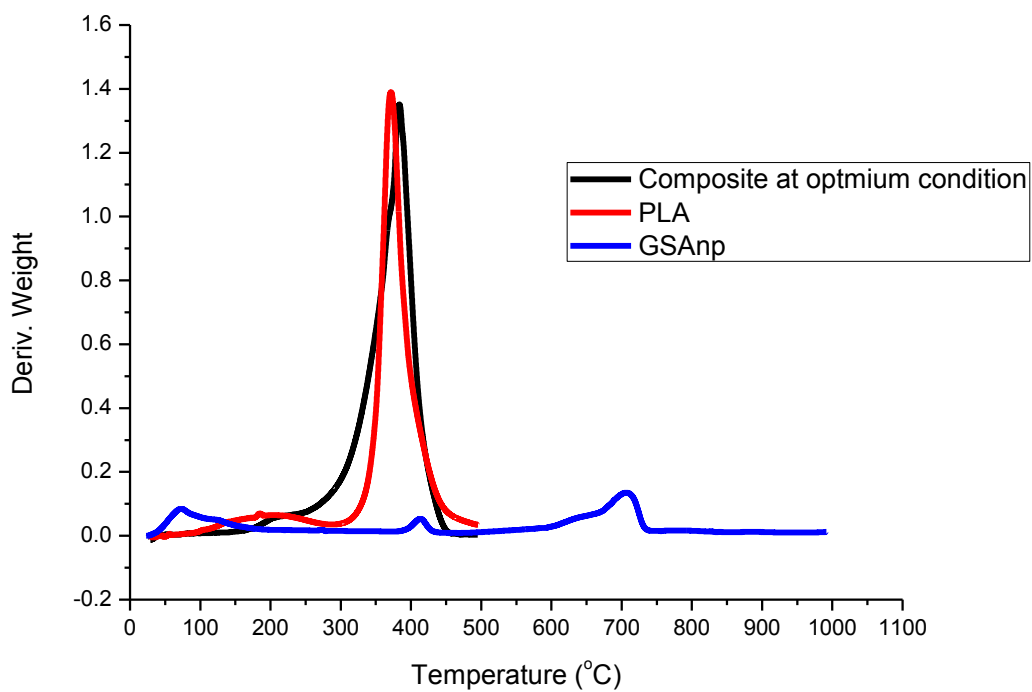


Figure 4.11: Derivative Weight curves of the GSAnp, PLA and Composite

4.4.10 DMA analysis

The variation of the storage modulus and damping factor($\tan\delta$) of the PLA and its composites as a function of temperature are shown in Figures 4.12- 4.13. It can be observed that the storage modulus of PLA composites in relation to the dynamic mechanical properties of PLA at different temperatures, decreased as the temperature increases. PLA has the typical curve of the storage modulus: a plateau firstly before the glass transition temperature, accompanied by a sharp decrease. At high temperatures, the produced composites have a relatively higher storage modulus than that of pure PLA, which can be attributed to the high stiffness and strength of GSAnp and the increase in crystallinity of PLA by GSAnp as confirmed by the XRD analysis. Therefore, the combination of GSAnp reinforcement and the enhanced crystallization of the PLA matrix lead to the better mechanical properties of the composite.

The storage modulus decreases at higher temperature due to a loss in stiffness of the GSAnp. The storage modulus of the PLA decreases from 3100 to 500MPa, while that of the composite from to 4250 to 700MPa at 30 and 90°C respectively, showing that the composite has better storage modulus. The increase in the storage modulus was attributed to the reinforcement effect in the PLA composites imparted by GSAnp which allows better stress transfer from the PLA matrix to the GSAnp. These effects are related to the improvement of the thermo-mechanical stability in PLA composites.

In Figure 4.13, it is observed that the addition of GSAnp decreases the damping factor ($\tan \delta$) in the glass transition region because the molecular mobility of the composites decreased and the mechanical loss to overcome interfriction between molecular chains is reduced. Hence the addition of GSAnp to PLA improves adhesion as composites show lower $\tan \delta$ than PLA at the peak.

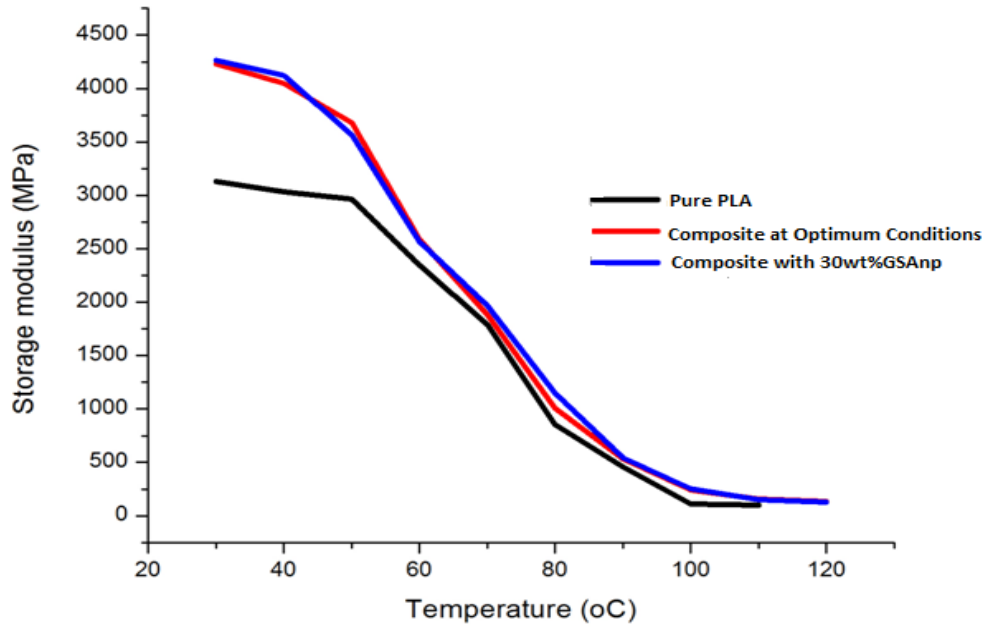


Figure 4.12: Variation of Storage Modulus with Temperature

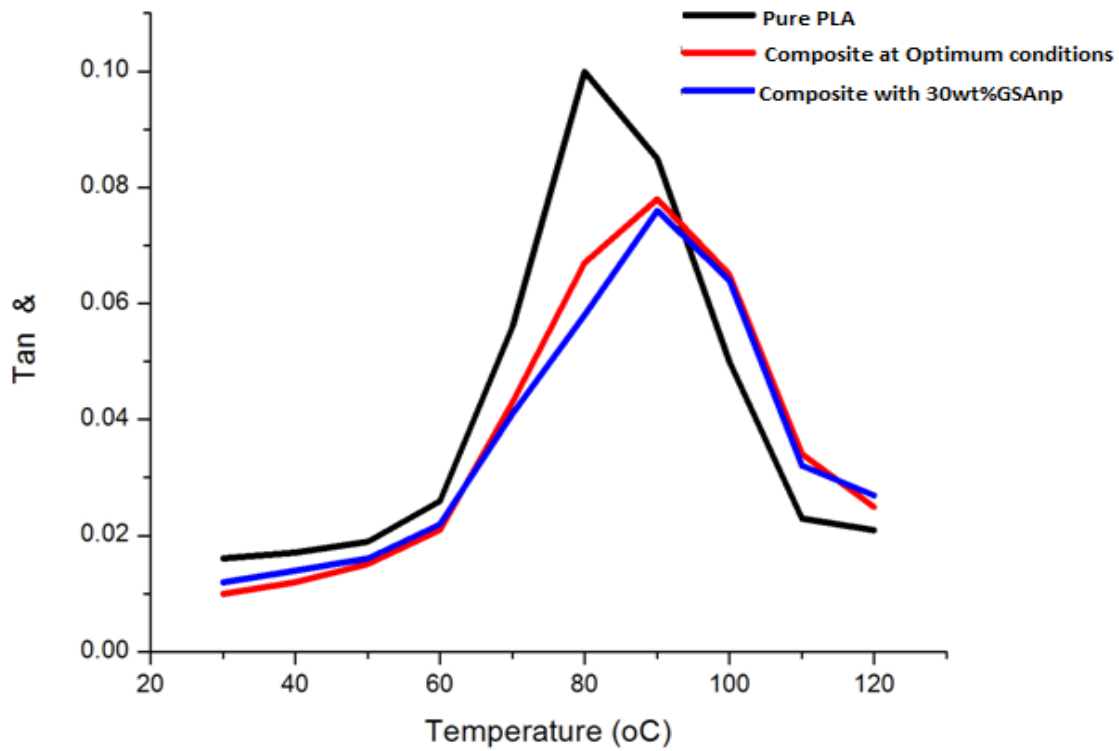


Figure 4.13: Variation of Damping factor with Temperature

4.4.11 Cone Calorimeter Analysis

Cone calorimeter test was used to further investigate the influence of GSAnp on the flammability of PLA/GSAnp composites during the combustion process. The details of the results obtained from the cone calorimeter test are shown in Table 4.12. Figure 4.14 shows the heat release rate (HRR) curves of PLA, optimum condition and 30wt%GSAnp composites. It can be seen that pure PLA burns fast after ignition and has a sharp HRR peak. While Figure 4.15 shows the total heat release (THR) curves of PLA, optimum condition and 30wt%GSAnp composites. The results showed that at the end of burning, pure PLA releases a total heat of 93.8 MJ/m². It can be observed clearly that the addition of GSAnp reduces the THR of the PLA from 93.8 to 79.2 MJ/m². The suggested mechanism, by which expanded GSAnp acts as fire retardant reducing HRR, involves the formation of char that serves as a potential barrier to both mass and energy transport between the flame and the burning polymer.

A PLA/GSAnp composite has a higher Time – to – Ignite (TTI) in comparison to pure PLA which indicates that they have better fire resistant properties see Table 4.11. Because the composite shows improvement in difficult – to – ignite, the oxygen consumed and smoke releases rate during burning was higher for the PLA than the composites. Figure 4.16, was used to validate the results obtained from the TGA. It would be observed that the samples lost weight as the temperatures increases. But the mass loss of the PLA is higher than the composites. e.g mass losses of 5123.3, 4928.2 and 4679.3g/m² were obtained for the PLA, optimum condition and 30wt%GSAnp respectively.

Table 4.12: Summary of results of Cone Calorimeter.

Sample	PLA	Optimum condition	30wt%GSAnp
HRR(Kw/m ²)	90.43	57.73	47.91
THR(MJ/m ²)	93.8	79.2	74.3
TOC(g)	63.5	54	50.2
Mass loss(g/m ²)	5123.3	4928.2	4679.3
TSR(m ² /m ²)	16.2	11.7	11.2
CO(kg/kg)	19.82	16.75	15.67
CO ₂ (kg/kg)	37.76	24.51	22.45
TTI(s)	74	78	78.2

Note: HRR=Heat release rate, THR=Total heat release TOC=total oxygen consumed TSR=Total smoke release, TTI=Time to ignition.

Also, the peak carbon monoxide yield and the peak carbon dioxide yield are summarized in Table 4.12. It can be observed that both the smoke emission and the carbon oxides yield of composites shows a significant decrease compared to PLA, which is attributed to the smoke suppression effect of the GSAnp.

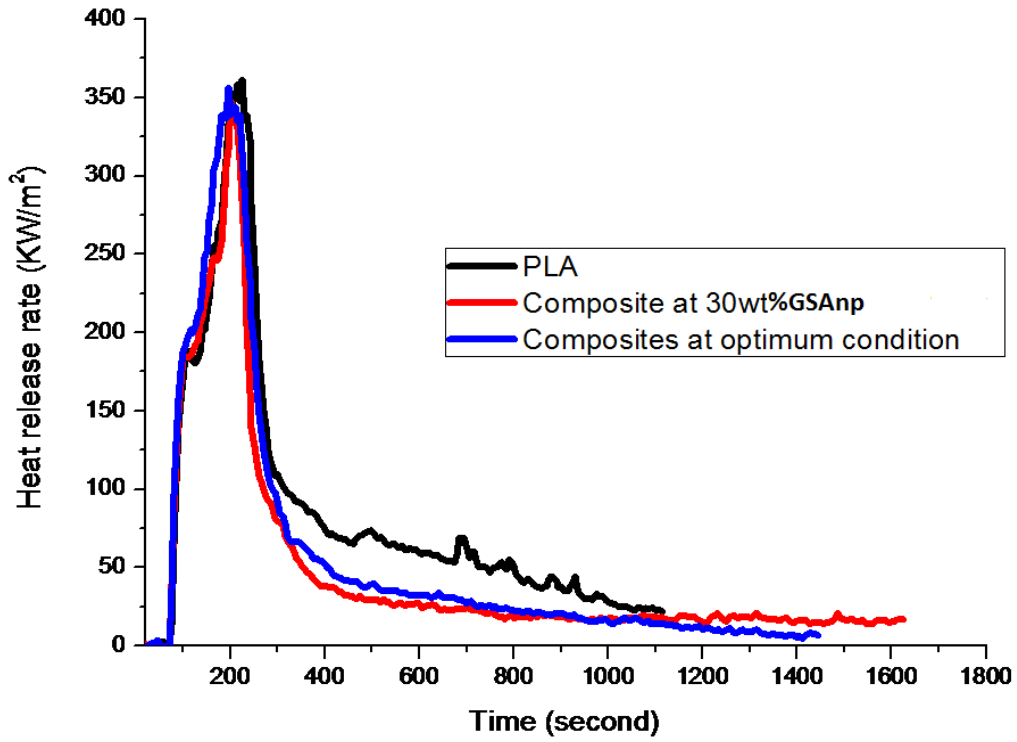


Figure 4.14: Variation of heat release rate with time

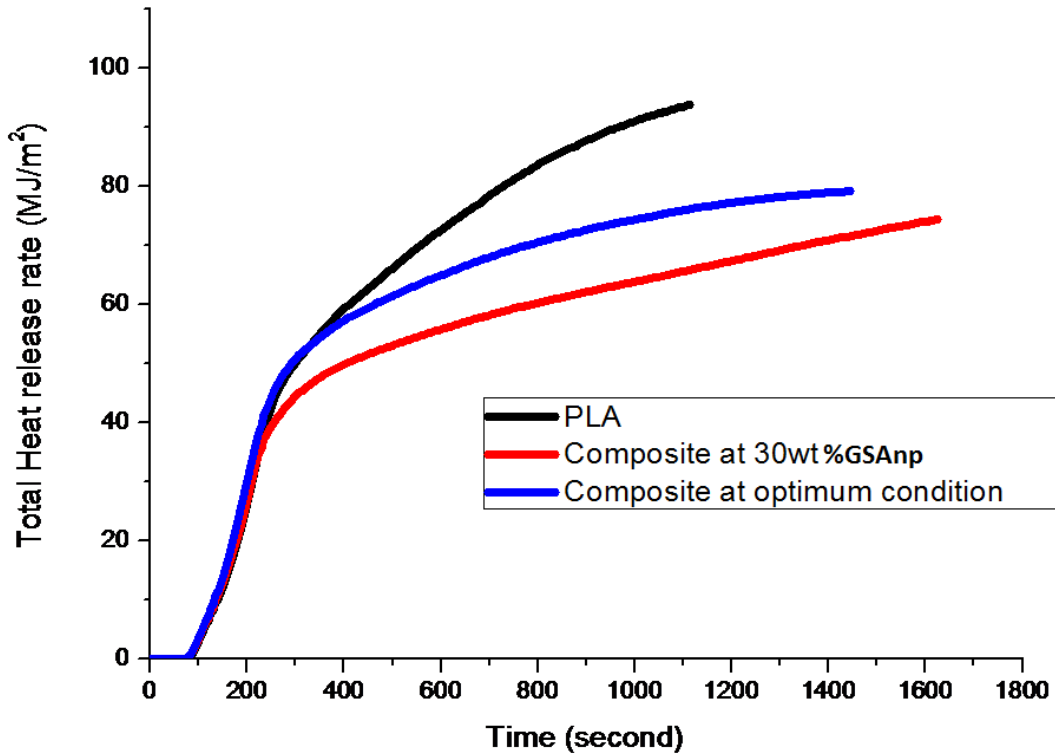


Figure 4.15: Variation of Total heat release rate with time

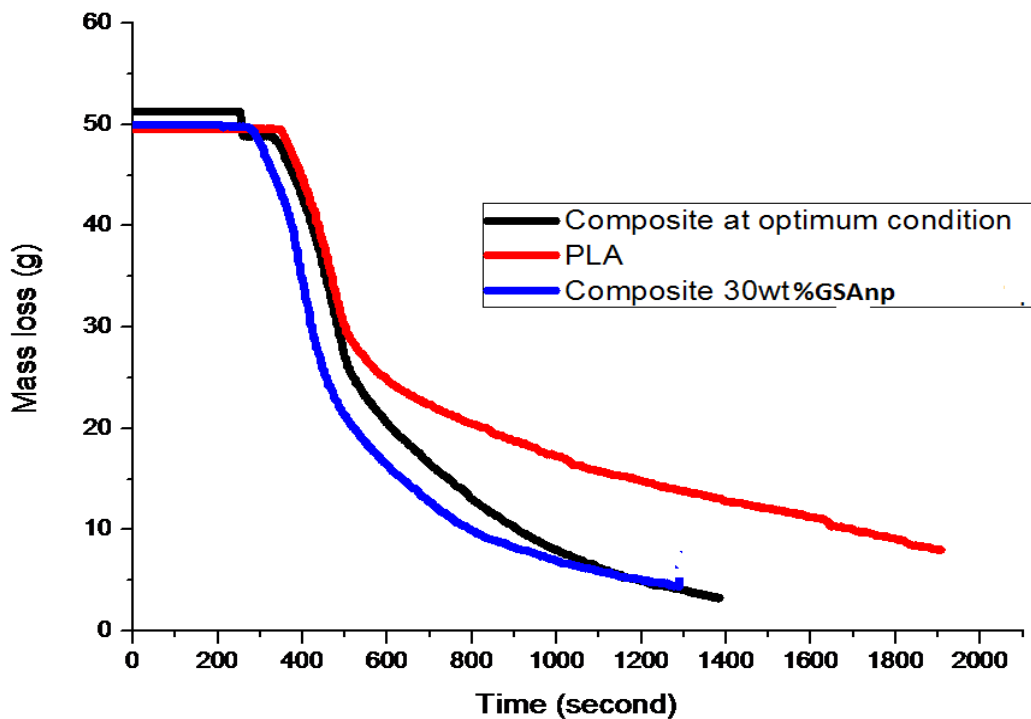


Figure 4.16: Variation of mass loss with time

Figure 4.16 revealed the variation of mass loss with time while Plate 4.10, shows the photo of the residues after the cone calorimeter experiment. It was observed that the PLA shows little or no residue after burning Plate 4.10a. The residue of the composite as shown in Plate 4.10b shows a compact and intumescent char layer, which could be the main reason for obtaining better flame retardancy of the composite.

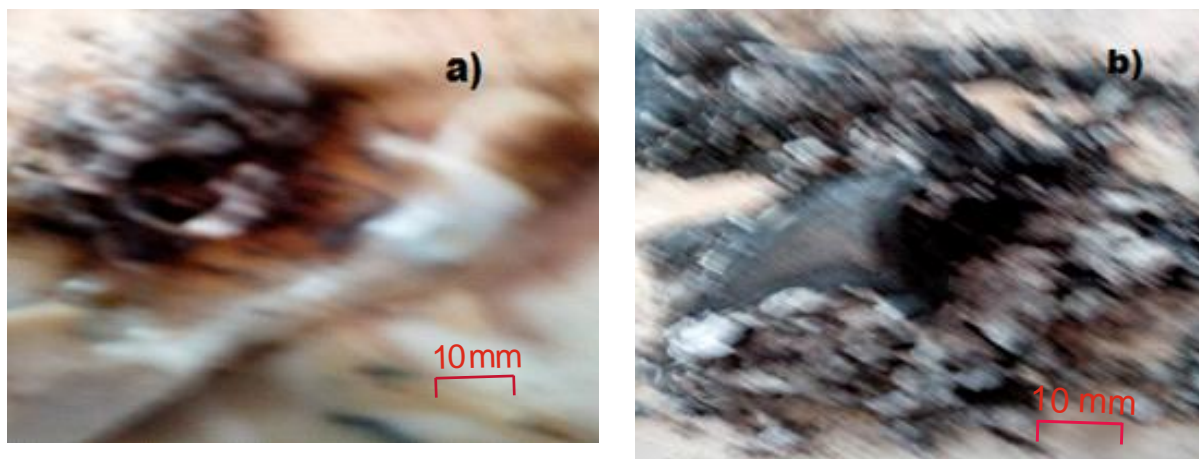


Plate 4.10: a) Residues of PLA after burning b) Residues of Composite after burning

4.4.12 Biodegradability Analysis

The weight loss at biodegradation of the PLA and composite with GSAnp ranges from 2.5-20.5% and 3.4 to 21.5% after 20 and 100days respectively (Figure 4.17). The above results clearly indicate that addition of GSAnp enhances the biodegradability of the composite, and may thereby facilitate the release of the entrapped cells into the environment.

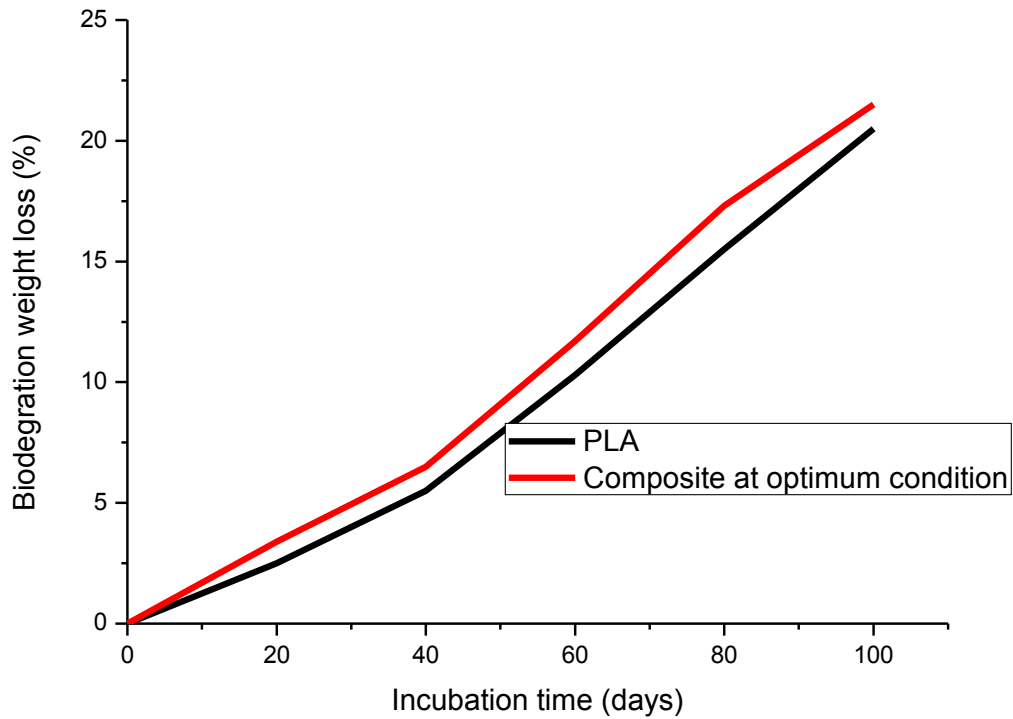


Figure 4.17: Variation of Biodegradation with incubation time

CHAPTER FIVE

5.0 CONCLUSIONS AND RECOMMENDATION

5.1 CONCLUSIONS

This research is centred on the development and characterization of PLA/GSAnp composites. From the results obtained and discussion the following conclusions could be drawn:

1. The optimal ball milling time required to produce nanoparticles of average diameter 20nm from the groundnut shell ash was 10hours using High energy intensity ball milling
2. The optimal condition for the production of the composite using tensile strength as a critical criterion was obtained at 20wt%GSAnp, 4wt%PEG, annealing temperature of 100°C and annealing time of 6hours.
3. From the XRD analysis, the composite is semi-crystalline. This is as a result of the introduction of the GSAnp into PLA chains.
4. The density of the composite (1.145g/cm³) is lower than that of the PLA (1.198g/cm³). This is because the density of the GSAnp is lower than that of the PLA matrix.
5. The composite has better mechanical properties (Hardness, Impact energy, Flexural and Tensile modulus) compared to the PLA.
6. The maximums of the endothermic peaks shift to higher temperature with GSAnp addition showing an increase in the thermal stability of the composite due to the incorporation of GSAnp particles.

7. The storage modulus of the PLA decreases from 3100 to 500MPa and that of the composite from 4250 to 700MPa at 30 and 90°C respectively. Showing that the composite has better storage modulus.
8. The composite has better flame retardancy and biodegradation properties than the PLA.

5.2 RECOMMENDATIONS

The current study has yielded some important information about the microstructure and properties of PLA/GSAnp composites. In the course of the investigation, some recommendations and new areas of research have been identified.

1. Other mechanical properties of the composite, such as wear resistance and fatigue can also be investigated in order to expand the potential applications.
2. The biodegradability of the composite was evaluated using weight loss techniques. It is recommended that the change in molecular weight technique be used and the mechanical properties determined after the test.
3. It is recommended that the matrix particle interface be investigated to determine the degree of bonding.
4. The resistance of the composite to chemical attack should be investigated.

5.3 CONTRIBUTION TO KNOWLEDGE

1. The research has established that GSAnp can be produced using High energy ball milling. The nanoparticles of average diameter 20nm and specific surface area of 56.7 m²/g were produced at 10 hours of ball milling.
2. The research has confirmed the suitability of using the GSAnp as reinforcement for the production of composites using PLA as the matrix.

3. The research also established that the optimum conditions and process parameters required for the production of the composite are 20wt%GSA_{np}, 4wt%PEG, annealing temperature and time of 100°C and 6hours respectively.
4. The storage modulus of the PLA decreased from 3100 to 500MPa and that of the composite from 4250 to 700MPa at 30 and 90°C respectively. Showing that the composite has better storage modulus.
5. The Tensile Strength of the composite as compared to injection moulded PLA and virgin PLA, was enhanced by 115.215% and 267% respectively, biodegradability was improved by 5% and there was decrease of the total heat released by 36.04%.
6. Two journal articles have already been published in peer review international journals.

(Appendix C)

REFERENCES

- Antonio J., Reilly T.O., Cavaille J.-Y. and Gandini A. (1997): The surface chemical modification of cellulosic fibres in view of their use in composite materials, *Cellulose*, vol. 4, pp. 305–320.
- Antonio J., Reilly T.O., Cavaille J.-Y., and Gandini A. (1997): "The surface chemical modification of cellulosic fibres in view of their use in composite materials," *Cellulose*, vol. 4, pp. 305–320.
- Araki J., Wada M., and Kuga S (2001): Steric Stabilization of a Cellulose Microcrystal Suspension by Poly(ethylene glycol) Grafting, *Langmuir*, vol. 17, pp. 21-27.
- ASTM standard (2002): Composite Materials Handbook Vol. 2. Polymer Matrix Composites Materials Properties, MIL-HDBK-17-2F Vol. 2 of 5.
- ASTM (2002) ASTM standard D 2240- 98 Standard test method for Rubber property – Durotometer Harness, in ASTM standards Vol 08 (3). New York: American Society for testing and materials.
- ASTM (1998): ASTM standard D570- 98. Standard Test methods for water absorption of Plastics, In ASTM standards Vol .08.01 New York, N.Y American society for testing and materials.
- ASTM D638-03 (2003) Standard test method for tensile properties of plastics. West Conshohocken ASTM international
- ASTM D6002(2010): Standard Guide for Assessing the compostability of environmentally degradable plastics.
- ASTM D256 (2005) Standard test methods for determining the Charpy Pendulum, impact Resistance of plastics.
- ASTM D 1037.06 standard (2006): Standard test method for evaluating properties of wood-based fibres and particle panel materials, Designation, West Conshohocken, PA, PP 142-171.
- Avella, M., Bogoeva-Gaceva, G., Buzarovska, A., Errico, M. E., Gentile, G. and Grozdanov, A (2008): Poly(lactic acid)-based biocomposites reinforced with kenaf fibres. *J. Appl. Polym. Sci.*, 108, 3542-3551.
- Avérous L., and Boquillon N (2004): Biocomposites based on plasticized starch: thermal and mechanical behaviours. *Carbohydrate Polymers*; 56: 111-122.
- Avérous L. and Le Digabel F. (2006): Properties of biocomposites based on lignocellulosic fillers. *Carbohydrate Polymers*; 66: 480-493.
- Bataille P., Ricard L., and Sapieha S. (1989): Effects of cellulose fibres in polypropylene composites," *Polymer Composites*, Vol. 10, pp. 103-108.
- Bax, B. and Mussig, J. (2008):

- Impact and tensile properties of PLA/Cordenka and PLA/flax composites. *Compos. Sci. Technol*, 68, 1601-1607.
- Belgacem M.N. and Gandini A (2005): The surface modification of cellulose fibres for use as reinforcing elements in composite materials, *Composite Interfaces*, Vol. 12, pp. 41-75.
- Ben – Gal (2005). The use of Data Compression Measures to Assess Robust Designs, *IEEE Trans on Reliability* Vol 54 N0 3 pp381-388
- Ben – Gal, Katz-R. and Bukchin J. (2008). Robust Eco- Design: A New Application for Quality Engineering, *IE transactions* Vol. 40 (10) pp 907- 918
- Biagiotti J., D., Puglia J. Kenny M (2004): A review on natural fibre-based composites Part I: Structure, processing and properties of vegetable fibres. *Journal of Natural Fibres*, Vol. 1, pp37-67.
- Bikiaris. D.N (2006): Isotactic polypropylene (iPP)/silica nanocomposites *J. Appl. Polym. Sci.*, Vol. 100, pp2684
- Bhatnagar A. and Sain M. (2005): Processing of cellulose nanofibre-reinforced composites, *Journal of Reinforced Plastics and Composites*, Vol. 24, pp. 1259-68.
- Chapple S., and Anandjiwala R (2013). Flammability of natural fibre reinforced composites and strategies for fire retardancy: A Review *Journal of Thermoplastic Composite Materials* 236 871-893
- Cheung H.-Y, Lau K.-T, Tao X.-M and Hui. D (2008): A potential material for tissue engineering: Silkworm silk/PLA. *Composites Part B*; Vol. 39: pp1026–1033
- Chiu, W.M., Chang, Y.A., Kuo, H.Y., Lin, M.H. and Wen, H.C (2008): A study of carbon nanotubes/bio-degradable plastic polylactic acid composites. *J. Appl. Polym. Sci.*, Vol. 108, 3024-3030.
- Cypus S. H., Saltzman W. M., and Giannelis E. P. (2003): Organosilicate-polymer drug delivery systems: controlled release and enhanced mechanical properties, *Journal of Controlled Release*, Vol. 90, pp.163-169, 2003.
- De Silva, A.L.N., Rocha, M.C.G. and Moraes, M.A.R (2002). Mechanical and Rheological properties of composites based on polythene and mineral Additive, *polymers Testing* 21(1): 57-60
- Ess J.W. and Hornsby P. R. (1987) *Plastic Rubber Process Appl*, Vol. 8, pp. 147.
- Facca, Angelo G., Mark., Kortschot, T. and Yan, N. (2006). Predicting the elastic modulus of natural fibre reinforced thermoplastics. *Composites part A* 37 pp 1660 – 1671
- Fang, Q. and Hanna, M.A. (2006) Rheological properties of amorphous and semicrystalline poly(lactic acid) polymers. *Ind. Crop Prod*, 10, 47-53.
- Fowler P.A., J.M. Hughes, R.M. Elias (2006). Biocomposites: technology, environmental

- credentials and market forces. *Journal of the Science of Food and Agriculture*; 86:1781-1789.
- Fukushima. K., Abbate C., Tabuani D., Gennari, M. and Camino G. (2009): Biodegradation of Poly(Lactic Acid) and Its Nanocomposites, *Polymer Degradation and Stability*, Vol. 94: pp1646-1655.
- Garlotta, D.A. (2002): Literature review of Poly(lactic acid). *J. Pol. Env. Vol.9*, pp63-84.
- Goswami J., Bhatnagar. N, Mohanty. S and Ghosh. A.K. (2013): Processing and characterization of poly(lactic acid) based bioactive composites for biomedical scaffold application, *express Polymer Letters* Vol.7, No.7 pp767-777
- Grozdanov, A., Buzarovska, A., Bogoeva-Gaceva, G., Avella, M., Errico, M.E., and Gentile, G. (2006): Rice straw as an alternative reinforcement in polypropylene composites. *Agron. Sustain. Dev.*, Vol. 26, pp251-255.
- Giita S. V. S., Nor A. I., Norhazlin Z., Wan M. Z. W. Y. and Hazimah A. H. (2012) Mechanical, Thermal and Morphological Properties of Poly(lactic acid)/Epoxidized Palm Olein Blend, *Molecules*, Vol 17, 11729-11747
- Guduri B.R, Rajulu A.V and Luyt A.S(2006): Effects of alkali treatment on the flexural properties of *Hildegardia* fabric composites. *Journal of Applied Polymer Science*, 102:1297-1302.
- Hanafi Ismail, U. S. Ishiaku, A. R. Arinab & Z. A. Mohd Ishak (2006) : The Effect of Rice Husk Ash as a Filler for Epoxidized Natural Rubber Compounds, *International Journal of Polymeric Materials and Polymeric Biomaterials*, 36:1-2, 39-51
- Herrmann A.S., Nickel J. and Riedel U. (1998): Construction materials based upon biological renewable resources— from component to finished parts. *Polymer Degradation and Stability*; 59:251-261.
- Heux L., Chauve G., and Bonini C. (2000): "Nonflocculating and Chiral-Nematic Self-ordering of Cellulose Microcrystals Suspensions in Nonpolar Solvents," *Langmuir*, Vol. 16, pp. 8210-8212.
- Hiremath. N, (2012): Recent Developments in Carbon Fibres and Carbon Nanotube-Based Fibres-A Review, *Polymer Reviews*, 1234-1237
- Huda, M.S., Mohanty, A.K, Drzal, L.T., Schut, E. and Misra, M (2005): Green composites from recycled cellulose and poly(lactic acid): Physico-mechanical and morphological properties evaluation. *J. Mater. Sci*, 40, 4221-4229.
- Huda M.S., Drzal, L.T., Mohanty A.K. and Misra, M. (2008): Effect of fibre surface-treatment on the properties of laminated biocomposites from poly(lactic acid)(PLA) and kenaf fibres. *Compos. Sci. Technology*, Vol. 68, pp 424-432.
- Hu R. and Lim J. K (2007): Fabrication and mechanical properties of completely biodegradable hemp reinforced PLA composites. *J. Compos. Mater*, 41, 1655-1669.

- Hu R and Lim J. K (2007): Fabricated hemp fibre reinforced PLA biodegradable composites *J Compos Mater*, 41:1655-69
- Ichazo, M. N. Albano, C. Gonzalez, J. Perera, R. Candal, M. V. (2001). Polypropylene/wood flour composites treatments and properties. *Composites structures* 54. 207 – 214
- Jancar J. (1989): Influence of filler particle shape on elastic modulus of PP/CaO₃ and PP/Mg(OH)₂ composites, *Journal of Materials Science*, vol. 24, pp. 3947–3955.
- Janewit, E., Faix, O. and Hill, F 2008. Thermal decomposition of milled wood lignins studied by thermogravimetry/ mass spectrometry. *Journal of Analytical and Applied Pyrolysis*. 40-41, 71-186
- Joseph, K. Mattoso L.H.C., Toledo S., Thomas R.D., de Carvalho L.H., Pothen L., Kala S. and James. B. (2000): Natural fibre reinforced thermoplastic composites. In *Natural Polymers and Agrofibrils Composites*, ed. E. Frollini, A.L. Leão and L.H.C. Mattoso, 159-201. São Carlos, Brazil: Embrapa, USP-IQSC, UNESP.
- Kim H. S., Park B.H., Choi, J.H. and Yoon, J. S. (2008): Mechanical properties and thermal stability of poly(L-lactide)/calcium carbonate composites. *J. Appl. Polym. Sci*, 109, 3087-3092.
- Ko E. K., Jeong S. I., Rim, N.G., Lee, Y.M., Shin H. and Lee, B. K (2008): *In vitro* osteogenic differentiation of human mesenchymal stem cells and *in vivo* bone formation in composite nanofibre meshes. *Tissue Eng. Pt A*, 14, 2105-2119.
- Kobashi, K., Villmow, T., Andres, T. and Pötschke, P. (2008): Liquid sensing of melt-processed poly(lactic acid)/multi-walled composite films. *Sensor Actuat. B-Chem* Vol. 134, 787-795
- Kolybaba M., Tabil L.G., Crerar W.J. and Wang B. (2003): Biodegradable polymers: Past, present and future. The Society for Engineering in Agricultural, Food and Biological Systems, ASA meeting presentation. Fargo, North Dakota, USA. 3-4
- Kozłowski R., M. Władyska-Przybylak (2008): Flammability and fire resistance of composites reinforced by natural fibres. *Polymers for Advanced Technology*; Vol. 19: pp446-453.
- Kumar, Sudhir, Kumar P. and Shan, H.S. (2008): Optimization of Tensile properties of Evaporative Pattern Casting Process Through Taguchi's Method. *Journal of Materials Processing Technology* Vol. 204 pp59-69.
- Kuan, C.F., Kuan, H. C., Ma, C.C.M. and Chen, C.H. (2008): Mechanical and electrical properties of multiwall carbon nanotube/poly(lactic acid) composites. *J. Phys. Chem. Solids*, Vol. 69, pp1395-1398.
- Le Duigou A., Piliñ I., Bourmaud A., P. and Davies, Baley C. (2008): Effects of recycling on

- mechanical behaviour of bio-compostable flax/poly(L-lactide) composites. *Composites Part A*; Vol. 39: pp1471-1478.
- Lee S. H, Wang S (2006): The effect of lysine-based diisocyanate (LDI) as a coupling agent, on the properties of bio-composites from poly(lactic acid) and bamboo fibre (BF), *Composites Part A*, 37 80-91
- Mammeri. F, Rozes H and Sanchez. C. (2003). filled PMMA coatings silica nanoparticles Sol-gel Sci. Techno. Vol. 26, 413
- Mathew A.P., Oksman K., and Sain M. (2006): "The effect of morphology and chemical characteristics of cellulose reinforcements on the crystallinity of polylactic acid," *Journal of Applied Polymer Science*, Vol. 101, pp. 300-310.
- Mathew, A.P., Oksman, K. and Sain, M (2005): Mechanical properties of biodegradable composites from polylactic acid (PLA) and microcrystalline cellulose (MCC). *J. Appl. Polym. Sci.* Vol. 97, pp2014-2025
- Mehta G., Mohanty A.K., Misra M. and Drzal L.T. (2004): Biobased resin as a toughening agent for biocomposites. *Green Chemistry*, Vol. 6: pp254-258.
- Metters, A. T. Anseth, K. S. and Bowman, C. N. (2000): Fundamental studies of a novel, biodegradable PEG-b-PLA hydrogel. *Polymer*, Vol.41, No.11, pp. 3993-4004, ISSN 0032-3861
- Mishra, A. Mohanty, L. Drzal, M. Misra, S. Parija, S. Nayak, S. Tripathy (2003): Studies on mechanical performance of biofibre/glass reinforced polyester hybrid composites, *Composite Science Technology*, Vol. 63 No. 10 pp. 1377-1385
- Mitsuishi K., S. Ueno, S. Kodama, and Kawasaki H. (1991): Crystallization behaviour of polypropylene filled with surface-modified calcium carbonate, *Journal of Applied Polymer Science*, vol. 43, pp. 2043-2049, 1991.
- Mohanty A.K., Misra M. and Drzal L.T (2002): Sustainable bio-composites from renewable resources: Opportunities and challenges in the green material world. *Journal of Polymers and the Environment* Vol. 10:19-26.
- Mohanty A.K., Misra M., Drzal L.T and Hinrichsen G. (2000): Biofibres, biodegradable polymers and biocomposites: An overview. *Macromolecular Materials and Engineering*; Vol. 276/277: pp1-24
- Nagata, F. and Miyajima, T. (2008): Fabrication of poly(D,L-lactide)/apatite nanocomposites through a modified surfactant-free process. *Key Eng. Mat*, 361-363, 523-526.
- Nourbakhsh, A. and Ashori, A. (2009): Preparation and properties of wood plastic composites

- made of Recycled High-density polyethylene. *Journal of composite materials*, vol. 43(8) pp 877-882.
- Ogata, N., Jimenez G., Kawai H. and Ogihara T. (1997): Structure and thermal/mechanical properties of poly (L-lactide)-clay blend. *Journal Polymer Science Part B: Polymer Physic*, Vol. 35, 389-396.
- OksmanK,SkriverM, and SelinJ. F. (2003):NaturalFibresasreinforcementinpolylacticacid(PLA) composites. *Composites Science and Technology*; 63:8.
- Onuegbu G.C., Nwanonyi S.C. and Obidiegwu M.U. (2013): The Effect of Pulverized Ground Nut Husk on Some Mechanical Properties of Polypropylene Composites,*International Journal of Engineering Science Invention*, Volume 2 Issue 6 pp.79-83
- Osman H., Ismail H. and Mustapha, M. (2010): Effect of Maleic Anhydride Polypropylene on Tensile, Water Absorption, And Morphological Properties of Recycled Newspaper filled Polypropylene/Natural Rubber Composites, *Journal of Composite Materials* Vol. 44, No. 12 pp1477 – 1490.
- OsmanK, SkrifvarsM. and SelinJ. F.(2003):PLA/flaxfibrecompositeshavingflaxfibre contentof30and40wt.%,*ComposSci Technology*, 63:1317-24.
- Osarenwinda, J.O. and Nwachukwu, J.C. (2007). Effect of particle size on some properties of Rice hush particle board. *Advance material Trans Tech Publish Ltd. Switzerland* **18-19**:43-48
- Osarenmwinda, J. O. and Nwachukwu, J. C. (2010). Development of Composite Materials from Agricultural waste. *International Journal of Engineering Research in Africa* Vol. 3 pp42 – 48.
- Qu. Y, Yang. F, and Yu. Z (1998): Effect of silica nanoparticles to nylon-6, *Journal of Polymer Science*. part B Polym Phys., 36, 789
- Peesan, M.;Supaphol,P.andRujiravanitR. (2005). Preparationandcharacterizationof hexanoyl chitosan/polylactide blendfilms. *CarbohydratePolymers*, Vol.60,No.3,pp.343-350,ISSN0144-8617
- Petinakis E, Yu L, Edward G, Dean K, Liu H. and Scully A. (2009): Effect of Matrix–Particle Inter- facial Adhesion on the Mechanical Properties of Poly(lactic acid)/Wood-Flour Micro- Composites. *Journal of Polymers and the Environment*;17(2):83-94.
- Pukanszky B.andFekete E (1999):AdhesionandSurfaceModification,*Advancesin Polymer Science*, vol. 139, pp. 109 -153, 1999.

- Pozsgay A., T. Fráter, L. Papp, I. Sajó, and Pukánszky B. (2002): Nucleating effect of montmorillonite nanoparticles in polypropylene, *Journal of Macromolecular Science, Part B Physics*, vol. 41, pp. 1249-1265.
- Pukánszky B. (1993): Interfacial interactions in particulate filled thermoplastics: mechanism, strength, properties, *Makromol. Chem., Macromol. Symp.*, Vol. 70/71, pp. 213-223.
- Ray S.S., Y. Kazunobu, M. Okamoto, Y. Fujimoto, A. Ogami, and Ueda K. (2003): New polylactide/layered silicate nanocomposites. 5. Designing of materials with desired properties, *Polymer*, Vol. 44, pp. 6633-6646.
- Raju A. G. U., Kumarappa B. S. and Gaitonde C. V. N. (2012), Mechanical and physical characterization of agricultural waste reinforced polymer composites, *Journal of material environmental science*, Vol. 3, pp 907-916
- Reddy N., Nama, D. and Yang, Y. (2008). Polylactic acid/polypropylene polyblend fibres for better resistance to degradation. *Polymer Degradation and Stability*, Vol. 93, No. 1, pp. 233-241, ISSN 0141-3910
- Rhim, J. W. Hong, S. I. and Ha, C. S. (2009): Tensile, water vapour barrier and antimicrobial properties of PLA/Nano clay composite films. *LWT - Food Sci. Technology*, Vol. 42, 612-617.
- Rong. M. Z, Zhang. M. Q, Liu. H, and Zeng H. M (2001): Epoxy/TiO₂ nanocomposites Ind. Lubr. Tribol., 2, 72
- Rothon R (1995): Particulate-Filled Polymer Composites: Longman Scientific and Technical, 1995.
- Roy, R. K (1990). A primer on Taguchi method van Nostrand Reinhold, New York.
- Serizawa S, Inoue K. and Lji M (2006): Developed high-performance composites (PLA/kenaf fibre and PLA/kenaf fibre/flexibilizer) *Journal Application Polymer Science*, Vol. 100: 618-24.
- Shibata M, Ozawa K, Teramoto N, Yosomiya R, Takeishi H. (2003): Biocomposites made from Short Abaca Fibre and Biodegradable Polyesters. *Macromolecular Materials Engineering Journal*; 288:9.
- Sheth, M. et al., (1997) Biodegradable polymer blends of poly(lactic acid) and poly(ethylene glycol). *Journal of Applied Polymer Science*, Vol. 66, No. 8, pp. 1495-1505, ISSN 0021-8995
- Sobkowicz, M. J., Dorgan, J. R., Gneshin, K. W., Herring, A. M. and McKinnon J. T (2008): Renewable cellulose derived carbon nanospheres as nucleating agents for polylactide and polypropylene. *J. Pol. Env.*, 16, 131-140.
- Song M., Pan C., Chen, C., Li, J., Wang, X. and Gu, Z. (2008): The application of new nanocomposites: Enhancement effect of polylactide nanofibres/nano-

TiO₂ blends on biorecognition of anticancer drug daunorubicin. *Appl. Surf. Sci.*, 255, 610-612

Taguchi G. (1987) System of experimental design, NY: BUN. White Plains

Tserki V, Matzinos P. and Panayiotou C (2006): Novel Biodegradable composites based on treated lignocellulosic waste flour as filler Part II. Development of Biodegradable composites using treated and compatibilized waste flour. *Composites: Part A*, Vol. 37:8.

Tokiwa Y., Calabia, B. P. Ugwu C.U. and Aiba S. (2009): Biodegradability of Plastics. *Molecular Sciences*; 10:3722-3724

Vaia R.A. and Wagner H.D. (2004): Framework for nanocomposites, *Mater. Today*, Vol. 7, pp. 32-37, 2004.

Verbeek, C. J. R. and Pickering, K. L. (2007) Recent Developments in Polymer Consolidated Composites, *Journal of Reinforcement and Composites*, Vol. 26, No. 16 pp1607 – 1624.

Vignesh X. M., Weilan X., Zuoxiang Z. and Wanyu Z. (2016) Synthesis and properties of polyamide/LLDPE composites with compatibilizer used as hot melt adhesive *Journal of Adhesion Science and Technology*, pp104-116

Vu. C, Ferte. O. L and Eranian N. (2002): Effect of silica nanoparticles in UV- curable acrylate coatings. *Eur. Coatings. Journal*, Vol. 64, pp66

Wang, S., Cui, W. and Bei J. (2005). Bulk and surface modifications of polylactide. *Analytical and Bioanalytical Chemistry*, Vol. 381, No. 3, pp. 547-556, ISSN 1618-2642

Winey K.I. and Vaia R.A. (2007): Polymer nanocomposites, *MRS Bulletin*, Vol. 32, pp. 314-319.

Wu D., Wu L., Zhang, M. and Zhao, Y. (2008): Viscoelasticity and thermal stability of polylactide composites with carbon nanotubes. *Polymer. Degrading. Stabil*, Vol. 93, 1577-1584.

Xu, C. et

al., (2009). Preparation and characterization of polylactide/thermoplastic konjac glucomannan blends. *Polymer*, Vol. 50, No. 15, pp. 3698-3705, ISSN 0032-3861

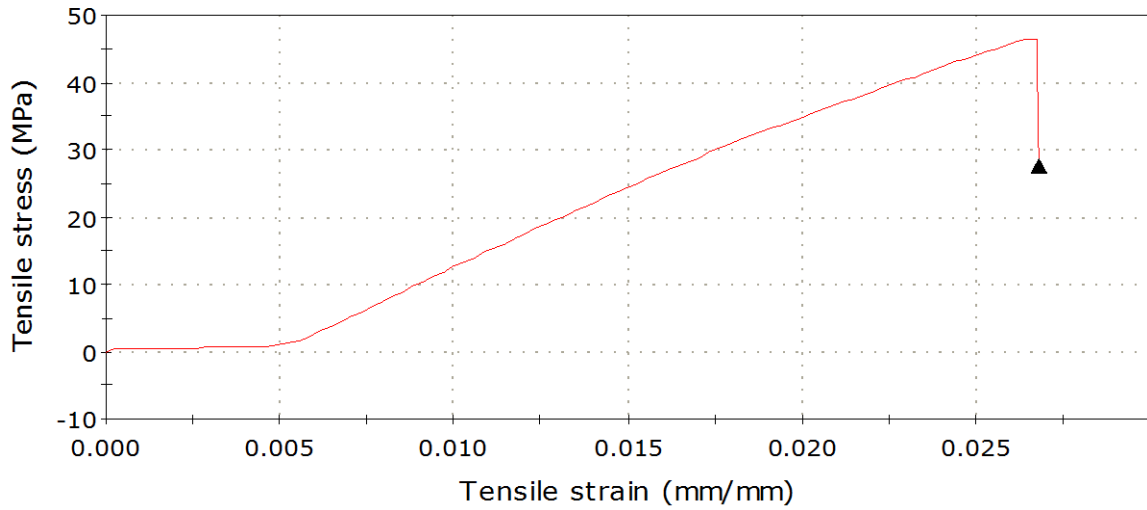
Yang. F and Nelson. G. L. (2004): PMMA/silica nanocomposites by solution polymerization, *Journal Application Polymer. Science.*, Vol. 91, pp3844

Yang, H., Joong -Hynn. P., Hee – Jun. L., Bum – Jae. H., and Taek – Sung (2006): Water Absorption Behavior and Mechanical Properties of Lignocellulosic filler – Polyolefin Bio-Composite. *Composite Structure*: Vol. 72 pp429 – 437.

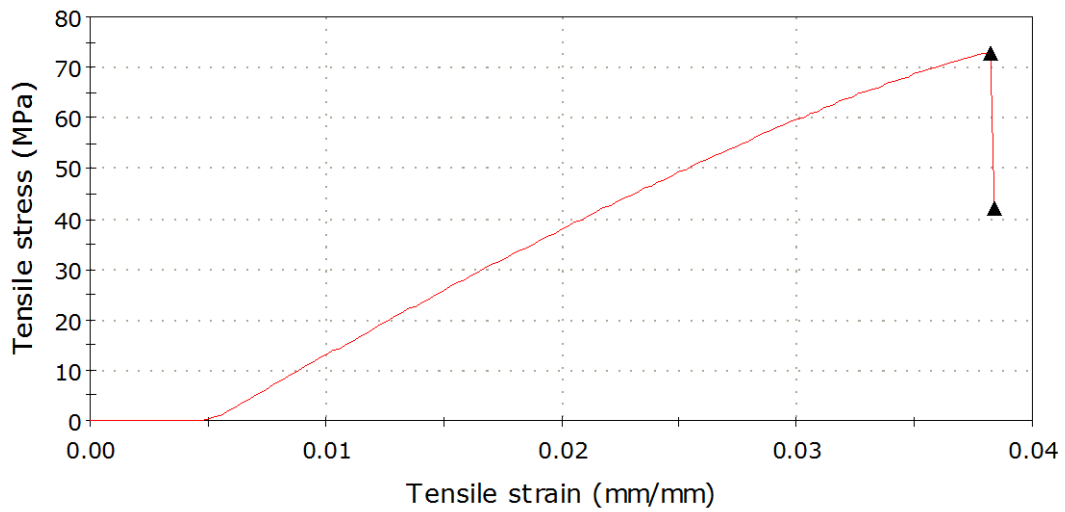
Yew G. H. Mohd Yusof A. M. M. Ishak Z. and Ishiaku U. S. (2005): PLA, rice starch (RS) (0-50 wt.%) and epoxidized natural rubber Composites, *Polymer. Degrading Stab*, Vol. 90, pp 488-500

- Youngquist, R., (1999): Wood-based composition and panel products. In: wood handbook. Wood as an Engineering material. USDA forest service, for prod. Lab general technological report FPL –GTR Vol. 113 pp 10
- Yuan, J., Shen, J. and Kang, I. K. (2008): Fabrication of protein-doped PLA composite nanofibrous scaffolds for tissue engineering. *Polymer. Int*, Vol. 57, 1188-1193
- Yuan, W., Wang, P., Cao, H. and Lei, H. (2008): Structure and properties of polylactide nano-composite polymerized in situ under microwave irradiation. *Chin. Synth. Resin Plast. Vol. 25*, pp61-64.
- Yu, T., Ren, J., Chen D. K. and Yang, S. (2008): Effect of polycaprolactone on the properties of poly(lactic acid)/montmorillonite nanocomposites. *Mater. Sci. Technology*, Vol. 16, 206-210
- Zhao Y. Q., Lau K. T., Liu T., Cheng S., Lam P. M. and Li, H. L. (2008): Production of a green composite: Mixture of poly(lactic acid) and keratin fibres from chicken feathers. *Adv. Mat. Res.*, 47-50, 1225-1228.
- Zhuang W., Zhang J., Liu J., Zhang Q., Hu B. and Shen J. (2008): Preparation and characterization of nano-TiO₂/polylactide composites. *Acta Mater. Compos. Sinica*, Vol. 25, pp8-11.

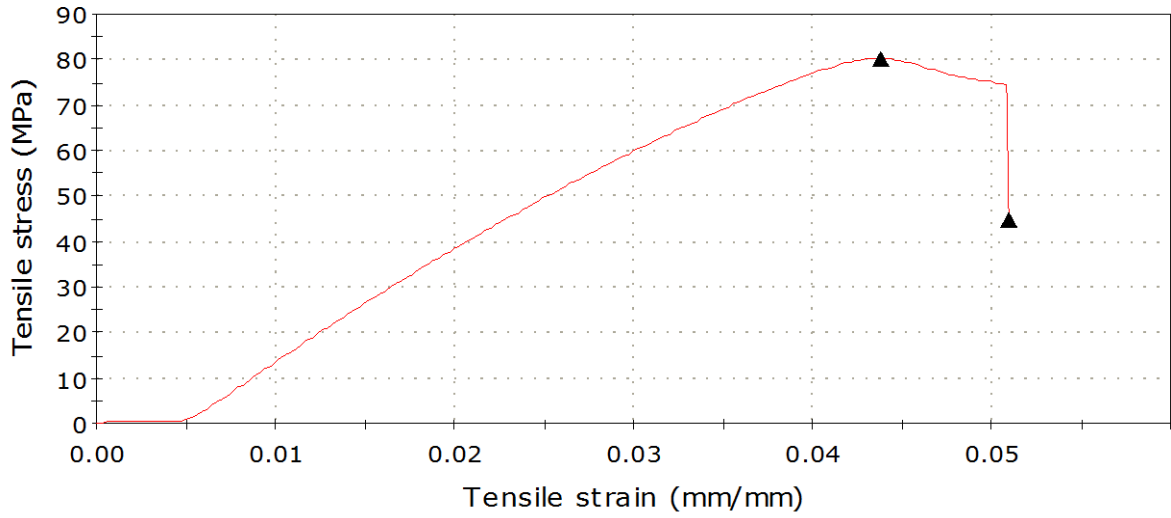
APPENDIX A



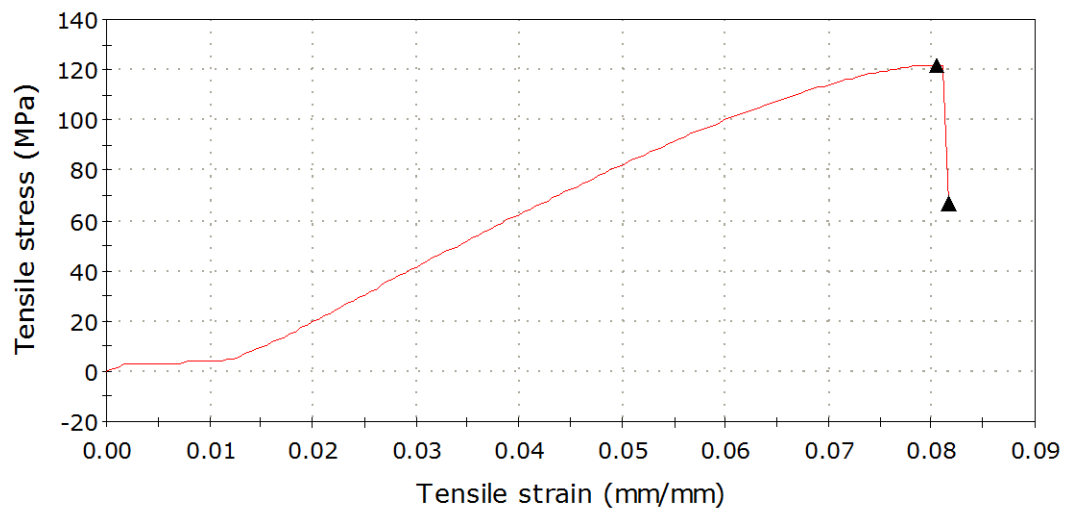
Appendix A1: Stress- Strain curve of Control(pure PLA)



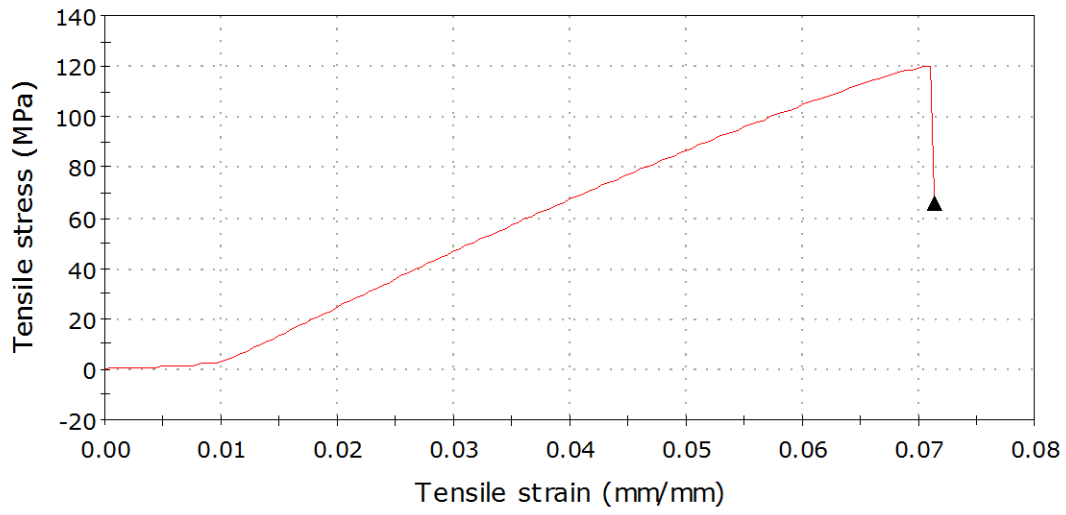
Appendix A2: Stress- Strain curve of S1



Appendix A3: Stress- Strain curve of S2

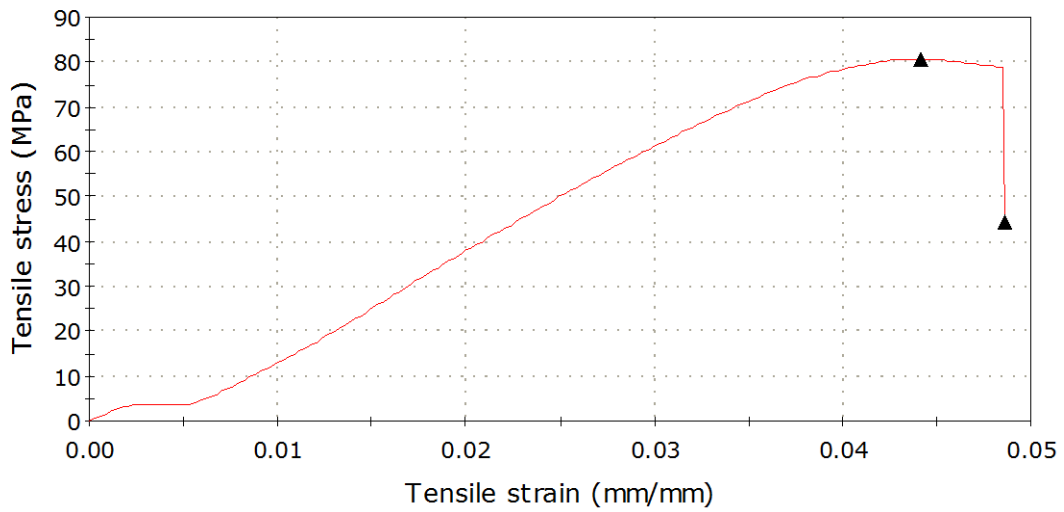


Appendix A4: Stress- Strain curve of S3



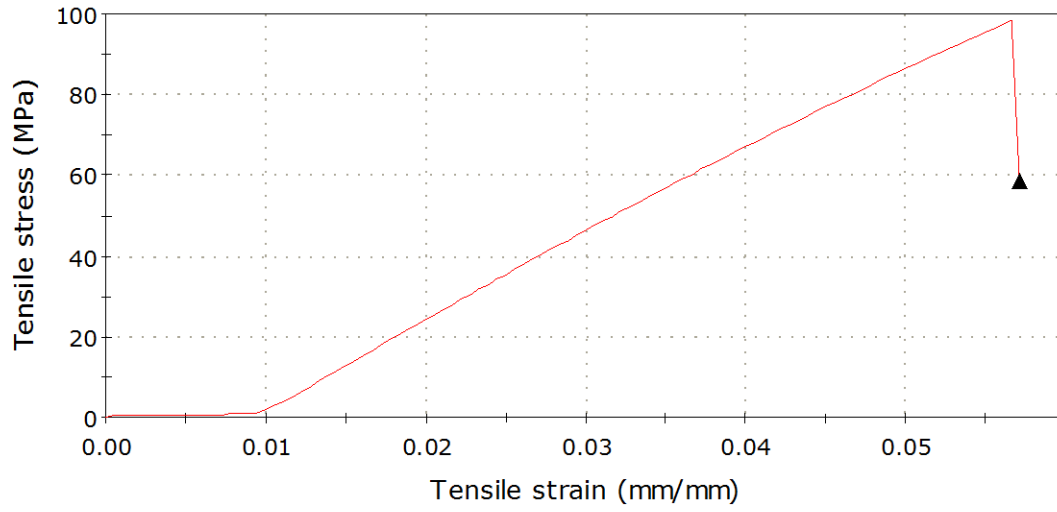
Figure

AppendixA5: Stress- Strain curve of S4



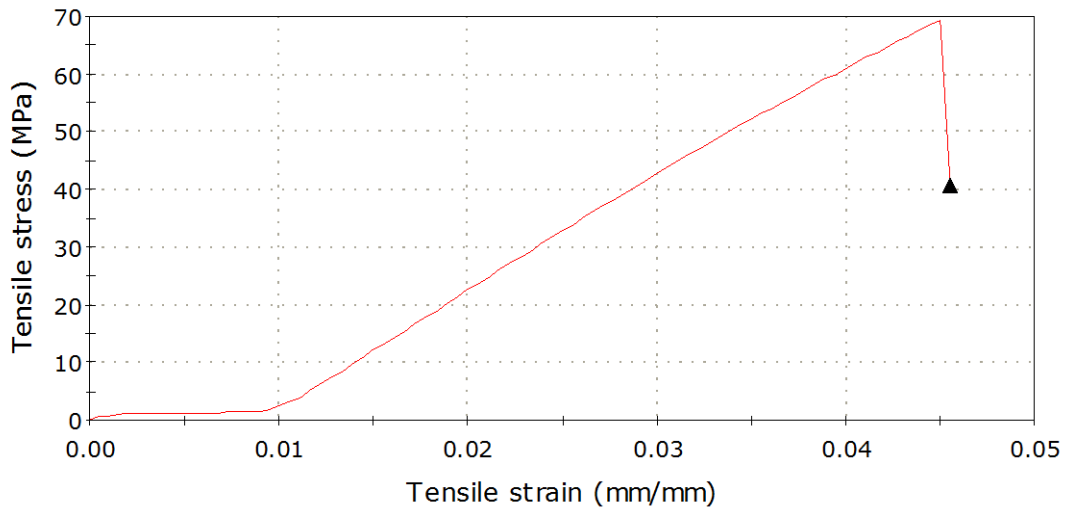
Figure

AppendixA6: Stress- Strain curve of S5



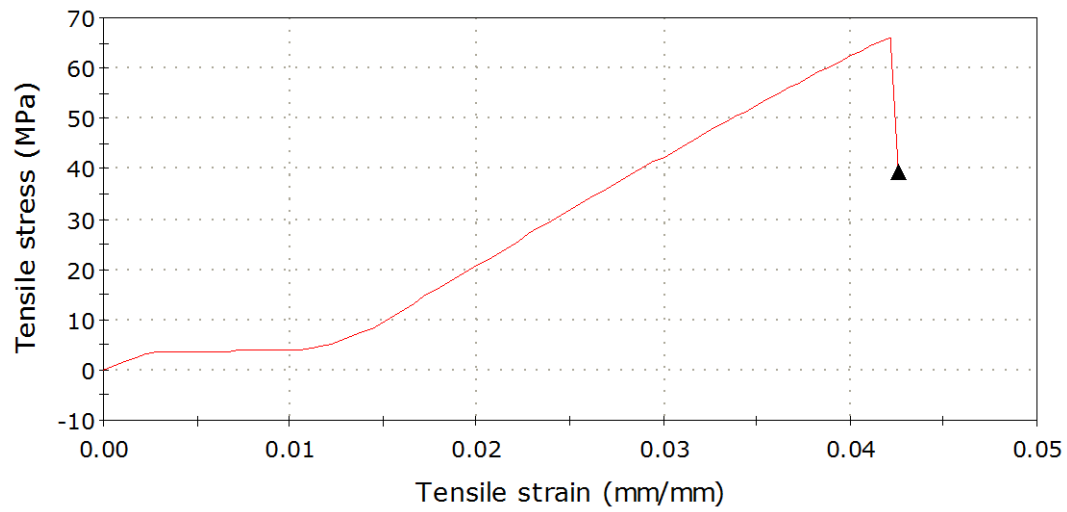
Figure

AppendixA7: Stress- Strain curve of S6

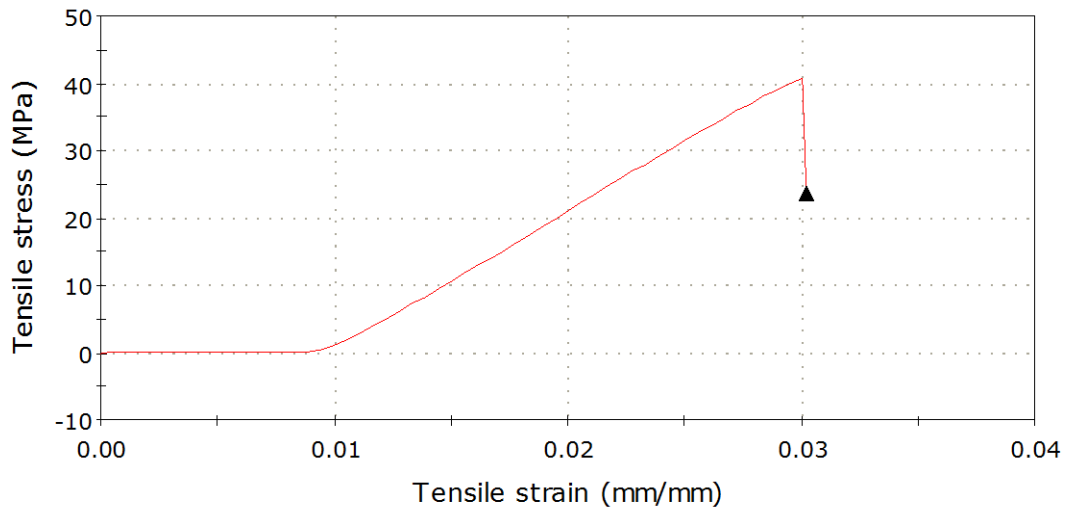


Figure

AppendixA8: Stress- Strain curve of S7



Appendix A9: Stress- Strain curve of S8



Appendix A10: Stress- Strain curve of S9

APPENDIX B



Appendix B1:Retsch Ball Mill used for the milling



Appendix B2: Photograph of TEM (Jeol, JSM2010)



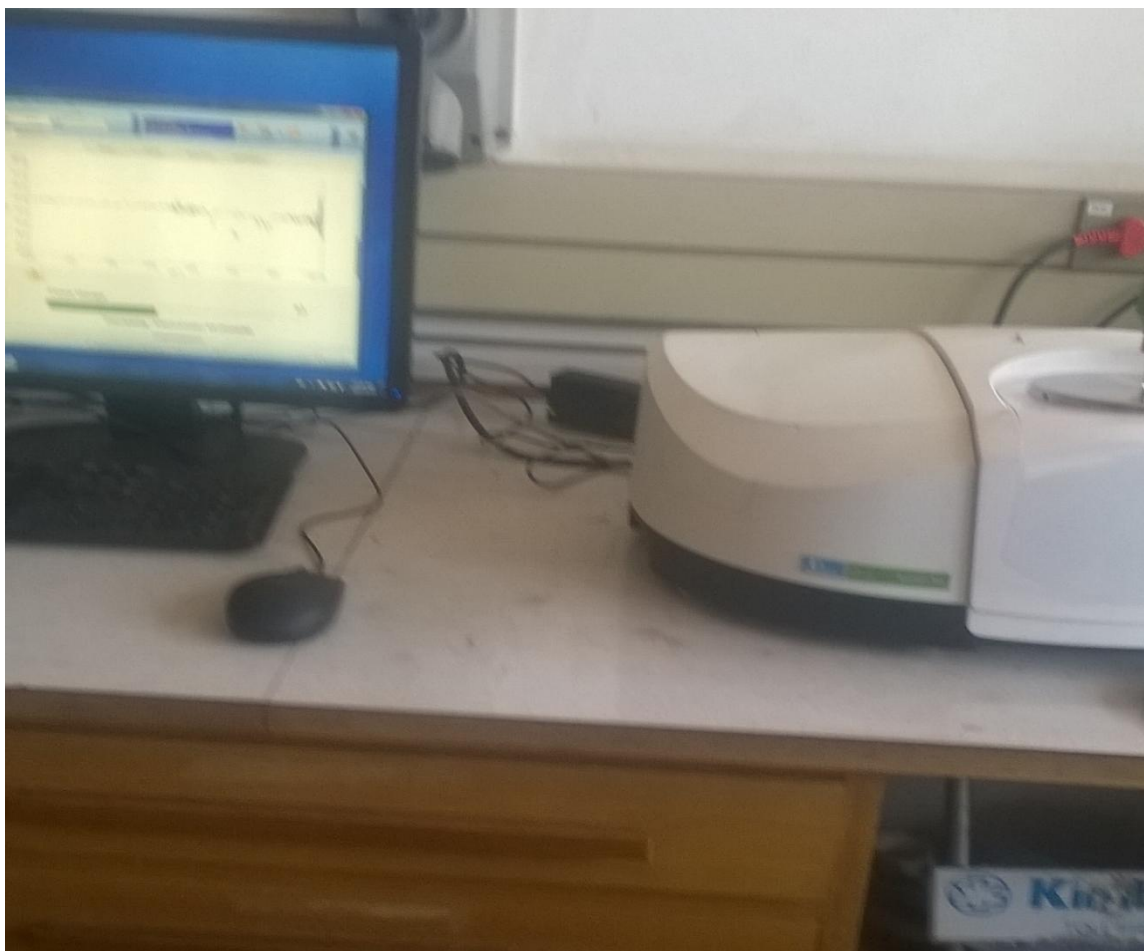
Appendix B3: Photograph of ASAP 2020 Micromeritics surface area analyzer



Appendix B4: Photograph of the X'PertPro PANalytical(XRD)



Appendix B5: Photograph of nanoparticle analyzer



Appendix B6: Photograph of Perkin Elmer spectrum 100 FT – IR spectrometer



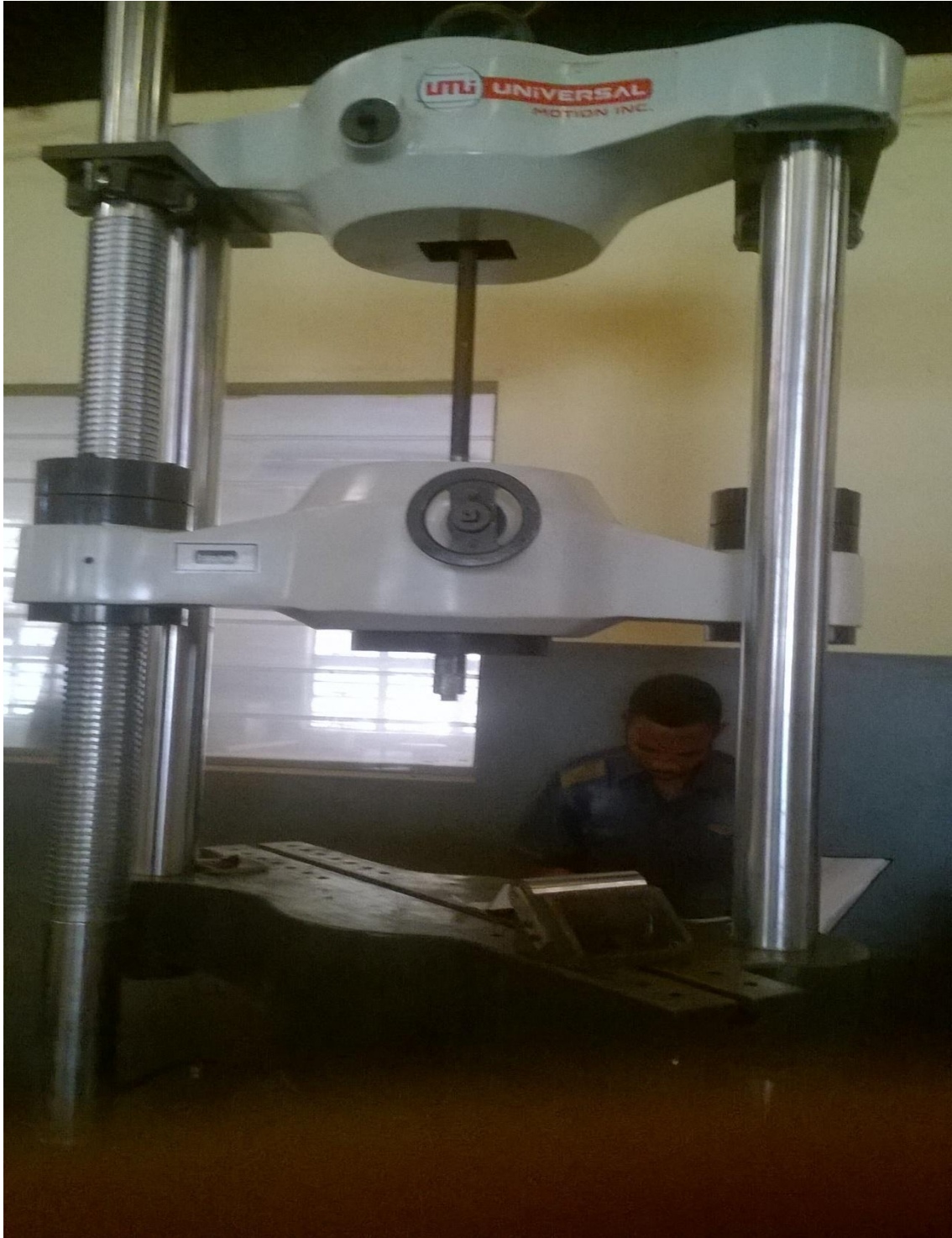
Appendix B7: Photograph of TE-30 Co-rotating screw extruder



Appendix B8: Photograph of pelletizing of the extrudates



Appendix B9: Photograph of the ENGEL e-mac 50, injection moulding machine



Appendix B10: Universal strength testing machine



Appendix B11: photograph of Instron impact Energy machine



AppendixB12: photograph of JEOL 6480 LV electron microscope



Appendix B13: Photograph of the TGA/DTA thermal analyser



AppendixB14: The cone calorimeter and burning panel inside the calorimeter.



(A)



(B)

Appendix B15: Photograph of the produced samples (B) and (B)



Plate B16: Samples encapsulated in the Bacillus bacterial

APPENDIX C

Articles published in peer review International Journal from the research work

1. Synthesis of groundnut shell ash nanoparticles: characterization and particle size determination. The International Journal of Advanced manufacturing technology. Volume 91. Pp 1111-1116. Springer. (2017).
2. Experimental correlation between process parameters and tensile strength of polylactic acid/groundnut shell ashnanoparticle biocomposites. The International Journal of Advanced manufacturing technology. DOI 10.1007/s00170-017-0448-1. Springer. (2017).